UNIVERSITY OF CAPE COAST

OPTIMIZATION OF RADIOLOGICAL PROTECTION OF PATIENTS UNDERGOING MAMMOGRAPHY EXAMINATION IN GHANA

BY

EDEM KOBLA SOSU

Thesis submitted to the Department of Physics of the School of Physical Sciences, College of Agriculture and Natural Sciences, University of Cape Coast, in partial fulfilment of the requirements for the award of Doctor of Philosophy degree in Physics

FEBRUARY 2018

DECLARATION

Candidate's Declaration

I hereby declare that this thesis is the result of my own original research and that no part of it has been presented for another degree in this university or elsewhere.

Candidate's Signature: ……. Date:…….

Name: Edem Kobla Sosu

Supervisors' Declaration

We hereby declare that the preparation and presentation of the thesis were supervised in accordance with the guidelines on supervision of thesis laid down by the University of Cape Coast.

Principal Supervisor's Signature: Date:…….....

Name: Professor Mary Boadu

Co-Supervisor's Signature: Date:.....

Name: Professor Samuel Yeboah Mensah

ABSTRACT

Quality control tests have been undertaken on thirteen mammography systems with the aim of optimizing procedures and patient radiation protection, establishing diagnostic reference levels (DRLs) and establishing quality control (QC) baseline data for the diagnostic mammography practice in Ghana. Quantitative image quality analysis was performed with "ImageJ" software using the "Rose Model" while all other tests were performed using internationally accepted protocols. Results from tube voltage accuracy and repeatability, output linearity and repeatability and half value layer measurements indicated satisfactory performance of all the systems. Results from the mammography units' assembly evaluation, compression plate assessment and short term automatic exposure control (AEC) test showed in some systems malfunctioning of compression paddles, misalignment of the compression plate and faulty AEC systems. Estimated parameters of signal-to-noise ratio (SNR) indicate that all images were not of standard quality. Results from mean glandular dose (MGD) measurements show that doses being received are within the acceptable levels with the exception of two systems whose MGD estimates exceeded the limit by 17.07% and 3.92% for the 60 mm and 75 mm equivalent breast thicknesses (EBT) respectively. Another system also exceeded the limit by 9.52% for the 75 mm EBT. DRLs based on phantom measurements have been established. Data from measurements undertaken was used to develop a model using MINITAB application software that predicts the exposure parameters, mean glandular dose and image quality before exposure is taken. Results from modelled equations proved to aid the mammography process.

KEY WORDS

Compressed breast thickness

Diagnostic reference level

Half value layer

Image quality

Mammography

Mean glandular dose

ACKNOWLEDGEMENTS

I thank the Almighty God who strengthened and encouraged me as I travelled across the country to do this work. Secondly, I will take this opportunity to express my sincere thanks to my supervisors, Prof. Mary Boadu and Prof. Samuel Yeboah Mensah for their helpful advice, thoughtful corrections and great encouragement throughout this work. I could not have come this far without them and for that I am grateful. I like to also thank the Head of Department and Staff of the Department of Physics for their support throughout my stay.

To my employer, the Ghana Atomic Energy Commission (GAEC), I say a big thank you for granting me the permission to undertake this study. For granting me days off to undertake the assessment nationwide is very much appreciated.

I also wish to thank all Heads and staff of the participating Centres. To Althea, Priscilla, Florence, Sika, Adelaide, Xoxali, Esi, Richard, Theresa, Mark, Tagoe, James, Ebenezer, Jeffrey and Sena, I am grateful for your commitment and dedication during the work.

Special and heartfelt appreciation to Dr. and Mrs. Atuwo-Ampo who hosted me during my work in the Ashanti Region. I am very grateful.

To my siblings, Mawugbonya, Makafui, Delali and Pearl, I could not have asked for better brothers and sister.

Last but not the least, to my wife, Mrs. Louisa Ama Sosu, I am grateful to have you in my life. Thanks for your love, commitment and encouragements.

God richly Bless you all.

DEDICATION

To my children: Jasmine, Jessica and Jeremy

TABLE OF CONTENTS

LIST OF TABLES

LIST OF FIGURES

LIST OF ACRONYMS

ACR	American College of Radiology
ACS	American Cancer Society
AEC	Automatic Exposure Control
ALARA	As Low As Reasonably Achievable
AJCC	American Joint Committee on Cancer
BSF	Backscatter factor
BMP	Bitmap
CBT	Compressed Breast Thickness
CC	Cranio-caudal
CD	Contrast-detail (phantom)
COV	Coefficient of Variation
CR	Computed Radiology
CT	Computed Tomography
DCIS	Ductal Carcinoma in situ
DES	Diethylstilbestrol
DICOM	Digital Imaging and Communication in Medicine
DRL	Diagnostic Reference Level
EBT	Equivalent breast thickness
EC	European Commission
ESAK	Entrance surface air kerma
EUREF	European Reference Organisation for Quality Assured Breast Screening and Diagnostic Services
FFDM	Full field digital mammography

FITS	Flexible Image Transport System
GIF	Graphics Interchange Format
HVL	Half value layer
IAEA	International Atomic Energy Agency
ICRP	International Commission on Radiological Protection
ICRU	International Commission on Radiation Units and measurements
IHC	Immune-histochemical
ITC	Isolated Tumour Cells
IPEM	Institute of Physics and Engineering in Medicine
JPEG	Joint Photographic Experts Group
LCIS	Lobular carcinoma in situ
MGD	Mean Glandular Dose
MLO	Mediolateral oblique
MRI	Magnetic resonance imaging
MTF	Modulation Transfer Function
PMMA	Polymethyl methacrylate (plexiglass or acrylic glass)
PSP	Photostimulable Storage Phosphor
QA	Quality assurance
QC	Quality control
ROI	Region-of-interest
SD	Standard deviation
SF	Screen-film
SFM	Screen-film mammography
SID	Source-to-image distance

SNR	Signal-to-noise ratio
SPR	Scatter-to-primary ratio
TIFF	Tag Image File Format
TNM	Tumour Node Metastasis
UICC	Union International Cancer Centre
WHO	World Health Organisation

CHAPTER ONE

INTRODUCTION

The study is based on the medical imaging modality of mammography. Mammography can be used for either diagnosis or screening. A mammogram reveals the anatomical features of the breast that will help detect a cancerous growth or any abnormalities in breast tissue at an early stage, allowing early treatment to produce an improved outcome for the patient.

Background to the Study

Breast cancer refers to the erratic growth and proliferation of cells that originate in breast tissues (Khuwaja, 2006). It is the most frequent female cancer and it's responsible for most cancer induced deaths in women around the world (WHO, 2002). During the process of development, breast tumour cells sometimes break away and spread to other parts of the body causing further complications if not properly managed as early as possible. In advanced stages, breast cancers are much difficult to treat in order to achieve better outcome (IMAGINIS, 2008). Primary prevention of breast cancer is still a distant goal thus secondary prevention through early detection is the only feasible approach at present. Breast self-examination, clinical breast examination and mammography have been incorporated into different screening programmes worldwide to aid early detection (EMRO, 2006).

Breast self-examination (BSE) is a domestic screening method performed by the woman herself in an attempt to detect breast cancer early (Kösters & Gøtzsche, 2003). Breast self-exams helps the woman to familiarize herself with the shape, size, and texture of her breasts. This is important because it can help her

determine if what she is feeling is normal or abnormal (Krans, 2012). The method involves the woman looking at and feeling each breast for possible lumps, distortions or swelling. It has helped to detect tumours, cysts and other abnormalities in the breast. However over the years and with the introduction of modern methods of screening, a self-exam is considered to be less effective than other techniques, such as regular mammograms. A breast self-exam is useful but optional (Baxter, 2001).

The clinical breast examination (CBE) is an important tool in the care of women (Bryan & Snyder, 2013). A clinical breast examination (CBE) is a physical exam done by a health care provider (this may be a physician, nurse practitioner or other trained medical staff). It's often done during your regular medical check - up. Even though it can lead to the detection of breast cancer and other breast abnormalities, the American Cancer Society does not recommend clinical breast examination for breast cancer screening especially because it is a subjective process (ACS, 2016). The United States. Preventive Services Task Force feels there's not enough scientific evidence to recommend for or against clinical breast examination (Siu, 2016).

Mammography is an X-ray examination of the breast using tube voltage between 25 kVp and 32 kVp to visualise fine details of breast tissue. It is a non - invasive imaging technique for detecting calcification or soft tissue masses, enabling detection and diagnosis of breast cancer in the early stages of the disease (IAEA, 2005; IPEM, 2005; Masselink, 2005). It is the mainstay of all current breast screening/diagnosis programmes. The ideal mammogram (either for diagnosis or

screening) will detect a cancerous growth or any abnormalities in breast tissue at an early stage, allowing early treatment to produce an improved outcome (Elmore, Miglioretti, & Carney, 2003). Since the early 90's, mammography has been the gold standard for early detection of breast cancer. Its principal purpose is to facilitate the detection of breast cancer at a point earlier than is possible by clinical breast examination or breast self - examination. It has been demonstrated that routine screening with high quality mammography is effective in reducing mortality from breast cancer in women aged 40 – 69 years. Mammography is also useful in refining the diagnosis of breast cancer (assessment or workup) after a suspicious area in the breast has been detected and for localizing a lesion for therapy (WHO, 2002; TABAR, 2003).

In order to achieve diagnosis accurately and at the earliest possible stage, the image from mammography examination must have excellent contrast to reveal mass densities and speculated fibrous structures radiating from them that are characteristic of cancer. In addition, the spatial resolution must be excellent to reveal the calcifications, their number and their shape. The imaging system must have adequate latitude to provide this contrast and resolution over the entire breast effectively. The geometrical characteristics of the mammography unit and the positioning of the breast by the radiographer must be such that as much breast tissue as possible is included in the mammogram. Finally, the noise (signal fluctuation) of the image must be sufficiently low to reveal the subtle structures in a reliable manner and the X-ray dose must be As Low As Reasonably Achievable (ALARA) while being compatible with image quality requirements (IAEA, 2001).

Statement of the Problem

In Ghana, there has not been any comprehensive study aimed at optimizing the radiological protection of patient undergoing mammography examinations through effective quality control (QC). QC in mammography is not receiving the needed attention – it is literally absent. There has not been any thorough work done in the mammography centres across the nation to ascertain whether the doses being received by the patient and the quality of images (mammograms) are within internationally accepted limits and standards. This work will carry out this task.

Objectives of the Study

The primary objective of this work is to assess mammography installations in the country in order to determine their performance status with respect to optimizing procedures and patient radiation protection. There would be comparison of results from the various facilities with international standards to ensure that patients undergoing mammography procedures have the maximum benefit.

The specific objectives are:

a) to undertake a comprehensive radiological quality control assessment on mammography units in the country

b) to quantitatively determine image quality over different equivalent breast thicknesses

c) to determine the mean glandular dose delivery accuracy for the Full Field Digital Mammography (FFDM) systems,

d) to determine the mean glandular dose using the American College of Radiology Mammography Accreditation Phantom (ACR MAP) for the FFDM systems

e) to establish a national quality control baseline data for the diagnostic mammography practice in Ghana

f) to establish Diagnostic Reference Levels (DRLs) based of Polymethyl-methacrylate (PMMA) phantom to help optimize mammography practice in Ghana

g) to design a model to predict the tube voltage, tube current, mean glandular dose (MGD) and image quality which will aid in reducing mammography re-takes.

Relevance and Justification

The risk of radiation – induced breast cancer has long been a concern in the practice of mammography and has driven the efforts to reduce the radiation dose per examination (NIH, 1997). In order to reduce this risk, an efficient and effective mammography quality assurance programme must be established and implemented throughout the country. Radiation has been shown to cause breast cancer in women, and the risk is proportional to dose. The younger the woman at the time of exposure, the greater her lifetime risk for breast cancer (Gordis et al, 1997).

The breast glandular tissue has tissue-weighting Factor of 0.12. This indicates that the breast is one of the most radiosensitive organs in the body and has a high risk of developing cancer from ionizing radiation (Blamey, Wilson, & Patnick, 2000). For this reason optimal equipment performance and dose management per mammogram is essential and cannot be overemphasized.

This research will enable the establishment of quality procedures for obtaining high quality mammograms to improve mammography practices in

Ghana. The research will also provide baseline data on diagnostic mammography practices in Ghana.

In the optimisation of protection in diagnostic radiology particularly in mammography, there is the need for improvement of image quality whiles reducing patient dose. Therefore, to determine how well a patient is protected there is a need for the implementation of a total quality assurance programme with relevant quality control procedures. With the relevant quality assurance programme in place, the carcinogenic risk associated with mammography can be estimated to determine whether the mammography equipment used is contributing to the increase in breast cancer risks or not.

This work seeks to improve diagnostic outcomes in mammography whiles reducing the dose received by patients. It is therefore important to perform an extensive quality control assessment of all mammography installations in the country to determine which equipment are operating within specific requirements and those that have a potential to induce breast cancer in women at a later stage due to low or high exposures as a result of equipment malfunction.

Scope and Limitation

The research is phantom based and will cover thirteen (13) out of nineteen (19) existing centres undertaking diagnostic mammography procedures in the entire country as at December 2015.

Organisation of the Study

The thesis report is presented in Five chapters. Chapter One of this thesis report gives a general overview of the research topic. It offers a brief background,

highlights the objective of the study, the benefit of the study and the scope and limitations of the study. Chapter Two reviews literature pertaining to the study. These include a review of literature on the anatomy of the breast, breast cancer and breast imaging. The chapter highlights the theory of mean glandular dose which is the main parameter used to estimate the amount of radiation deposited in the breast. It also introduces the theory on quantitatively image quality assessment in mammography. Chapter Three introduces the material and methods used in the research work to achieve the objectives set for the study. Chapter Four highlights results and discusses the outcomes of these results. The results are presented in graphs, tables and figures. Conclusions and relevant recommendations are presented in Chapter Five.

Chapter Summary

In summary a brief background information of the study has been given. The problem has been identified and objectives has been clearly setout to achieve the desired goal. Furthermore, it explained the scope and justification for the research and its importance in the health delivery system of Ghana. The chapter concludes with a summary of the organization of the thesis.

CHAPTER TWO

LITERATURE REVIEW

Introduction

Mammography plays an important role in the diagnosis and treatment of a large number of breast diseases. Imaging the breast with mammography easily helps to locate tumour or any sign or symptom of disease within it. This chapter reviews the anatomy of the female breast, breast cancer and its causes, staging of breast cancer and breast cancer treatment. It will also review imaging of the breast which will include mammography, ultrasound and magnetic resonance imaging. The chapter concludes with review of the principle of optimization, theory on image quality, dosimetry and diagnostic reference level (DRL).

The Female Breast

The female breast (Figure 1) is the tissue overlying the chest (pectoral) muscles (Web MD, 2015). They are made of specialized tissue that produces milk (glandular tissue) as well as fatty tissue. The amount of fat determines the size of the breast. The milk-producing part of the breast is organized into 15 to 20 sections, called lobes. Within each lobe are smaller structures, called lobules, where milk is produced. The milk travels through a network of tiny tubes called ducts. The ducts connect and come together into larger ducts, which eventually exit the skin in the nipple. The dark area of skin surrounding the nipple is called the areola. Connective tissue and ligaments provide support to the breast and give it its shape. Nerves provide sensation to the breast. The breast also contains blood vessels, lymph vessels, and lymph nodes (Web MD, 2015). The female Breast is also an external

symbol of beauty and womanhood (Nsiah-Akoto, Andam, Adisson, & Forson, 2011).

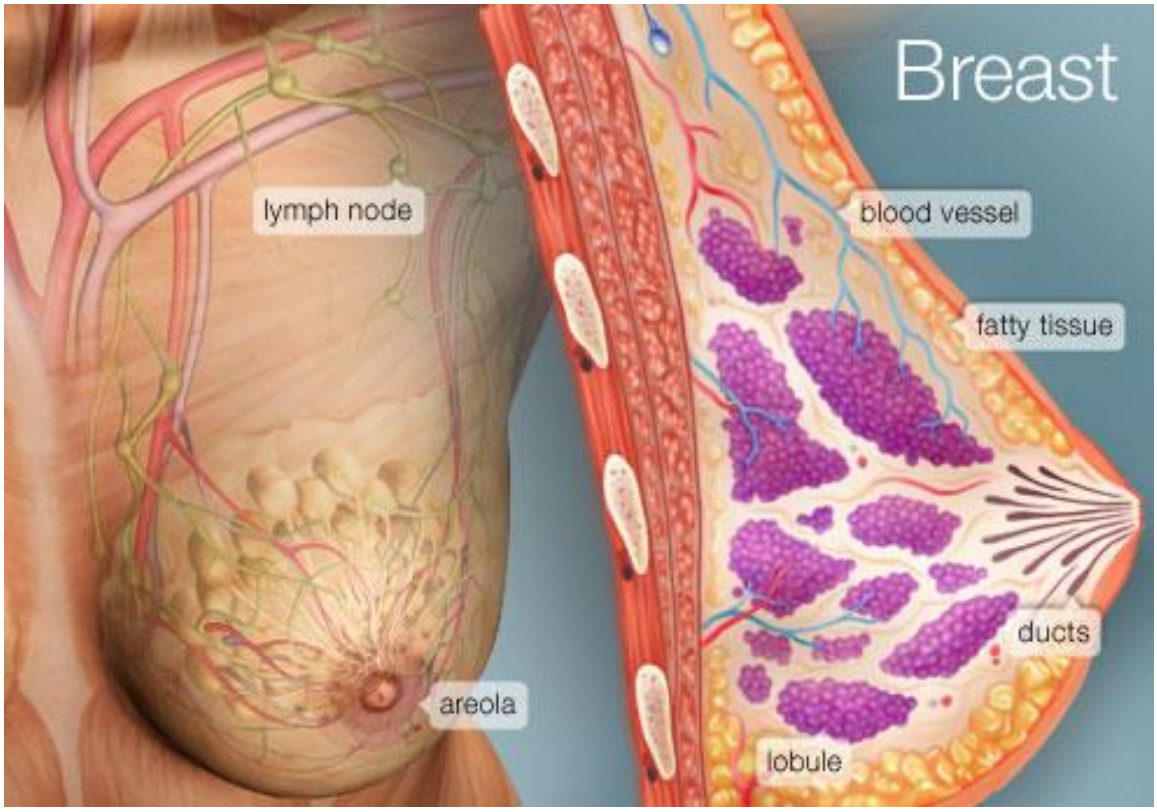

Figure 1: Anatomy of the female breast
(Web MD, 2015)

Breast Cancer

Breast cancer is a malignant tumour that starts in the cells of the breast. Most breast cancers begin in the cells that line the ducts (ductal cancers). Some begin in the cells that line the lobules (lobular cancers), while a small number start in other tissues (ACS, 2014).

It is the second most common cancer in the world and, by far, the most frequent cancer among women with an estimated 1.67 million new cancer cases diagnosed in 2012 (25% of all cancers). It is the most common cancer in women

both in more and less developed regions with slightly more cases in less developed (883,000 cases) than in more developed (794,000) regions. Incidence rates vary nearly four-fold across the world regions, with rates ranging from 27 per 100,000 in Middle Africa and Eastern Asia to 96 in Western Europe. Breast cancer ranks as the fifth cause of death from cancer overall (522,000 deaths) and while it is the most frequent cause of cancer death in women in less developed regions (324,000 deaths, 14.3% of total), it is now the second cause of cancer death in more developed regions (198,000 deaths, 15.4%) after lung cancer. The range in mortality rates between world regions is less than that for incidence because of the more favourable survival of breast cancer in (high-incidence) developed regions, with rates ranging from 6 per 100,000 in Eastern Asia to 20 per 100,000 in Western Africa (GLOBOCAN, 2012).

Global incidence and mortality of breast cancer is on the rise, and Ghana is no exception. It was reported that 2,000 Ghanaian women were diagnosed with the disease in 2012. The report indicated that, 1,000 of the figure, representing 50 per cent of the cases died and so there was an increasing danger of complications for women in Ghana and the whole of Africa. Breast cancer has been identified as the second leading cause of cancer deaths in Ghana, with about 2,900 cases being diagnosed annually and at least one of eight women with the disease dying (GNA, 2015). In Ghana also, data available from The National Centre for Radiotherapy and Nuclear Medicine shows an increase in breast cancer treatment and management even though there seems to be increased awareness on the disease (Sackey & Yarney, 2009).

Imaging of the breast with ionizing radiation like many other organs in the human body requires highly trained personnel as well as an efficient and reliable equipment. Without which accurate diagnosis may not be achieved and treatment outcomes of little impact to the life of the patient. Hence in order to achieve optimal results from breast imaging and to reduce the risk of inducing cancer, the dose administered to the patient as part of the imaging process should be of great concern to all because risk to cancer is approximately proportional to dose (Mole , 1978). The "state" of the imaging equipment is of great importance. Low or high (excess) dose to the patient apart from human factors can also be a result of equipment malfunction. Any risk of inducing breast cancer by mammography must definitely be smaller than the expected benefits (Berrington de Gonzalez & Reeves , 2005; Land, 1979) . A recent survey in Ghana, shows that quite a large number of women younger than 50 years undergo mammography for different purposes (Boadu, Sosu, Hasford, Nani, Sackey, Schandorf & Addison, 2012). This should be of great concern since about half of the radiation – induced breast cancer deaths were estimated to occur after age 50 years (Hall & Giaccia, 2012).

Causes of Breast Cancer

Researchers have so far shown no single cause of breast cancer but some factors appear to increase the risk of developing the disease.

Many of the most important risk factors are beyond an individual's control and they include:

Gender

Simply being a woman is the main risk factor for developing breast cancer.

Although women have many more breast cells than men, the main reason they develop more breast cancer is because their breast cells are constantly exposed to the growth-promoting effects of the female hormones estrogen and progesterone. Men can develop breast cancer, but this disease is about 100 times more common among women than men (ACS, 2014).

Aging

Risk of developing breast cancer increases as you get older. About 1 out of 8 invasive breast cancers are found in women younger than 45, while about 2 out of 3 invasive breast cancers are found in women aged 55 or older (ACS, 2014).

Genetic risk factors

About 5% to 10% of breast cancer cases are thought to be hereditary, resulting directly from gene defects (called mutations) inherited from a parent. The most common cause of hereditary breast cancer is an inherited mutation in the *BRCA1* and *BRCA2* genes. In normal cells, these genes help prevent cancer by making proteins that keep the cells from growing abnormally. If you have inherited a mutated copy of either gene from a parent, you have a high risk of developing breast cancer during your lifetime. Although in some families with *BRCA1* mutations the lifetime risk of breast cancer is as high as 80%, on average this risk seems to be in the range of 55 to 65%. For *BRCA2* mutations the risk is lower, around 45%. Breast cancers linked to these mutations occur more often in younger women and more often affect both breasts than cancers not linked to these mutations. Women with these inherited mutations also have an increased risk for developing other cancers, particularly ovarian cancer. In the United States *BRCA*

mutations are more common in Jewish people of Ashkenazi (Eastern Europe) origin than in other racial and ethnic groups, but they can occur in anyone (ACS, 2015; USPSTF, 2009).

Family history of breast cancer

Breast cancer risk is higher among women whose close blood relatives have this disease. Having one first-degree relative (mother, sister, or daughter) with breast cancer approximately doubles a woman's risk. Having two (2) first-degree relatives increases her risk about 3-fold. The exact risk is not known, but women with a family history of breast cancer in a father or brother also have an increased risk of breast cancer. Altogether, less than 15% of women with breast cancer have a family member with this disease. This means that most (over 85%) women who get breast cancer do not have a family history of this disease (ACS, 2014).

Race and ethnicity

White women are slightly more likely to develop breast cancer than are African-American women. African-American women are more likely to die of this cancer. At least part of this seems to be because African-American women tend to have more aggressive tumours, although why this is the case is not known. Asian, Hispanic, and Native-American women have a lower risk of developing and dying from breast cancer (ACS, 2014; USPSTF, 2009).

Dense Breast Tissue

Breasts are made up of fatty tissue, fibrous tissue, and glandular tissue. Women with denser breast tissue (as seen on a mammogram) have more glandular tissue and less fatty tissue, and have a higher risk of breast cancer. Women with

dense breasts on mammogram have a risk of breast cancer that is 1.2 to 2 times that of women with average breast density. Dense breast tissue can also make mammograms less accurate. A number of factors can affect breast density, such as age, menopausal status, certain medications (including menopausal hormone therapy), pregnancy, and genetics. Unfortunately, dense breast tissue can also make it harder for doctors to spot problems on mammograms (ACS, 2014).

Certain benign breast conditions

Women diagnosed with certain benign breast conditions may have an increased risk of breast cancer. Some of these conditions are more closely linked to breast cancer risk than others (ACS, 2014).

Lobular carcinoma in situ

In lobular carcinoma in situ (LCIS), Figure 2, cells that look like cancer cells are growing in the lobules of the milk-producing glands of the breast, but they do not grow through the wall of the lobules. LCIS (also called *lobular neoplasia)* is sometimes grouped with ductal carcinoma in situ (DCIS) as a non-invasive breast cancer, but it differs from DCIS in that it doesn't seem to become an invasive cancer if it isn't treated (AJCC, 2012).

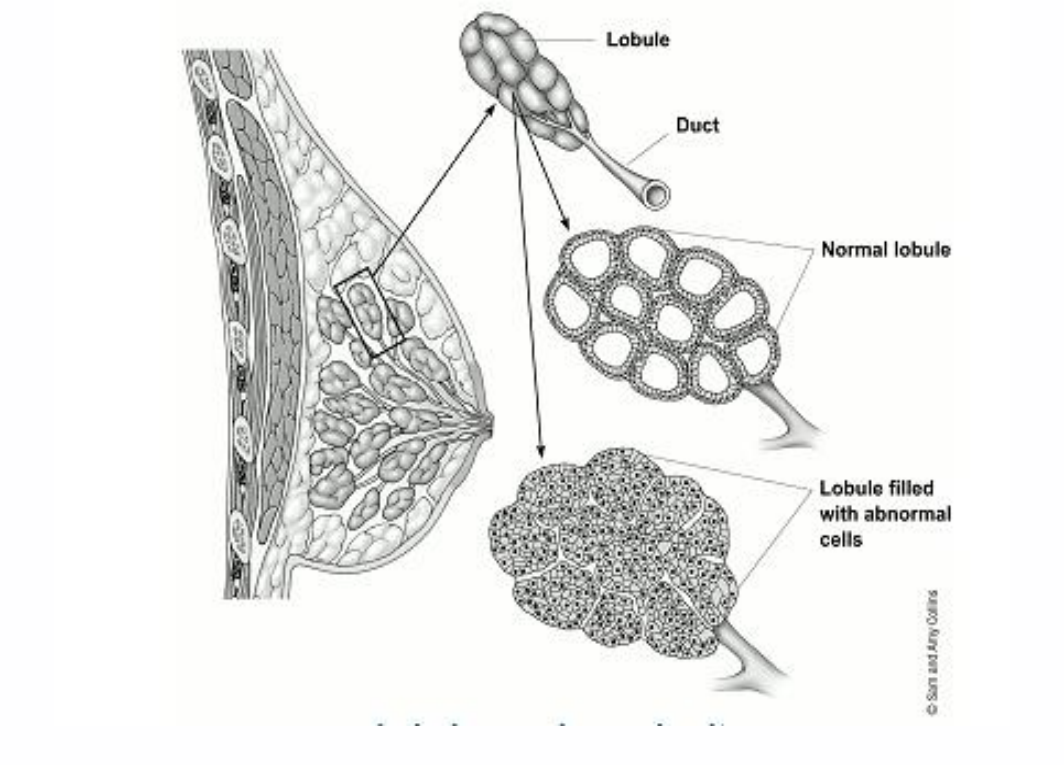

Figure 2: Lobular carcinoma in situ

(AJCC, 2012)

Women with lobular carcinoma in situ (LCIS) have a 7- to 11-fold increased risk of developing cancer in either breast (AJCC, 12).

Menstrual periods

Women who have had more menstrual cycles because they started menstruating at an early age (before age 12) and/or went through menopause at a later age (after age 55) have a slightly higher risk of breast cancer. This may be related to a higher lifetime exposure to the hormones estrogen and progesterone (ACS, 2014).

Previous chest radiation

Women who, as children or young adults, had radiation therapy to the chest area as treatment for another cancer (such as Hodgkin disease or non-Hodgkin lymphoma) are at significantly increased risk for breast cancer. This varies with the patient's age when they had radiation. The risk of developing breast cancer from chest radiation is highest if the radiation was given during adolescence, when the breasts were still developing. Radiation treatment after age 40 does not seem to increase breast cancer risk (ACS, 2014; Michigan Medicine, 2015; MCHG, 2012).

Diethylstilbestrol exposure

From the 1940s through the 1960s some pregnant women were given the drug diethylstilbestrol (DES) because it was thought to lower their chances of miscarriage (losing the baby). These women have a slightly increased risk of developing breast cancer. Women whose mothers took DES during pregnancy may also have a slightly higher risk of breast cancer (ACS, 2014; Michigan Medicine, 2015; MCHG, 2012).

However some risk factors are lifestyle related and they include:

Having children

Women who have had no children or who had their first child after age 30 have a slightly higher breast cancer risk. Having many pregnancies and becoming pregnant at a young age reduce breast cancer risk. Pregnancy reduces a woman's total number of lifetime menstrual cycles, which may be the reason for this effect (ACS, 2014; Michigan Medicine, 2015; MCHG, 2012).

Recent oral contraceptive use

Studies have found that women using oral contraceptives (birth control pills) have a slightly greater risk of breast cancer than women who have never used them. This risk seems to decline back to normal over time once the pills are stopped (ACS, 2014; Michigan Medicine, 2015; MCHG, 2012).

Hormone therapy after menopause

The increased risk from combined hormone therapy appears to apply only to current and recent users. A woman's breast cancer risk seems to return to that of the general population within 5 years of stopping combined treatment. Studies have shown that using combined hormone therapy after menopause increases the risk of getting breast cancer. It may also increase the chances of dying from breast cancer (ACS, 2014; Michigan Medicine, 2015; MCHG, 2012).

Breast-feeding

Some studies suggest that breast-feeding may slightly lower breast cancer risk, especially if breast-feeding is continued for 1½ to 2 years. One explanation for this possible effect may be that breastfeeding reduces a woman's total number of lifetime menstrual cycles (similar to starting menstrual periods at a later age or going through early menopause) (ACS, 2014; Michigan Medicine, 2015; MCHG, 2012).

Alcohol

The use of alcohol is clearly linked to an increased risk of developing breast cancer. The risk increases with the amount of alcohol consumed. Compared with non-drinkers, women who consume 1 alcoholic drink a day have a very small

increase in risk. Those who have 2 to 5 drinks daily have about 1½ times the risk of women who don't drink alcohol. Excessive alcohol consumption is also known to increase the risk of developing several other types of cancer (ACS, 2014; Michigan Medicine, 2015; MCHG, 2012).

Being overweight or obese

Being overweight or obese after menopause increases breast cancer risk. Before menopause your ovaries produce most of your estrogen, and fat tissue produces a small amount of estrogen. After menopause (when the ovaries stop making estrogen), most of a woman's estrogen comes from fat tissue. Having more fat tissue after menopause can increase your chance of getting breast cancer by raising estrogen levels. Also, women who are overweight tend to have higher blood insulin levels. Higher insulin levels have also been linked to some cancers, including breast cancer. But the connection between weight and breast cancer risk is complex. For example, the risk appears to be increased for women who gained weight as an adult but may not be increased among those who have been overweight since childhood. Also, excess fat in the waist area may affect risk more than the same amount of fat in the hips and thighs. Researchers believe that fat cells in various parts of the body have subtle differences that may explain this (ACS, 2014; Michigan Medicine, 2015; MCHG, 2012).

Physical activity

Evidence is growing that physical activity in the form of exercise reduces breast cancer risk. The main question is how much exercise is needed. In one study from the Women's Health Initiative, as little as 1.25 to 2.5 hours per week of brisk

walking reduced a woman's risk by 18%. Walking 10 hours a week reduced the risk a little more (ACS, 2014; Michigan Medicine, 2015; MCHG, 2012).

Breast Cancer Staging

The most important function of staging is to anatomically group patients to determine the treatment algorithm and prognosis. Accurate staging carries substantial importance to compare the treatment results among the studies (AJCC, 2012). The classification system (tumour node metastasis [TNM]) is based on the dissemination of cancer according to the features of the primary tumour (localization, size, and extension to the surrounding structures), regional lymph nodes, and the presence of metastases.

Currently, the TNM system which was formulated by Union International Cancer Centre (UICC) and the American Joint Committee on Cancer (AJCC) is being used worldwide (Ozsaran & Alanyali, 2013).

Breast cancer is staged according to the location of the primary tumour, metastases, clinical or pathological evidence. A description of details of the various types of staging of breast cancer is presented in Table 1 to Table 4 respectively. Figures 3 and 4 present image of cancer staging by primary tumour and pathology respectively.

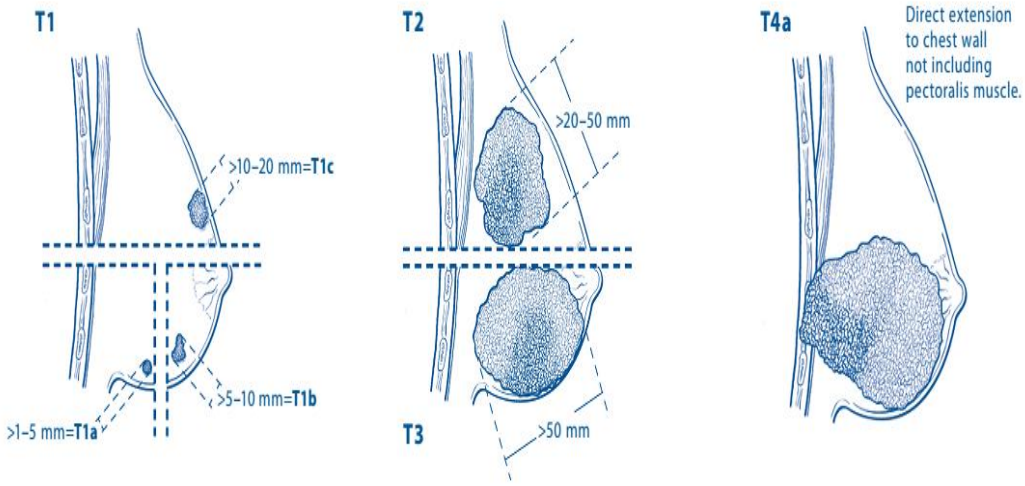

Figure 3: Cancer staging by Primary Tumour (T)

(AJCC, 2012)

Table 1: American Joint Committee on Cancer's staging of breast Cancer based to Primary Tumour (T)

SYMBOL	MEANING
TX	Primary tumour cannot be assessed
T0	No evidence of primary tumour
Tis	Carcinoma in situ
Tis (DCIS)	Ductal carcinoma in situ
Tis (LCIS)	Lobular carcinoma in situ
Tis (Paget's)	Paget's disease of the nipple NOT associated with invasive carcinoma and/or carcinoma in situ (DCIS and/or LCIS) in the underlying breast parenchyma. Carcinomas in the breast parenchyma associated with Paget's disease are categorized based on the size and characteristics of the parenchymal disease, although the presence of Paget's disease should still be noted
T1	Tumour ≤ 20 mm in greatest dimension
T1mi	Tumour ≤ 1 mm in greatest dimension
T1a	Tumour > 1 mm but ≤ 5 mm in greatest dimension
T1b	Tumour > 5 mm but ≤ 10 mm in greatest dimension
T1c	Tumour > 10 mm but ≤ 20 mm in greatest dimension
T2	Tumour > 20 mm but ≤ 50 mm in greatest dimension
T3	Tumour > 50 mm in greatest dimension
T4	Tumour of any size with direct extension to the chest wall and/or to the skin (ulceration or skin nodules)
T4a	Extension to the chest wall, not including only pectoralis muscle adherence/invasion
T4b	Ulceration and/or ipsilateral satellite nodules and/or edema (including peau d'orange) of the skin, which do not meet the criteria for inflammatory carcinoma
T4c	Both T4a and T4b
T4d	Inflammatory carcinoma

Table 1: American Joint Committee on Cancer's tumor node Metastasis (M) staging of breast cancer based on distant metastases

SYMBOL	MEANING
M0	No clinical or radiographic evidence of distant metastases
cM0(i+)	No clinical or radiographic evidence of distant metastases, but deposits of molecularly or microscopically detected tumor cells in circulating blood, bone marrow, or other nonregional nodal tissue that are no larger than 0.2 mm in a patient without symptoms or signs of metastases
M1	Distant detectable metastases as determined by classic clinical and radiographic means and/or histologically proven larger than 0.2 mm

Staging of breast cancer can also be on clinical or pathological bases.

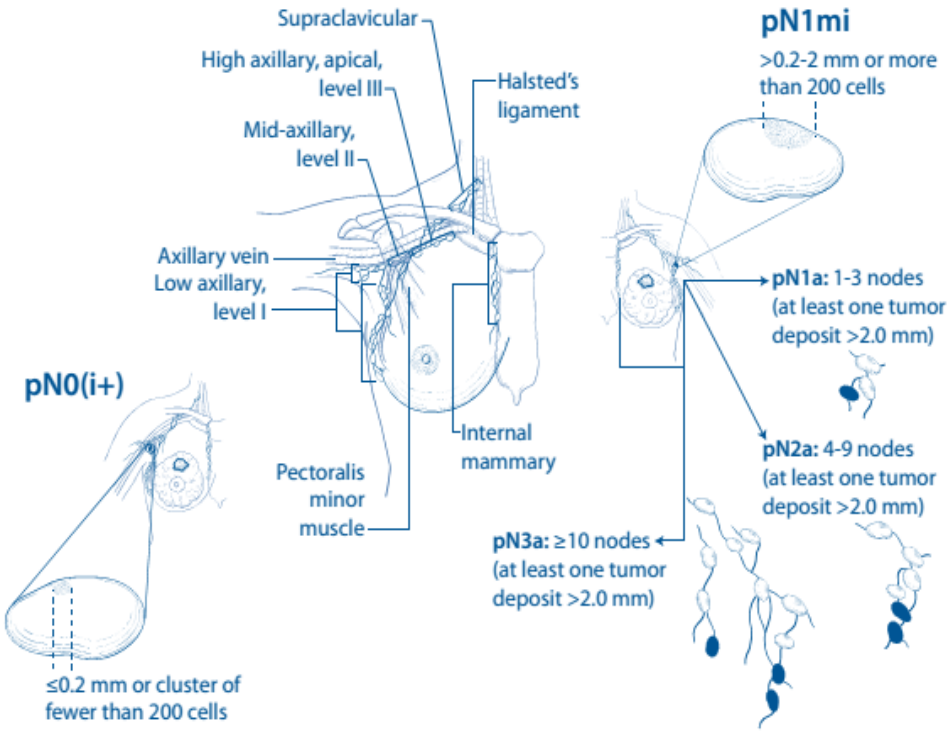

Figure 4: Cancer staging by Pathology (AJCC, 2012)

Table 2: American Joint Committee on Cancer's tumour node staging of breast cancer based on regional lymph nodes (clinical)

SYMBOL	MEANING
NX	Regional lymph nodes cannot be assessed (for example, previously removed)
N0	No regional lymph node metastases
N1	Metastases to movable ipsilateral level I, II axillary lymph node(s)
N2	Metastases in ipsilateral level I, II axillary lymph nodes that are clinically fixed or matted; or in clinically detected ipsilateral internal mammary nodes in the absence of clinically evident axillary lymph node metastases
N2a	Metastases in ipsilateral level I, II axillary lymph nodes fixed to one another (matted) or to other structures
N2b	Metastases only in clinically detected ipsilateral internal mammary nodes and in the absence of clinically evident level I, II axillary lymph node metastases
N3	Metastases in ipsilateral infra-clavicular (level III axillary) lymph node(s) with or without level I, II axillary lymph node involvement; or in clinically detected ipsilateral internal mammary lymph node(s) with clinically evident level I, II axillary lymph node metastases; or metastases in ipsilateral supraclavicular lymph node(s) with or without axillary or internal mammary lymph node involvement
N3a	Metastases in ipsilateral infra-clavicular lymph node(s)
N3b	Metastases in ipsilateral internal mammary lymph node(s) and axillary lymph node(s)
N3c	Metastases in ipsilateral supraclavicular lymph node(s)

Table 3: American Joint Committee on Cancer's tumour node staging of breast Cancer based on regional lymph nodes (Pathology)

SYMBOL	MEANING
pNX	Regional lymph nodes cannot be assessed (for example, previously removed, or not removed for pathologic study)
pN0	No regional lymph node metastasis identified histologically Note: Isolated tumor cell clusters (ITC) are defined as small clusters of cells not greater than 0.2 mm, or single tumor cells, or a cluster of fewer than 200 cells in a single histologic cross-section. ITCs may be detected by routine histology or by immune-histochemical (IHC) methods. Nodes containing only ITCs are excluded from the total positive node count for purposes of N classification but should be included in the total number of nodes evaluated.
pN0(i−)	No regional lymph node metastases histologically, negative IHC
pN0(i+)	Malignant cells in regional lymph node(s) no greater than 0.2 mm
pN0(mol−)	No regional lymph node metastases histologically, negative molecular findings (RT-PCR)
pN0(mol+)	Positive molecular findings (RT-PCR), but no regional lymph node metastases detected by histology or IHC
pN1	Micrometastases; or metastases in 1–3 axillary lymph nodes; and/or in internal mammary nodes with metastases detected by sentinel lymph node biopsy but not clinically detected
pN1mi	Micrometastases (greater than 0.2 mm and/or more than 200 cells, but none greater than 2.0 mm)
pN1a	Metastases in 1–3 axillary lymph nodes, at least one metastasis greater than 2.0 mm
pN1b	Metastases in internal mammary nodes with micrometastases or macrometastases detected by sentinel lymph node biopsy but not clinically detected
pN1c	Metastases in 1–3 axillary lymph nodes and in internal mammary lymph nodes with micrometastases or macrometastases detected by sentinel lymph node biopsy but not clinically detected
pN2	Metastases in 4–9 axillary lymph nodes; or in clinically detected internal mammary lymph nodes in the absence of axillary lymph node metastases

Table 4 continued

SYMBOL	MEANING
pN2a	Metastases in 4–9 axillary lymph nodes (at least one tumour deposit greater than 2.0mm)
pN2b	Metastases in clinically detected internal mammary lymph nodes in the absence of axillary lymph node metastases
pN3	Metastases in 10 or more axillary lymph nodes; or in infraclavicular (level III axillary) lymph nodes; or in clinically detected ipsilateral internal mammary lymph nodes in the presence of one or more positive level I, II axillary lymph nodes; or in more than three axillary lymph nodes and in internal mammary lymph nodes with micrometastases or macrometastases detected by sentinel lymph node biopsy but not clinically detected; or in ipsilateral supraclavicular lymph nodes
pN3a	Metastases in 10 or more axillary lymph nodes (at least one tumor deposit greater than 2.0 mm); or metastases to the infraclavicular (level III axillary lymph) nodes
pN3b	Metastases in clinically detected ipsilateral internal mammary lymph nodes in the presence of one or more positive axillary lymph nodes; or in more than three axillary lymph nodes and in internal mammary lymph nodes with micrometastases or macrometastases detected by sentinel lymph node biopsy but not clinically detected
pN3c	Metastases in ipsilateral supraclavicular lymph nodes

(Haffty , Buchholz, & Perez, 2008)

Breast Imaging

Breast cancer is sometimes found after symptoms appear, but many women with early breast cancer have no symptoms. Imaging tests using X-rays, magnetic fields, sound waves, or radioactive substances to create pictures of the inside of the body may be used to evaluate breast disease. It helps to find out whether a suspicious area might be cancerous, to learn how far cancer may have spread, and to help determine if treatment is working. Mammography, ultrasound and magnetic resonance imaging are usually used to image the breast (ACS, 2014).

Mammography

Mammography is the process of using low - energy ionizing radiation to examine the human breast. It is used as a diagnostic or a screening tool. The goal of mammography is the early detection of breast cancer, typically through detection of characteristic masses and/or micro calcifications (WIKIPEDIA, 2015). During mammography, the breast is compressed using a dedicated X-ray unit. Parallel-plate compression evens out the thickness of breast tissue to increase image quality by reducing the thickness of tissue that X-rays must penetrate, decreasing the amount of scattered radiation (scatter degrades image quality), reducing the required radiation dose, and holding the breast still (preventing motion blur).

There are two types of mammogram studies: screening mammograms and diagnostic mammograms. Screening mammograms are performed on a patient who presents with no symptoms and consists of only four standard X-ray images. For the average woman, the U.S. Preventive Services Task Force recommends (2009) mammography every two years in women between the ages of 50 and 74 (USPSTF, 2009).

The American College of Radiology (ACR) and American Cancer Society (ACS) recommend yearly screening mammography starting at age 40 (ACS, 2015). The Canadian Task Force on Preventive Health Care (2012) and the European Cancer Observatory (2011) recommend mammography every 2-3 years between 50 and 69 (CMAJ, 2011; EUCAN, 2015). In screening mammography, both head-to-foot (craniocaudal, CC) view and angled side-view (mediolateral oblique, MLO) images of the breast are taken (IMAGINIS, 2015). Mammography screening

reduces breast cancer mortality by 15% for women age 39–69 years (Nelson et al., 2009).

Diagnostic mammograms are reserved for patients with breast symptoms, changes, or abnormal findings seen on their screening mammogram. Diagnostic mammograms are also performed on patients with breast implants, breast reductions, and patients with personal and/or family history of breast cancer. Mammography was typically performed with screen-film cassettes. Diagnostic mammography may include both CC and MLO (Figure 5) and/or other views, including geometrically magnified and spot-compressed (magnification mammography) views of the particular area of concern (IMAGINIS, 2015).

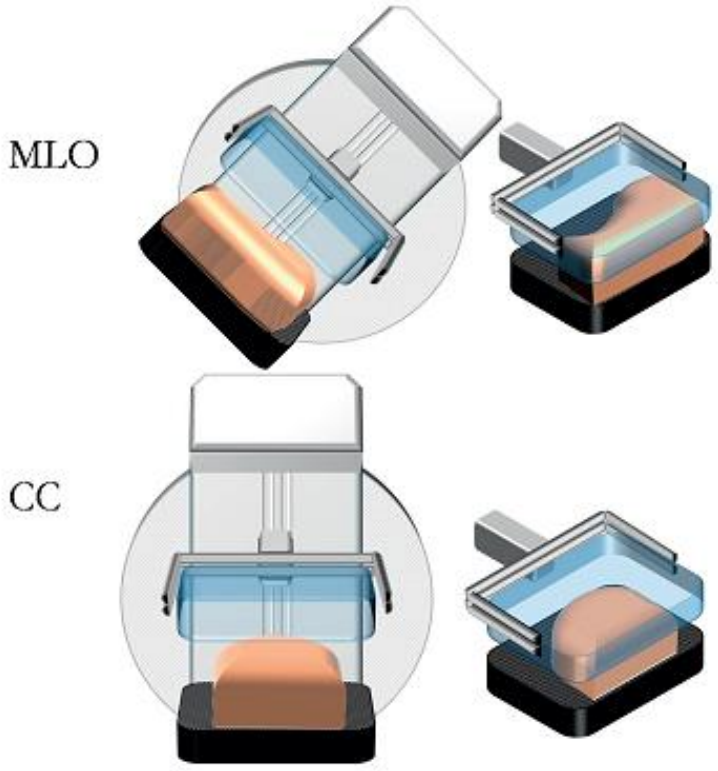

Figure 5: Illustration of mammography projection views CC & MLO (IAEA, 2014)

Screen Film mammography

Screen-film/Conventional mammography was invented in 1969 (Haus, 2001). The formation of the X-ray image on the film process includes the X-ray beam emerging from the patient being converted into a pattern of visible light by the cassette's intensifying screen, and the visible image is then captured permanently on the film. Upon chemical development of the film with a Processor, the emulsion that contains the latent X-ray image is converted into specks of metallic silver. The screen and film are arranged such that the X-rays pass through the cover of the cassette and the film to impinge upon the screen. Absorption is exponential, so that a larger fraction of the X-rays are absorbed and converted to light near the entrance surface of the screen. The screens are often constructed with rare earth phosphors such as gadolinium oxysulfide (Gd_2O_2S). Films have significant disadvantages and limitations which include the lack of ability to detect small differences in contrast, the poorly exposed nature of images due to the film's stringent requirements for proper exposure which leads to repeated exposures, reduced visibility of microcalcifications, increase in the examination time due to the chemical processing of film, films require large storage space in patient health records, and films must be transported physically to the physician for viewing (Haus, 2001; Säbel, 1996; Yaffe et al., 2009)

Digital mammography

Digital mammography was introduced in early 2000 (Haus, 2001). In digital mammography X-rays are used to produce images of the breast, but unlike the screen-film system, there are specially designed digital detectors that converts the X-rays to digital images and they are stored directly in a computer. In digital

mammography, image acquisition, processing, display and storage are performed independently, allowing optimization of each. There are currently two types of digital mammography systems: computed radiography (CR) which uses indirect digital detectors, and digital radiography (DR) which uses direct digital detectors. With a CR system, the X-rays transmitted through the breast are absorbed by the CR imaging plate, a Photostimulable storage phosphor (PSP) plate. Absorbed X-ray energy corresponding to anatomical variations in the breast produces an electronic latent image on the PSP. The cassette is then removed from the mammography system and placed in a CR reader with a scanning laser beam that stimulates the release of light corresponding to the incident X-ray intensity. The light information is captured, converted to a digital signal, and displayed at the workstation. However, with the DR system, the X-ray signal is directly converted to a digital signal at the acquisition stand. No cassette is used. The image is displayed at the workstation shortly after it is acquired (Lanca & Silva, 2013). Digital mammography systems offer a number of practical advantages and patient conveniences over conventional systems. Digital images are immediately available, therefore there is no waiting time, quality of the images can be evaluated as they are being taken, digital systems are fast, so patients spend less time in uncomfortable positions, also, contrast of images can be adjusted and sections of an image can be magnified after the mammogram is complete making it easier to see subtle differences between tissues. Digital images can easily be stored and retrieved and their transmission from one physician to another is quick and easy,

multiple copies can easily be printed with the digital system (Chevalier, Leyton, Tavares, Oliveira, Silva & Peixoto 2012).

Components of a mammography X-ray equipment

The mammography unit consists of an X-ray tube and an image receptor mounted on opposite sides of a mechanical assembly. Because the breast must be imaged from different aspects, the assembly can be rotated about a horizontal axis, as shown in Figure 6. Unlike most general radiography equipment, which is designed such that the image field is centred below the X-ray source, in mammography, the system's geometry is arranged as in Figure 7(a). Here, a vertical line from the focal spot of the X-ray source grazes the chest wall of the patient and intersects orthogonally with the edge of the image receptor closest to the patient. If the X-ray beam were centred over the breast as in Figure 7(b), some of the tissue near the chest wall would not be imaged. Radiation leaving the X-ray tube passes through a metallic spectral shaping filter, a beam defining aperture and a plastic plate, which compresses the breast on to the breast support platform. Those X-ray transmitted through the breast and breast support are incident on a specially designed anti-scatter grid, and then are incident on the image receptor, where they interact and deposit most of their energy locally. Other components of the equipment are the compression plate and breast support.

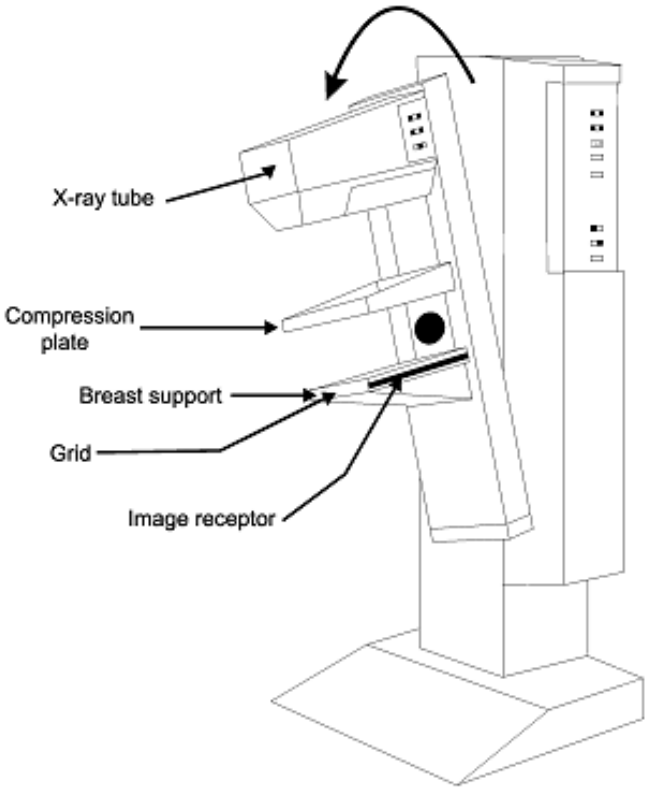

Figure 6: Schematic of a mammography imaging system

(IAEA, 2014)

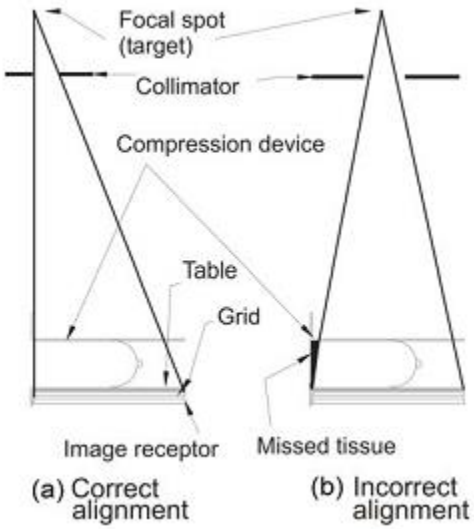

Figure 7: System geometry for image acquisition showing (a) correct alignment and (b) missed tissue associated with incorrect alignment
(IAEA, 2014)

X-ray Tube

In mammography, the X-ray tube is usually operated at a kilovoltage of 25 to 32 kVp with molybdenum and rhodium as target materials in the anode. Both molybdenum and rhodium are used as target materials in the anode because they produce characteristic X-ray radiation at optimal energy levels. (Bick & Diekmann, 2010). In mammography, the X-ray tube is arranged such that the cathode side of the tube is adjacent to the patient's chest wall (anode heel effect), this is because the highest intensity of X-rays is available at the cathode side and the attenuation of X-rays by the patient is generally greater near the chest wall (Dance, Christofides, Maidment, McLean & Ng, 2014).

Compression Plate

Compression (which has to be firm) causes the various breast tissues to be spread out, minimizing superposition from different planes and thereby improving the conspicuity of structures. This effect may be accentuated by the fact that different tissues (fatty, fibroglandular and cancerous) have different elasticities, resulting in the various tissues being spread out by different amounts and potentially making a cancer easier to see. Compression decreases the ratio of scattered to directly transmitted radiation reaching the image receptor. It also decreases the distance from any plane within the breast to the image receptor, and in this way reduces geometric unsharpness. The compressed breast provides lower overall attenuation to the incident X-ray beam, allowing the radiation dose to be reduced. The compressed breast also provides more uniform attenuation over the image which reduces the exposure range that must be recorded by the imaging system. It also provides a clamping action, which reduces anatomical motion during

the exposure, thereby reducing this source of image unsharpness. It is important that the breast be compressed as uniformly as possible and that the edge of the compression plate at the chest wall be straight and aligned with both the focal spot and image receptor to maximize the amount of breast tissue that is included in the image. The mechanical properties of the breast are non-linear; after a certain reduction in thickness, application of additional pressure provides little benefit in terms of improved image quality (Saunders & Samei, 2008). An important disadvantage of compression is the pain and discomfort that women experience during and after the examination (Broeders, Veldkamp, Engen, Landsveld – Verhoeven, Jong – Gunneman, Win, Kitty, Greve, Paap & Heeten, 2015).

Filters

Filters are placed in the path of the X-ray beam in order to absorb those X-rays with energies above and below the desired spectrum. Filters lower the amount of radiation dose the patient receives. Filters shortens the exposure time giving the patient only the radiation doses needed to obtain a good quality radiography. Filters ensure that less scatter radiations are produced and the X-ray beam is able to penetrate the breast leading to good quality images (Barnes & Ho, 2016)

Grids

Scattered radiation reduces contrast in mammography images. Reducing the effects of scattered radiation has been achieved through the use of scatter absorbing grids. In the absence of this anti-scatter device, 37–50% of the total radiation incident on the image receptor would have experienced a scattering interaction within the breast. According to ACR (1999), the scatter-to-primary ratio (SPR) will

range from 0.3 to 1.2, depending upon the breast size. In addition to contrast reduction, the recording of scattered radiation reduces the useful dynamic range of the image receptor and adds stochastic noise to the image. When a grid is used, the SPR is typically reduced by a factor of about 5, leading in most cases to a substantial improvement in image contrast (Dance et al., 2014).

Automatic Exposure Control (AEC)

AEC, also known as phototiming, is designed to automatically provide the radiation exposure needed to produce a mammogram with an acceptable and consistent optical density (Huda, Sajewicz, Ogden, and Dance, 2003). For screen film (SF) mammography and for cassette based digital systems, the AEC radiation sensor(s) is/are located behind the image receptor to avoid casting a shadow on the image. The sensors measure the X-ray fluence transmitted through both the breast and the image receptor and provide a signal to discontinue the exposure when a preset amount of radiation has been received by the image receptor. The location of the sensor is adjustable so that it can be placed behind the appropriate region of the breast to obtain proper exposure. With DR equipment, AEC is generally microprocessor based, so that relatively sophisticated corrections can be made during the exposure to achieve the same effect as in the SF system (Yaffe, 2006).

Magnification

Magnification mammography is often used intentionally to improve the diagnostic quality of the image. This is accomplished by elevating the breast above the image receptor, in effect reducing the focus to object distance and increasing the distance from the object to the image receptor. Magnification mammography

ensures increased SNR, improved spatial resolution and dose efficient scatter rejection. Magnification causes structures to appear larger when projected on to the image receptor, thereby increasing the effective modulation transfer function (MTF) of the receptor with respect to structures within the breast. In screen film mammography, the limiting resolution of the image receptor is already quite high and is rarely a limiting factor. The increase in focal spot unsharpness that occurs as a result of magnification, even with a small focal spot, typically offsets any improvement in the MTF of the image receptor. The main benefit of magnification is to increase the size of the projected anatomical structures compared with the granularity of the image, thereby improving the SNR in the image. This improvement can be valuable, particularly for the visualization of fine calcifications and spiculations. In digital mammography, where the film grain noise has been eliminated, but where the limiting spatial resolution of the detector is lower than that provided by the screen film image receptor, the benefits of magnification may be different in nature. In this case, the increase in projected size of anatomical features does improve the effective resolution of the detector, which in some cases is a limiting factor. However, by moving the breast closer to the X-ray source in magnification mammography, the dose to breast tissue increases compared with that in contact mammography (IAEA, 2014).

Source-to-image distance

This is the entire distance of the X-ray beam from the focal spot (source) to the image receptor, the greater the distance, the lesser the occurrence of geometric blurring. This affects the focal spot size, which in turn affects the size of the object being imaged. The larger the SID the larger the field size. With a larger source to image distance “65cm”, more beam penetrability is required, which in turn increases the heel effect (Yaffe, Barnes, Conway, Haus, Karellas, Kimme-Smith, Lin, Mawdsley, Rauch, Rothenberg, 1990).

Breast support/bucky

It is the platform which supports the breast during compression. For screen film (SF) mammography and for cassette based digital systems it serves as a cassette holder.

Magnetic Resonance Imaging

Magnetic resonance imaging (MRI) is a diagnostic examination that uses a combination of a large magnet, radio waves and a computer to produce detailed images of organs and structures within the body. The magnetic field, along with radio waves, alters the hydrogen atoms' natural alignment in the body. Computers are then used to form a two-dimensional (2D) image of a body structure or organ based on the activity of the hydrogen atoms. Cross-sectional views can be obtained to reveal further details. MRI does not use radiation.

During the proceedure, a magnetic field is created and pulses of radio waves are sent from a scanner. The radio waves knock the nuclei of the atoms in your body out of their normal position. As the nuclei realign into proper position, they

send out radio signals. These signals are received by a computer that analyzes and converts them into an image of the part of the body being examined. This image appears on a viewing monitor. For a breast MRI, the woman usually lies face down, with her breasts positioned through openings in the table.

A breast MRI usually requires the use of contrast that is injected into a vein in the arm before or during the procedure. The dye helps create clearer images that outline abnormalities more easily.

MRI, used with mammography and breast ultrasound, can be a useful diagnostic tool. Recent research has found that MRI can locate some small breast lesions sometimes missed by mammography. It can also help detect breast cancer in women with breast implants and in younger women who tend to have dense breast tissue in which mammography may not be as effective. Since MRIs do not use radiation, they may be used to screen women younger than 40 and to increase the number of screenings per year for women at high risk for breast cancer.

Although it has distinct advantages over mammography, breast MRI also has potential limitations. For example, it is not always able to distinguish the difference between cancerous abnormalities, which may lead to unnecessary breast biopsies. This is often referred to as a "false positive" test result. Recent research has demonstrated that using commercially available software programs to enhance breast MRI scans can reduce the number of false positive results with malignant tumours. Thus, the need for biopsies may decrease with computer-aided enhancement.

Another disadvantage of breast MRI is that it has historically been unable to identify calcifications or tiny calcium deposits that can indicate breast cancer (John Hopkins Medicine, 2015).

Ultrasound

Ultrasound, also known as sonography, uses sound waves to outline a part of the body. For this test, a small, microphone-like instrument called a transducer is placed on the skin (which is often first lubricated with ultrasound gel). It emits sound waves and picks up the echoes as they bounce off body tissues. The echoes are converted by a computer into a black and white image that is displayed on a computer screen. This test is painless and does not expose you to radiation. Ultrasound has become a valuable tool to use along with mammography because it is widely available and less expensive than other options, such as MRI. Usually, breast ultrasound is used to target a specific area of concern found on the mammogram. Ultrasound helps distinguish between cysts (fluid-filled sacs) and solid masses and sometimes can help tell the difference between benign and cancerous tumours. In someone with a breast tumour, it can also be used to look for enlarged lymph nodes under the arm. The use of ultrasound instead of mammograms for breast cancer screening is not recommended. However, clinical trials are now looking at the benefits and risks of adding breast ultrasound to screening mammograms in women with dense breasts and a higher risk of breast cancer (ACS, 2014).

Comparison of Imaging Techniques

Consideration for imaging of the breast is always dependent on the radiation to be used and the breast density. From studies, exposure to ionizing radiation at a younger age has a higher risk of inducing cancer because the breast is highly sensitive to radiation (Hendrick, 2010.). Younger women are more likely to have dense breast than older women. Mammography has relatively lower sensitivity in breast tissue that is dense or heterogeneously dense, especially in younger women. Ultrasound is not significantly affected by breast density (Kolb, Lichy, & Newhouse, 2002). With increasing Breast Imaging Reporting and Data Systems (BIRADS) destiny classifications, sensitivity of mammography decreases from 100% to 47%. Sensitivity of Ultrasound remains in the range of 80% - 88% at all densities (Berg et al., 2004). Data from five different studies to compare the sensitivities of Mammography and Ultrasound breast imaging modalities in women, shows that in younger women the sensitivity of ultrasound is significantly (10% – 23%) greater than that of mammography. The sensitivity of ultrasound is very high (> 92%) in women under age 40. Specificity of ultrasound in women less than 30 years is 80.50%. It was recommended that for mammography routine screening be conducted in women over 40 years and diagnostic imaging in symptomatic women age 30 years and older. Ultrasound should be used in diagnostic imaging in symptomatic women under age 30 years. Screening MRI is recommended for women with an approximately 20–25% or greater lifetime risk of breast cancer, including women with a strong family history of breast or ovarian cancer and women who were treated for Hodgkin disease. MRI has the highest

sensitivity and lower specificity and can be used in pre-surgical planning (Parikh, 2007; Saslow et al., 2007).

Breast Cancer Treatment

The main types of treatment for breast cancer are: Surgery, Radiation therapy, Chemotherapy, Hormone therapy, Biological therapy (targeted therapy) and Bone - directed therapy. One or a combination of methods may be used for treatment. The type or combination of treatments you have will depend on how the cancer was diagnosed and the stage it's at. Breast cancer diagnosed at screening may be at an early stage, but breast cancer diagnosed when you have symptoms may be at a later stage and require a different treatment (ACS, 2014; NHS, 2016).

Optimisation of Patient Dose

In diagnostic radiology, patient protection is governed by three (3) basic principles as recommended by the International Commission of Radiological Protection (ICRP): justification of practice, optimisation of protection and diagnostic reference levels. Justification, being the first step in radiological protection, is to ensure that medical exposure is justifiable with a valid clinical indication, no matter how good the imaging performance may be. Every examination must result in a net benefit for the patient. And once a diagnostic examination has been clinically justified, the radiological protection of the patient must be optimised, which means that the doses should be as low as reasonably achievable, consistent with obtaining the appropriate image quality (IAEA, 2002).

In the area of optimization in diagnostic radiology there is considerable scope for reducing doses without loss of diagnostic information, but the extent to

which the measures available are used varies widely. The optimization of protection in diagnostic radiology does not necessarily mean the reduction of doses to the patient — it is paramount that the image obtained contains the diagnostic information as intended (IAEA, 2004). Dedicated high sensitivity, high resolution mammography screen film combinations or equivalent digital imaging systems need to be used to produce the image quality required at a low dose (IAEA, 2006). Therefore to determine how well a patient is protected, calls for the implementation of a total quality assurance programme with relevant quality control procedures. With the relevant quality assurance programme in place, the carcinogenic risk associated with mammography can be estimated to determine whether the mammography equipment used is contributing to the increase in breast cancer risks or not.

Theory on Image Quality

Image quality assessment is very crucial for the optimisation process (Sandborg, Tingberg, Ullman, Dance & Carlsson, 2006). The quality of the images depends critically on the design and performance of the X-ray unit and image receptor, and on how that equipment is used to acquire and process the mammogram (Yaffe et al, 2009). One way of describing the overall system performance of the system in terms of image quality is to use a contrast-detail (CD) phantom (de Paredes, Fatouros, Thunberg, Cousins, Wilson and Sedgwick, 1998). The phantom can be made of PMMA. Human observers are subjective, can get tired and have limited time hence methods for objective and quantitative computer-assisted evaluation have been developed (Young, Alsager, Oduko, Bosmans,

Verbrugge, Geertse and Engen 2008a). A problem with CD phantoms is their homogeneous background. According to the Rose model (Rose, 1948), the contrast must increase when the diameter decreases for a CD object to be visible. This is normally found in practice with phantoms of homogeneous background. However, in observer performance studies of lesion detection in an anatomical background it has been shown (Burgess, Jacobson & Judy 2001) that this is not valid for structures with an extension of about 1 mm or larger. Instead, larger objects may be more difficult to see than smaller due to the anatomical background. It is likely that this applies to detection of masses (i.e. tumours) in mammograms, a detection task for which the anatomical background dominates (Ruschin, Timberg, Svahn, Andersson, Hemdal, Mattsson, Båth & Tingberg, 2007). A conclusion drawn from literature is that CD phantoms with a homogeneous background are questionable as tools for optimisation (Månsson, Båth & Mattsson, 2005). However, their use as a tool for image quality control on a regular basis is well justified (EC, 2006; Young, Alsager, Oduko & Gundogdu 2008b). It has been shown (Young *et al*. 2008a) that evaluation with computer aid can be made both efficiently and with results comparable to those from human observers.

Rose Model

The "Rose Model" seeks to establish the relationship between the number of image quanta deposited and the amount of detail embodied. The Model established the fact that image quality is ultimately limited by the statistical nature of image quanta. It describes the signal-to-noise ratio (SNR) for the detection of a uniform object of area *A* in a uniform background having a mean $\overline{q_b}$ quanta per

unit area. If $\overline{q_o}$ is the mean number of quanta per unit area in the region of the object, the resulting contrast can be written as

$$C = \frac{(\overline{q_b} - \overline{q_o})}{\overline{q_b}} \quad (1)$$

Rose defined signal to be the incremental change in the number of image quanta due to the object, $A(\overline{q_b} - \overline{q_o})$, and noise to be the standard deviation in the number of quanta in an equal area of uniform background, σb. For the special case of uncorrelated background quanta, noise is described by Poisson statistics and

$$\sigma b = \sqrt{A\overline{q_b}} \quad (2)$$

so that the Rose SNR, SNR_{Rose}, is given by

$$SNR_{Rose} = \frac{A(\overline{q_b} - \overline{q_o})}{\sqrt{A\overline{q_b}}} \quad (3)$$

Rose showed that SNR_{Rose} must have a value of approximately five or greater for reliable detection of an object (Rose, 1953; Cunningham & Shaw, 1999).

Theory of Breast Dosimetry

The estimation of the absorbed dose to the breast is an important part of the quality control of the mammographic examination because there is a small but significant risk of radiation induced carcinogenesis associated with it (Dance, 1990; ICRP, 1991). Knowledge of breast dose is essential for the design and performance assessment of the mammographic imaging systems. It also helps to optimise both equipment and technique so that the desired image quality is obtained at the lowest possible dose (IPSM, 1994).

Breast dose can be estimated on the basis of measurements on patients or phantoms. Phantoms measurements are well suited to quality control and inter-system comparison. It can form the basis for dose – surveys (Law, 1995). The quantity mostly used in determining the amount of radiation deposited in the breast is the mean glandular dose (MDG). It is defined as the average dose to the glandular tissue of the breast and it is the most appropriate dosimetric quantity used to predict the risk of carcinogenesis (Hogg, Kelly & Mercer, 2015).

Because it is difficult to measure the mean glandular dose to the breast directly and it is usual to employ conversion factors which relate the incident air kerma to this dose, such factors have been measured by some authors (Hammerstein et a1., 1979, Stanton et a1., 1984) and have been calculated by others using Monte Carlo techniques (Dance 1980, Rosenstein et a1., 1985) for the conventional X-ray spectra used in screen/film or Xero-mammography. No factors are presently available for the spectra from a tungsten target filtered with K-edge filters which are sometimes used in screen film mammography (Beaman et a1., 1983, Sabel et a1., 1986). The most comprehensive of the existing tabulation of factors are those of Stanton et a1 (also given in NCRP 85, 1986) and (Rosenstein et a1., 1985).The tables of Stanton et a1 have some data missing for compressed breast thicknesses of 3 cm, 7 cm and 8 cm. They are based on the integration of depth-dose curves and do not account for variation of the dose laterally within the breast. The tables provide data for a range of breast shapes but factors for firm compression are only given for a thickness of 6 cm (Rosenstein et a1). Breast dose varies widely with breast composition and thickness as well as the choice of imaging equipment and

radiographic technique. To facilitate a comparison of variations due to the imaging system alone, the IPSM (1989) has developed a protocol for estimating the dose to a 4.5 cm thick standard breast from measurements using a Perspex phantom, and appropriate conversion factors. This paper describes the Monte Carlo calculation of these conversion factors for a wide range of X-ray spectra including K-edge filtered spectra from both molybdenum and tungsten targets. For comparison purposes, and in order to supplement the existing tabulations, the incident air kerma to mean glandular dose conversion factor has also been evaluated for breast thicknesses in the range 2 cm - 8 cm (Stanton et a1., & Rosenstein et a1.,)

Perspex is a cheap and convenient material for constructing breast phantoms and the Monte Carlo program has also been used to calculate equivalent thicknesses of Perspex and breast tissue which will be of value in the practical assessment of the performance of breast imaging systems for different breast sizes (Dance, Skinner, Young, Beckett & Kotre, 2000).

According to Dance (1990), mean glandular breast dose, is calculated using

$$\mathrm{MGD} = \mathrm{K.g} \qquad (4)$$

where K is the incident air kerma at the upper surface of the breast, measured without backscatter, and g is the incident air kerma to mean glandular dose conversion factor (g - factor). As noted earlier, the tabulated g - factors correspond to a glandularity of 50%. It is proposed that equation (4) is now extended to

$$\mathrm{MGD} = \mathrm{K.g.c.s} \qquad (5)$$

where the factor g is unchanged, the factor c corrects for any difference in breast composition from 50% glandularity and the factor s corrects for any difference from the original tabulation by Dance (1990) due to the use of a different X-ray spectrum.

The conversion factors g and c were determined by interpolation using equation 6 from look up tables (Dance et al., 2000, 2009 & 2011).

$$Y_2 = \frac{(X_2 - X_1)(Y_3 - Y_1)}{(X_3 - X_1)} + Y_1 \quad (6)$$

where X_1, X_2, X_3, Y_1, Y3 are all known parameters and Y_2 is the unknown being determined.

Diagnostic Reference Level (DRL)

A diagnostic reference level (DRL) is a dose level for a typical X-ray examination of a group of patients with standard body sizes and for broadly defined types of equipment. These levels are expected not to be exceeded for standard procedures when good and normal practice regarding diagnostic and technical performance is applied. They assist in the optimisation of the medical exposure in a certain region as it allows detecting unnecessarily high doses to the patient. DRLs have already proved useful as a tool in support of dose audit and practice review for promoting improvements in patient protection (MED, 1997; RPoP, 2013; ICRP, 2001).

DRLs were first successfully implemented in relation to conventional radiography in the 1980s and subsequently developed for other modalities in the 1990s (RPoP, 2013).

At present, in mammography practice, it is assumed that the glandular tissue is vulnerable to radiation induced cancer, whereas fatty tissue and skin tissue are less critical. It is proposed that the mean X-ray dose to the glandular tissue (MGD) is the most appropriate dosimetric quantity to predict the risk of carcinogenesis (RPoP, 2013; IPEM, 2004).

Ideally, MGD that is representative of patients should be used for the establishment of DRLs however measurements on phantoms are valid and provide a good estimate of the mean patient dose (Sams, Bosmans, Xiao, Carton, Marshall, Young & Marchal, 2004).

Chapter Summary

In summary, a review of the literature on the female breast and breast cancer (causes and staging of disease) were done. Furthermore the various types of breast imaging and the advantages and disadvantages of each modality were also reviewed. The concept of optimization was also introduced in this chapter. The final review was on the theory of image quality, breast dosimetry and Diagnostic Reference Levels.

CHAPTER THREE

MATERIALS AND METHODS

Introduction

This chapter provides information on the materials and methodology that was used to measure and analyse the data. It describes the "ImageJ", "Ocean 2014" and Minitab softwares that were used to achieve the objectives of the study. The chapter concludes with description of the systematic procedures that were followed to arrive at the modelled equations.

Materials

The materials that were used for the research include mammography equipment, semi-circle polymethylmethacrylate (PMMA) plates, Piranha quality control kit, American College of Radiology mammography accreditation phantom (ACR MAP), towel, bathroom scale, meter rule, lawn tennis ball and Styrofoam, Ocean 2014 software, "ImageJ" software, Minitab software and ArcGIS software.

Mammography equipment

A total of thirteen (13) mammography centres (A – M) with digital mammography systems agreed to participate in this study. Four (4) were located in public/government hospitals, two (2) in private hospitals and seven (7) in private diagnostic imaging centres throughout the Ghana. The four (4) in the public hospital were full-field digital mammography (FFDM) systems whiles the remaining nine (9) were computed radiology (CR) systems. Table 5 to Table 7 gives details of the mammography systems that were used.

Table 5: Specification of mammography systems A to C

MAMMOGRAPHY SYSTEMS	A	B	C
Type of system	CR	CR	CR
X-ray Unit Manufacturer / Year	Planmed / 2009	Philips / 2009	General Electric / 2010
Year Installed	2011	2015	2012
Model	Nuance Classic	MammoDiagnost AR	Alpha RT
Mode of operation	Both AEC and Manual	Both AEC and Manual	Both AEC and Manual
SID (mm)	650	650	600
Applied Anode/filter type	Mo/Rh	Mo/Rh	Mo/Rh
kVp range	20 - 35	20 - 35	23 - 35
mAs range	10 - 450	1 - 640	4 - 450

Table 6: Specification of mammography systems D to F

MAMMOGRAPHY SYSTEMS	D	E	F
Type of system	CR	CR	CR
X-ray Unit Manufacturer / Year	General Electric / 2003	General Electric / 2013	Varian Medical Systems / 2005
Year Installed	2009	2014	2016
Model	Senographe 700T	Alpha RT	GE Diamond
Mode of operation	Both AEC and Manual	AEC only	Manual only
SID (mm)	660	600	660
Applied Anode/filter type	Mo/Mo	Mo/Rh	Mo/Mo
kVp range	22 - 35	23 - 35	20 - 39
mAs range	4 - 600	4 - 450	4 – 350

Table 7: Specification of mammography systems G to M

MAMMOGRAPHY SYSTEMS	G	H	I	PUBLIC HOSPITALS
Type of system	CR	CR	CR	FFDM
X-ray Unit Manufacturer / Year	BEMEMS / 2014	Hologic / 2005	Siemens / 2003	DRGEM Corporation / 2011
Year Installed	2014	2011 & 2016	2010	J 2015 K 2012 L 2016 M 2012
Model	Pinkview – *AT*	LORAD M - IV	Mammomat 3000 Nova	Fujifilm – AMULET F
Mode of operation	AEC only	Manual only	Manual only	AEC only
SID (mm)	660	650	650	650
Applied Anode/filter type	Mo/Mo	Mo/Rh	Mo/Rh	W/Rh
kVp range	20 - 35	20 - 35	23 - 35	23 - 35
mAs range	4 - 350	3 - 400	2 - 400	2 - 600

The location of the nineteen (19) available mammography systems in the country and the Centres that participated in the study is presented in Figure 8. Alphabet 'P' in the map represents the number of facilities present in that region of Ghana that participated in the study.

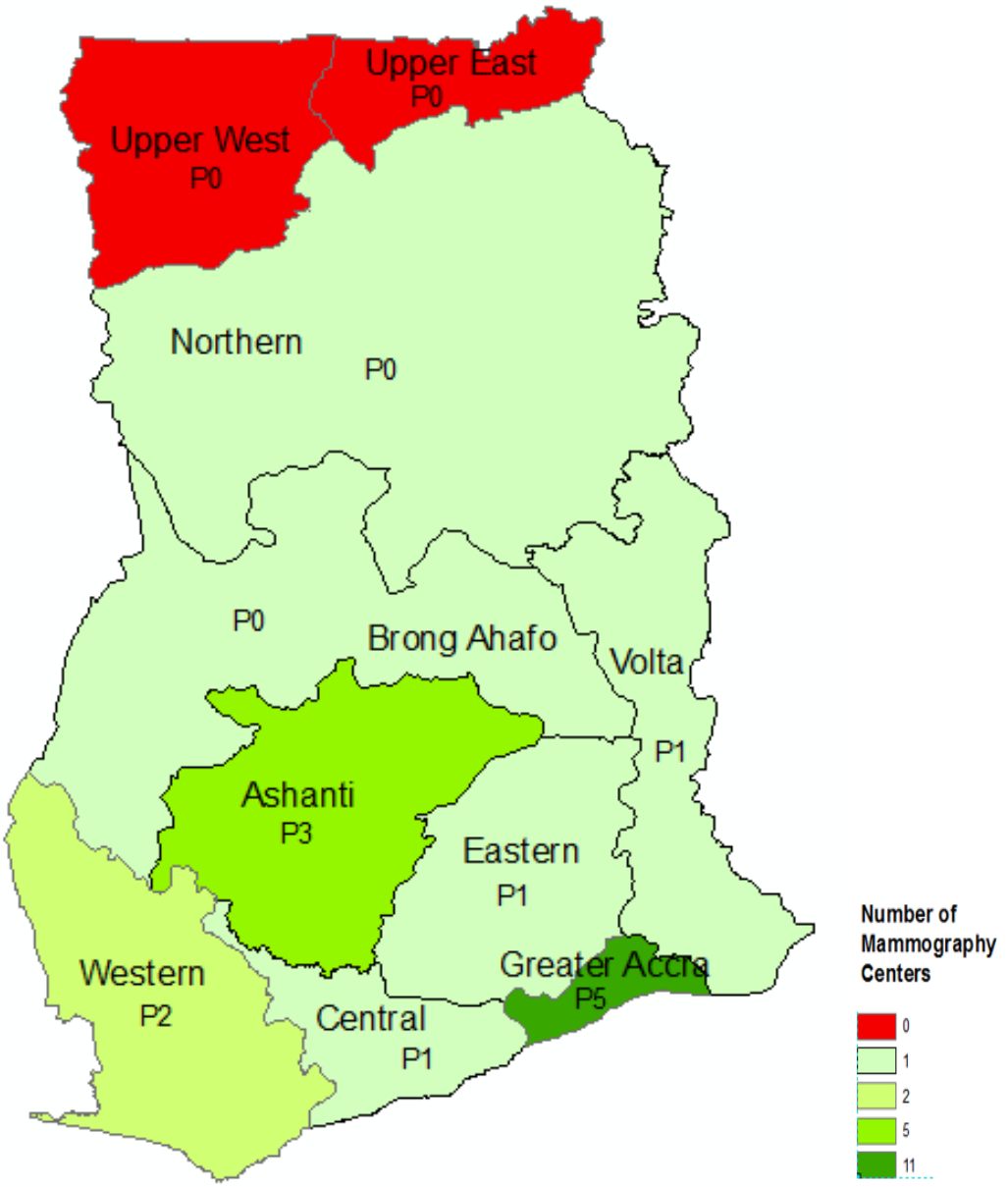

Figure 8: Mammography map of Ghana as at December 2015

Polymethyl methacrylate (PMMA) slabs

Polymethyl methacrylate (PMMA), also known as acrylic glass or Perspex is a transparent thermoplastic often used in sheet or slab form. PMMA is a human tissue equivalent material and is one of the mostly used phantoms for studying breast dosimetry in mammography because it has a good repeatability. It is a strong and lightweight material having a density of 1.17–1.20 g/cm^3 (Meyers, 1995; DATA TABLE, 2016; Boulet, Gérardin, Acem, Parent, Collin, Pizzo & Porterie, 2014). It does not melt or char. Figure 9 shows a single semi – circular PMMA slab. A total of nine (9) slabs were used. Seven (7) were 10 mm thick whiles two (2) were 5 mm thick. These slabs were combined to get the different desired thicknesses.

Figure 9: A single slab of Polymethylmethacrylate

Piranha Quality Control Meter

The Piranha is a solid state detector which can measure all the required parameters such as tube voltage (kVp), milliampere second (mAs), exposure

(mGy), exposure rate (mGy/s), exposure time (s), total filtration and half value layer (HVL). When an external probe is connected, it can measure dose and dose rate. It finds use in diagnostic radiology specifically in conventional X-ray, fluoroscopy, mammography, dental and computed tomography (CT) ranges. The Piranha system version 5.5C was used in this study. The system has the ability to generate a tube voltage waveform and a dose rate waveform.

The Piranha is designed for fast set-up and use, to enhance productivity and reduce errors particularly during repetitive X-ray system output measurement and analysis routines. All measurements were displayed immediately after exposure (RTI, 2014). Figure 10 shows the Piranha system that was used for this study.

Figure 10: Piranha Quality Control Meter

Styrofoam

Styrofoam is a closed-cell extruded polystyrene foam currently made for thermal insulation and craft applications. Styrofoam is composed of 98% air, making it lightweight and buoyant. It finds its application in medical practice as a 'spacer' during quality control measurements in diagnostic radiology and radiotherapy (Wikipedia, 2016). Figure 11 shows Styrofoam boards that were used as spacers.

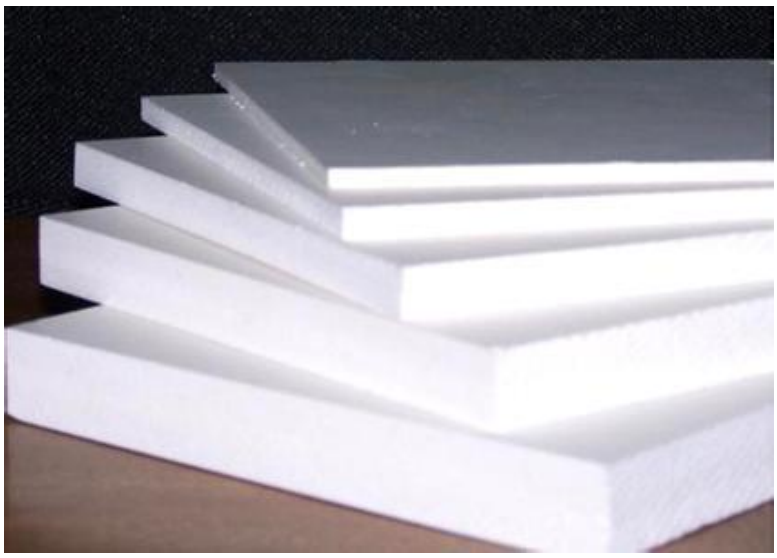

Figure 11: Styrofoam boards
(WIKIPEDIA, 2016)

American College of Radiology Mammography Accreditation Phantom (ACR MAP)

The Mammography Accreditation Phantom is made up of a wax block containing 16 various sets of test objects, a 3.3 cm (1.3 in.) thick acrylic base, a tray for placement of the wax block, and a 0.3 cm (0.12 in.) thick cover. It is used to simulate X-ray attenuation of 4.2 cm compressed human breast composed of 50%

adipose and 50% glandular tissue. Five (5) groups of simulated micro-calcifications, six (6) different size nylon fibers simulate fibrous structures, and five (5) different size tumour - like masses are included in the wax insert (MAP, 1997). Figure 12 shows ACR MAP that was used in the study.

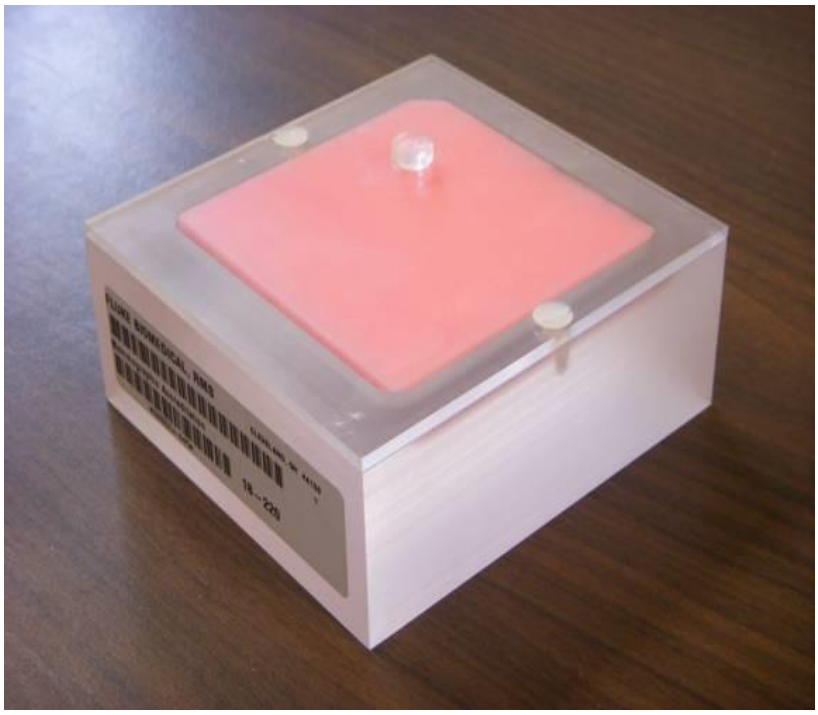

Figure 12: American College Radiology Mammography Accreditation Phantom (ACR MAP)

Ocean 2014 software

The Piranha quality control Meter is connected to a laptop or tablet via the "Ocean 2014" software. It's a powerful software with diverse applications and abilities. Ocean 2014 allows one to set up templates to automate X-ray equipment testing, analyze the test data and store the data, waveforms and analyze the results by selecting appropriate icon on the software interface. It has a special 'Quick Check' feature which is launched automatically when "Ocean 2014" starts and the

Piranha Meter is detected. The software automatically recognizes what type of Meter being used. It is full plug-and-play system. One can manually save data, print or export measured data to Excel (Ocean 2014 Manual, 2015). Figure 13 shows the interface of the Ocean 2014 software.

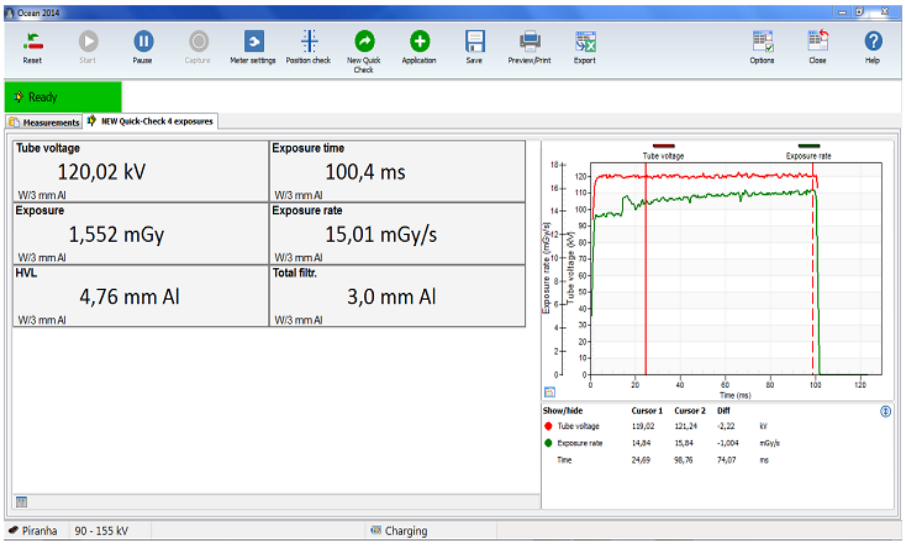

Figure 13: Interface of Ocean 2014 Software

ImageJ software

"ImageJ" is a public domain Java image processing program created by the National Institute of Health, United States of America that performs image quality assessment quantitatively. It can display, edit, analyze, process, save and print 8-bit, 16-bit and 32-bit images. It can read many image formats including Tag Image File Format (TIFF), Graphical Interchange Format (GIF), Joint Photographic Experts Group (JPEG), Bitmap (BMP), Digital Imaging and Communication in Medicine (DICOM) and Flexible Image Transport System (FITS) formats. It can calculate area and pixel value statistics of user-defined selections. It can measure distances and angles and can create density histograms and line profile plots. It

supports standard image processing functions such as contrast manipulation, sharpening, smoothing, edge detection and median filtering. It does geometric transformations such as scaling, rotation and flips (Rasband, 2012). Figure 14 shows the interface of the "ImageJ" version1.50i that was used for the study.

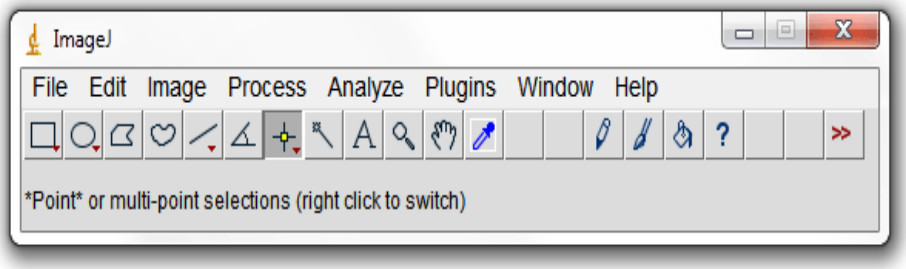

Figure 14: Interface of ImageJ Software

MINITAB Application software

Minitab is a statistical package that provides a broad range of basic and advanced data analysis techniques. It includes regression techniques (general and logistic), analysis of variance, experimental design, control charts and quality tools, survival analysis, multivariate analyses (principal components, cluster and discriminant), time series, descriptive and non-parametric statistics, exploratory data analysis, power and sample-size calculations (MINITAB, 2017).

The major regression analysis of the Minitab software was used to produce a statistical modelled relationship between the compressed breast thickness (CBT), tube voltage (kVp), tube current (mAs), mean glandular dose and image quality (SNR).

ArcGIS Software

ArcGIS is a geographic information system (GIS) software for working with maps and geographic information. It is used for creating and using maps, compiling geographic data, analyzing mapped information, sharing and discovering geographic information, using maps and geographic information in a range of applications, and managing geographic information in a database. The system provides an infrastructure for making maps and geographic information available across an organization, community and country (ArcGIS, 2017).

This software was used to draw the mammography map of Ghana.

Methodology

The main reason for undertaking the quality control assessment was to ensure optimal operation of the mammography systems and safety of both patients and operators. Quality control assessment performed on all thirteen (13) mammography systems were unit assembly evaluation, X-ray tube performance test which included tube voltage accuracy and repeatability, output repeatability and linearity, half value layer, short term automatic exposure control (AEC). The Breast Compression system was assessed by evaluating the Compression force, thickness and alignment. Quantitative Image quality and dosimetry at different thicknesses were also determined.

Unit assembly evaluation

The mammography system contains many mechanical components. These are subject to wear or degradation over time, resulting in possible safety or performance problems. Therefore, they must be checked on a regular basis. The test

was performed to ensure that all locks, detents, angulation indicators and mechanical support devices for the X-ray tube and breast support assembly are operating properly, and that the Digital Imaging and Communications in Medicine" (DICOM) system file headers are correctly populated. The test was conducted in reference to the International Atomic Energy Agency, Human Health Series 2 and 17 (IAEA , 2009; IAEA, 2011). The list of tests undertaken are presented in Appendix A. The results from the evaluation is presented in Table 8 to Table 11. Results are given in terms of compliance/pass (YES represented by Y), failure to comply/fail (NO represented by N) and test non-applicable to system represented by N/A.

X-ray Tube Performance Test

Tube voltage accuracy and repeatability

The test was performed to verify the accuracy and repeatability of the tube voltage at fixed kVp and over a range of clinically applicable tube voltages. The test was conducted in reference to the International Atomic Energy Agency, Human Health Series 2 (IAEA, 2009). A tube voltage of 28 kVp was selected on the console. The Piranha was placed centrally in the radiation field on the breast support and compressed. In manual mode (without AEC), five (5) exposures were carried out with 40 mAs. The measured tube voltage values were recorded onto a data collection sheet which was prepared using Microsoft Excel. Mean and standard deviation of the measured values was determined. Accuracy (deviation), difference and repeatability (Coefficient of variation - COV) of the tube voltage was calculated from recorded data using equations 7, 8 and 9 respectively. Tolerance

level for Accuracy was ±5 % whiles for Repeatability - difference ≤5 % and COV ≤2 %. Set-up for the test is presented in Figure 15.

Figure 15: Set – up for kVp Accuracy and Repeatability measurement

$$Deviation\ (\%) = \left(\frac{kVp_{nom} - kVp_{measured}}{kVp_{nom}}\right) \times 100 \qquad (7)$$

where kVp_{nom} is the value indicated on the equipment and $kVp_{measured}$ is the Piranha measured value. This percentage deviation is a measure of the accuracy.

$$Difference\ (\%) = \left(\frac{Max\ measurement - Min\ measurement}{Min\ measurement}\right) \times 100 \qquad (8)$$

where *Max measurement* is the maximum tube voltage measured and *Min measurement* is the minimum tube voltage measured.

$$COV = \left(\frac{\bar{X}}{\sigma_{\bar{X}}}\right) \times 100 \qquad (9)$$

where $\bar{X}$ is the mean of the tube voltage values measured and $\sigma_{\bar{X}}$ is the standard deviation of the tube voltage values measured . Results for this test for all thirteen (13) mammography systems are presented in Table 12.

Output repeatability and Linearity

The output repeatability and linearity was performed to evaluate the repeatability of the air kerma for a given mAs and the linearity with the mAs. The Piranha was laterally centred on the breast support and 40 mm from the chest wall, so that the sensitive volume of the Piranha remains completely irradiated. A fixed tube voltage of 28 kVp was selected and exposures made with three (3) different values of mAs (40, 80 or 85 and 120 or 125 – based on the potential of the mammography equipment). For the 40 mAs, five exposures were taken whiles two exposures were taken for both the 80 mAs or 85 mAs and the 120 mAs or 125 mAs. The exposure readings of the Piranha was recorded onto a data collection sheet. The percentage difference between the measurements under 28 kVp / 40 mAs was calculated using equation 8. Coefficient of variation was calculated using equation 9. For each mAs selected, the average value of the obtained readings of air kerma was calculated and recorded on the data collection sheet. The output, *Y*, was

calculated by dividing each average air kerma value obtained by the corresponding mAs and the results recorded. The output linearity (L) was calculated using the equation 10.

$$Linearity\ (L) = \left(\frac{(Y_1 - Y_2)}{(Y_1 + Y_2)}\right) \times 100 \qquad (10)$$

where Y_1 and Y_2 are two output values at consecutive mAs settings.

The tolerance (acceptable) limit according to the International Atomic Energy Agency Human Health Series 2 (IAEA, 2009) is repeatability - difference ≤5 % and COV ≤5 % whiles that of linearity is <10 %. Results for this test for all thirteen (13) mammography systems are presented in Table 13.

Short Term AEC

The performance of the Automatic Exposure Control (AEC) system can be described by the reproducibility and accuracy of the automatic optical density control. The Piranha was positioned in the path of the X-ray beam but without covering the AEC – detector. The short term reproducibility of the AEC system is calculated by the deviation of the exposure meter reading of ten (10) routine exposures of the 45 mm PMMA slabs. The test was performed according to European guidelines for quality assurance in breast cancer screening and diagnosis Fourth edition and the results presented in Table 14. Set – up for determination of the reproducibility of the AEC is presented in Figure 16.

Figure 16: Set – up for determination of Short Term AEC

Half Value Layer (HVL)

The purpose of the test was to confirm that the total filtration of the X-ray beam over a wide range of kVp's is in agreement with International Standards. The Piranha system was placed on the breast support, centred laterally, and 40 mm away from the chest wall edge, so that the sensitive volume of the Piranha remains completely within the radiation field. The compression paddle was applied. Exposures were made by setting the kVp from the lowest to the highest with increments of 1, 2 or 3 depending on the system's ability to select a particular tube voltage. The exposures were repeated for each kVp set and the data recorded from the Piranha was entered into a data collection sheet. The mean and standard deviation was calculated. Tolerance limit for the HVL was determined by using

equations 11 and 12. The results for the HVL measurements are presented in Table 15 to Table 27.

$$HVL\ (measured)min \geq \frac{X\text{-}ray\ tube\ voltage\ (KV)}{100} + 0.03 \quad (11)$$

$$HVL\ (measured)max \leq \frac{X\text{-}ray\ tube\ voltage\ (KV)}{100} + C \quad (12)$$

where 0.03 is a factor that compensates for the thickness of the compression plate and C is a factor that compensates for the anode/filter combination used (Elmore et al., 2003; IAEA, 2011). Each equipment used has a C factor depending on the anode/filter combination. C factors were chosen from Mo/Mo – 1.000, Mo/Rh – 1.017, Rh/Rh – 1.061, W/Rh – 1.042 and W/Ag – 1.042.

Compression Test

Adequate compression is essential for high quality mammography. The compression test was performed to check that the mammography system provides adequate compression in manual and automatic mode; to check the accuracy of the compression force indicator, if present on the equipment; to check the accuracy (or deviation) of the compression thickness indicator (IAEA, 2011). The alignment of the compression device at maximum force was also visualized and measured (EC, 2006).

Compression Force

Automatic Compression Mode

The bathroom towel was placed on the breast support and the bathroom scale was placed on it centrally directly under the compression paddle. A lawn tennis ball was placed on the scale to protect the compression plate and such that it

does not obscure the reading on the scale. The reading on the scale was adjusted to point “Zero”. The compression paddle was activated so that it operated and stopped at the maximum available powered force of 150 N. The compression foot pedal was activated for a second time to secure the compression plate. The deflection on the bathroom scale and the value of the displayed compression force were both recorded in kilogrammes (Kg) and Newtons (N) respectively. The compression plate was released. Displayed value accuracy should be within ±20 N. Results are presented in Table 28.

Manual compression mode

Using the same set-up as the automatic compression, the compression plate was moved downwards manually until it stopped. The deflection on bathroom scale and the value of the compression force were both recorded on the data collection sheet in Kilogrammes (Kg) and Newtons (N) respectively. The compression plate was released. Displayed maximum manual compression force should be less than 300 N. Displayed value accuracy should be ± 20 N. Results are presented in Table 28. Set – up for measuring compression force in Automatic and Manual mode is presented in Figure 17.

Figure 17: Set – up for measuring Compression force in both Automatic and Manual Mode

Compression Thickness

The PMMA slabs (20 mm, 45 mm and 70 mm) were aligned with the chest wall edge of the breast support platform. The compression paddle was activated so that it operated and stopped at the maximum available powered force. The measurement of the thickness of the slabs was taken centrally. The measured thickness and the displayed thickness were all recorded and inputted into the data sheet. Tolerance limit is for the displayed thickness to be within ±5 mm of phantom

thickness. Results are presented in Table 29. Set – up for measuring compression thickness is presented in Figure 18.

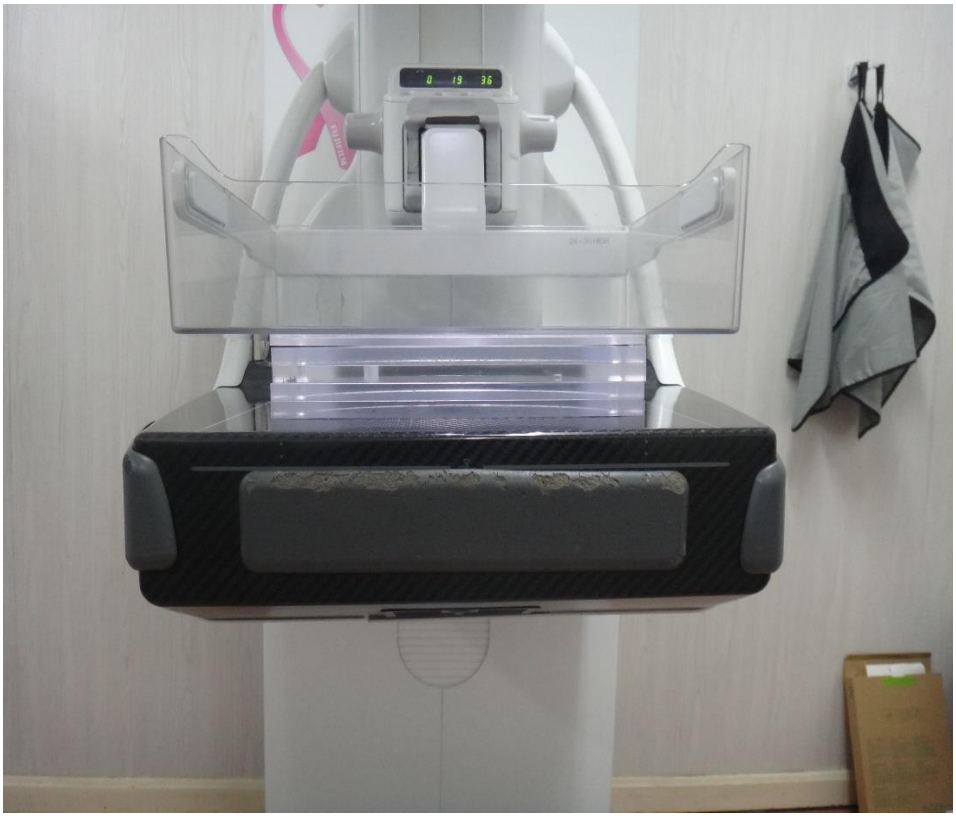

Figure 18: Set – up for measuring Compression thickness

Compression Alignment

The alignment of the compression device at maximum force was visualized and measured when the lawn tennis ball was compressed. The distance between breast support surface and compression device on each corner was measured. The compression device was released. Minimal misalignment of the compression plate is allowed, the difference between the measured distances at the left and the right side of the compression paddle should be ≤ 5 mm for symmetrical load. Results are

presented in Table 30. Set – up for measuring compression alignment is presented in Figure 19.

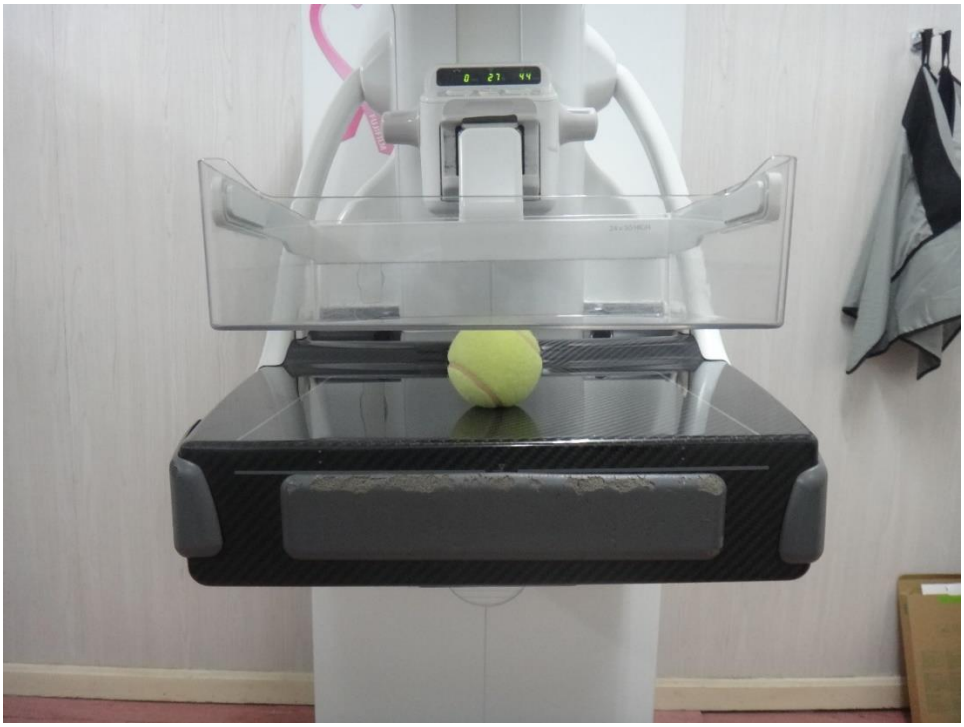

Figure 19: Set – up for measuring Compression alignment

Image Quality Test

Image quality assessment plays an essential role in the imaging process. It seeks to quantify a visual quality or, anatomically, an amount of distortion or degradation in a given image (Nisha, 2013).

Signal-to-noise ratio (SNR)

SNR was achieved through the exposure of PMMA plates with varying thicknesses (20 mm, 45 mm and 70 mm) using the automatic exposure control mode. The PMMA plates were positioned on the breast support and in order to produce a contrast area, an aluminium foil 0.2 cm thick measuring 2 x 2 cm was placed 6 cm far from the chest wall. After exposures, the images were registered as

"raw data". The images were imported into the ImageJ software and same dimension circular regions-of-interest (ROI) were drawn on the images – one inside the Aluminium sheet region and four (4) outside the Aluminium sheet region. The mean pixel value (MPV) and the standard deviation (σ) for the area inside the Aluminium sheet region and the area outside it were extracted from the image. The value of SNR for the 20 mm, 45 mm and 70 mm was calculated according to the "Rose Model" using equation 3. The results of the test are presented in Table 31. Set-up for image quality test is presented in Figure 20 to Figure 22.

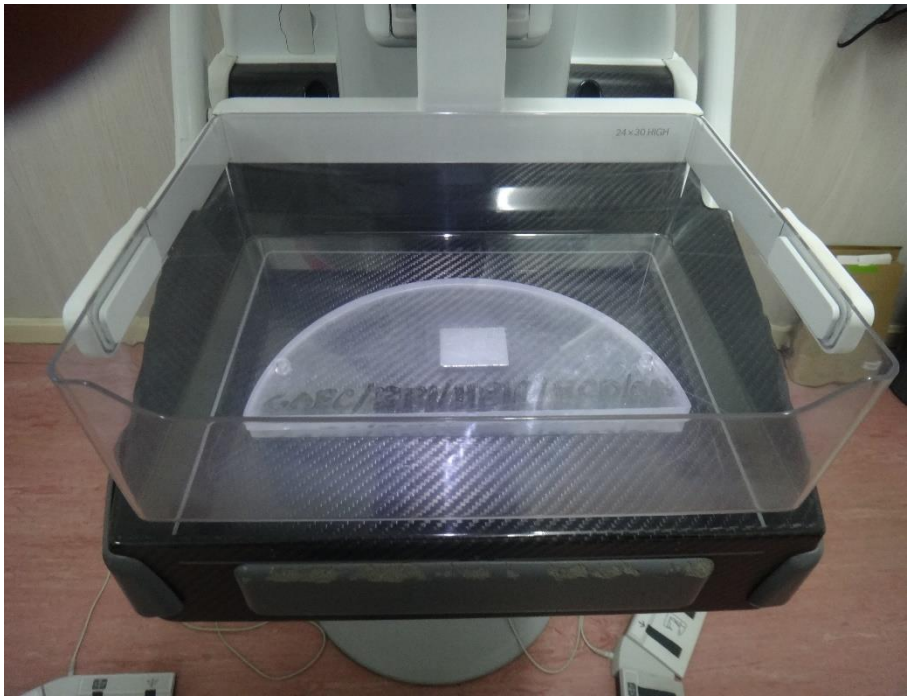

Figure 20: Set – up for Image quality test on 20 mm phantom

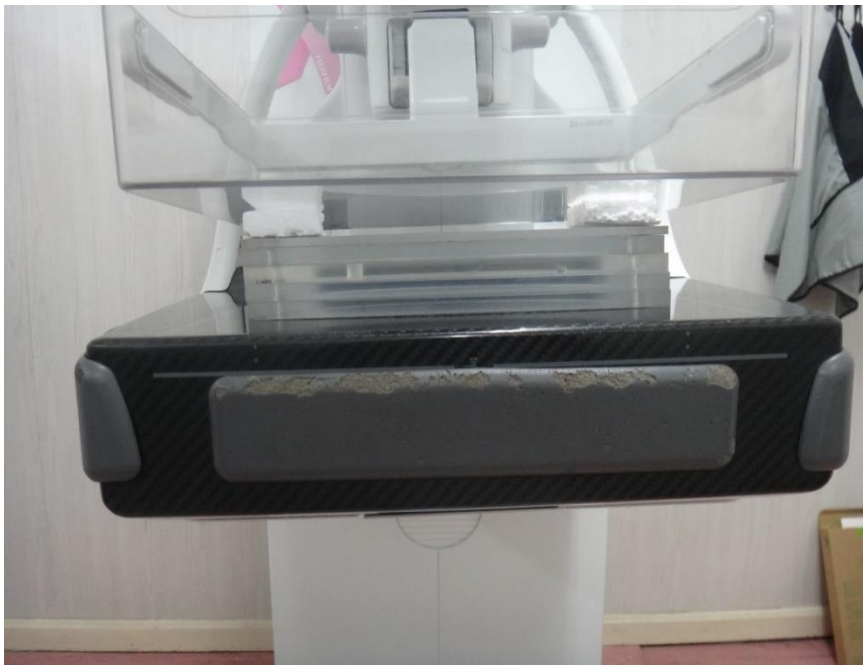

Figure 21: Set – up for Image quality test on 45 mm phantom with spacer to obtain an equivalent breast thickness of 53 mm

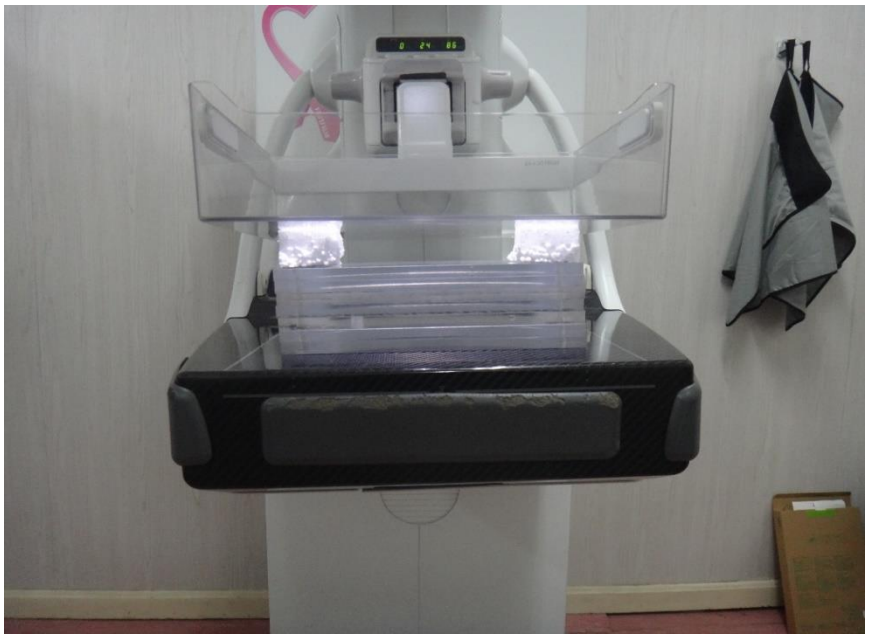

Figure 22: Set – up for Image quality test on 70 mm phantom with spacer to obtain an equivalent breast thickness of 90 mm

Mean Glandular Dose (MGD) Estimation

The purpose of the test was to estimate the mean dose to the glandular tissue of the breast which was calculated using equation 4. The MGD values are based on measurements of Entrance Surface Air Kerma (ESAK) and Half Value Layer. A thickness of 20 mm was simulated using two (2) 10 mm PMMA plates. The Piranha system was positioned centrally on the breast support and positioned 4 cm away from the chest wall. The compression plate was lowered and the exposure made in AEC mode. Set – up for estimation of mean glandular dose is presented in Figure 23. The same set-up was used for an exposure in the Semi – automatic mode with 50 mAs. The entrance surface air kerma and half value layer reading were recorded from the Ocean software and entered in the data sheet designed in Microsoft Excel. To get the actual ESAK, the Inverse Square Law (equation 13) was employed.

$$\frac{I_1}{I_2} = \frac{(d_2)^2}{(d_1)^2} \tag{13}$$

where I_1 and I_2 are the initial and final intensity of radiation respectively and d_1 and d_2 are the initial and final distances respectively.

This was necessary because, the distance at which the detector was measuring the incident radiation was different from the distance at which the various simulated breast thicknesses received the incident radiation. The actual mAs of the exposure was also corrected. The conversion factors g, c, s, used for this study was extrapolated from Dance et al publication (2000, 2009, and 20011). The procedure was repeated for a thickness of 30 mm, 40 mm, 45 mm, 50 mm, 60 mm and 70 mm PMMA thickness. The results for the calculated mean glandular dose are presented

in Table 32. For the FFDM systems, the displayed MGD was also recorded and the deviation between the displayed and the calculated was also determined. The results are presented in Table 33.

Figure 23: Set – up for estimation of MGD using PMMA slabs

Mean Glandular Dose (MGD) measurement using ACR MAP

The purpose of the test was to measure the mean dose to the glandular tissue of the breast using the ACR MAP. The ACR MAP was positioned centrally on the breast support and positioned 4 cm away from the chest wall. The compression plate was lowered and the exposure made in semi - automatic mode using tube voltage of 28 kVp. Set - up for the test is presented in Figure 24. The results are presented in Table 36.

Figure 24: Set – up for estimation of MGD using ACR MAP

Modelling process

The experimental modelling process was done using analytical modelling technique. The models were designed from the acquired phantom data and used to establish the relationship between the compressed breast thickness (CBT) and the tube voltage (kVp) and output (mAs). In addition, the experimental analytical modelling technique was used to model the relationship between pre-set exposure parameters (mAs, kVp) and the expected delivered mean glandular dose and the image quality. With a known CBT, mean glandular dose and image quality are predicted before the procedure starts i.e. patient is imaged.

The modelling procedure involved the use of mathematical regression analysis to determine the mathematical relationship between two or more variables. The idea of linear regression equation predictor which is used to estimate the relationship between two unknown variables in the form of the model equation predictor as in:

$$\boldsymbol{A = \gamma_0 + \gamma_1 \alpha} \tag{14}$$

where A is the unknown variable and $\boldsymbol{\alpha}$ is the predictor with $\boldsymbol{\gamma_0}$ and $\boldsymbol{\gamma_1}$ as the intercept on the axis of the unknown variable and slope of the relationship between the two variables respectively. In addition, each predictor in a regression equation has an estimated coefficient associated with the sample population regression coefficients. That is by using the estimated coefficients ($\boldsymbol{\gamma_1}$) with the predictors to calculate the fitted value of the response. Furthermore, the model equations were verified by estimating $\boldsymbol{\gamma_1}$ and $\boldsymbol{\gamma_0}$ and comparing them with the modelled linear regression equation predictor above. In addition the coefficient ($\boldsymbol{\gamma_1}$) was also estimated using the formula in simple linear regression:

$$\boldsymbol{\gamma_1 = \frac{\Sigma(X_1 - X)(Y_1 - Y)}{\Sigma(X_1 - X)^2}} \tag{15}$$

whereas the formula for the intercept ($\boldsymbol{\gamma_0}$) was estimated using:

$$\boldsymbol{\gamma_0 = A - \gamma_1 \alpha} \tag{16}$$

The mathematical model equations are presented in chapter 4.

Limitations of Model

One very crucial limitation of the model is the fact that all measurements were based on phantoms therefore getting enough data for the study presents a serious challenge. It doesn't take into consideration gender, age and clinical history. Another limitation is the anode/target combination of the system. Different systems have different anode / target combination. This impacts the final dose delivered to the glandular tissue as indicated in equation 4. This current model is based on the Tungsten / Rhodium (W/Rh) combination.

Chapter Summary

This chapter gave into details the materials and the methodology used to achieve the study objectives. It describes the different measurements that were undertaken and the process of obtaining the primary data in order to undertake further analysis. The chapter also gave details on the modelled equations. It conclude with a description of the application software and statistical models that were used to analysed the data, in addition to the limitations encounter during the modelling of the equations.

CHAPTER FOUR

RESULTS AND DISCUSSION

Introduction

The results of the unit assembly evaluation, radiological equipment performance test (tube voltage accuracy and repeatability, output repeatability and linearity, half value layer, short term automatic exposure control (AEC), compression (force, thickness and alignment) test, quantitative image quality and dosimetry are all presented in this chapter. Results from dose assessment using the ACR MAP and dose delivery accuracy are also presented. Modelled equations that predict exposure parameters, mean glandular dose and image quality are presented in this chapter. The chapter also has information on how the diagnostic reference levels were established.

Equipment Assembly Evaluation

The test was performed to ensure that all locks, detents, angulation indicators and mechanical support devices for the X-ray tube and breast support assembly are operating properly. It was also to ensure that the DICOM file headers are correctly populated. The results are presented in Table 8 to Table 11. The results show that for most of the mammography systems, their mechanical features are functioning correctly with the exception of systems ‘F’ and ‘I’ whose compression paddles were not functioning hence compression plate is only brought down manually. This tends to affect positioning of breast since two (2) hands are required to position the breast effectively. Angular indicator on system ‘F was also not functioning hence angular positions of both Craniocaudal (CC) and mediolateral

oblique (MLO) projections are based only on MLO button of the system and working experience of the radiographer. Even though system 'E' is a CR system, the image capturing and processing is that of a screen film system. Hence images don't contain the institute's details and the DICOM header is also not populated with patients ID and technique factors used for the exposure. For CR systems 'G', 'C', 'E' and FFDM systems 'K' and 'L' the DICOM is not activated on the system. The package was not part of the installation at the time of purchase. Images are only obtained through printing. It was confirmed that appropriate, operator technique control charts were not posted in the imaging room of all thirteen (13) Centres under the study even though for some systems, once awhile the radiographer uses the Manual exposure mode and for other systems the radiographer uses Manual exposure mode all the time. In such cases, the selection of the exposure parameters is based solely on the radiographer's working experience which is not the best especially when two (2) or more radiographers rotate at the Mammography unit. This usually happens when broad breast are imaged in parts and also when further details are required of very dense breast. Since systems J – M were FFDM systems, it means questions 6 – 8 were not applicable to them. The results of the unit assembly evaluation which was undertaken according to the IAEA Human Health Series 2 and 17 protocols respectively (IAEA 2009, IAEA 2011) indicate that systems A – E and G – M passed all the evaluation tests.

Table 8: Results of mammography equipment assembly evaluation for systems A – C

	MAMMOGRAPHY SYSTEMS	A	B	C
1	Free standing unit is mechanically stable.	Y	Y	Y
2	Indicator lights working properly	Y	Y	Y
3	All moving parts move smoothly, without obstructions to motion.	Y	Y	Y
4	All locks and detents work properly.	Y	Y	Y
5	Angulation indicators function properly	Y	Y	Y
6	Image receptor and holder is free from vibrations during exposure	Y	Y	Y
7	Image receptor slides smoothly into holder assembly	Y	Y	Y
8	Image receptor is held securely by assembly in any orientation	Y	Y	Y
9	The compression plate is in good condition	Y	Y	Y
10	The compression breast thickness scale (analog or digital) is accurate and reproducible	Y	Y	Y
11	The automatic compression release following exposure functions correctly	Y	Y	Y
12	The manual release of compression is possible when power fails	Y	Y	Y
13	The compression release override works properly	Y	Y	Y
14	The radiation shield for the operator is adequate	Y	Y	Y
15	There are no sharp edges on the breast support or compression paddle	Y	Y	Y
16	The face guard is in place	Y	Y	Y
17	Confirm that appropriate, current operator technique control charts are posted.	N	N	N
18	Panel switches, Indicator lights and meters working properly	Y	Y	Y
19	Images contain institution ID, patient ID, image acquisition time and date and technique factors	Y	Y	Y
20	DICOM header is populated correctly with institution ID, patient ID, image acquisition time and date, and technique factors etc.	Y	Y	N

NB: Results are given in terms of compliance (Y) and failure to comply (N)

Table 9: Results of mammography equipment assembly evaluation for systems D – F

MAMMOGRAPHY SYSTEMS		D	E	F
1	Free standing unit is mechanically stable.	Y	Y	Y
2	Indicator lights working properly	Y	Y	Y
3	All moving parts move smoothly, without obstructions to motion.	Y	Y	N
4	All locks and detents work properly.	Y	Y	Y
5	Angulation indicators function properly	Y	Y	N
6	Image receptor and holder is free from vibrations during exposure	Y	Y	Y
7	Image receptor slides smoothly into holder assembly	Y	Y	Y
8	Image receptor is held securely by assembly in any orientation	Y	Y	Y
9	The compression plate is in good condition	Y	Y	Y
10	The compression breast thickness scale (analog or digital) is accurate and reproducible	Y	Y	Y
11	The automatic compression release following exposure functions correctly	Y	Y	Y
12	The manual release of compression is possible when power fails	Y	Y	Y
13	The compression release override works properly	Y	Y	Y
14	The radiation shield for the operator is adequate	Y	Y	Y
15	There are no sharp edges on the breast support or compression paddle	Y	Y	Y
16	The face guard is in place	Y	Y	Y
17	Confirm that appropriate, current operator technique control charts are posted.	N	N	N
18	Panel switches, Indicator lights and meters working properly	Y	Y	Y
19	Images contain institution ID, patient ID, image acquisition time and date and technique factors	Y	N	Y
20	DICOM header is populated correctly with institution ID, patient ID, image acquisition time and date, and technique factors etc.	Y	N	Y

NB: Results are given in terms of compliance (Y) and failure to comply (N)

Table 10: Results of mammography equipment assembly evaluation for systems G – I

	MAMMOGRAPHY SYSTEMS	G	H	I
1	Free standing unit is mechanically stable.	Y	Y	Y
2	Indicator lights working properly	Y	Y	Y
3	All moving parts move smoothly, without obstructions to motion.	Y	Y	N
4	All locks and detents work properly.	Y	Y	Y
5	Angulation indicators function properly	Y	Y	Y
6	Image receptor and holder is free from vibrations during exposure	Y	Y	Y
7	Image receptor slides smoothly into holder assembly	Y	Y	Y
8	Image receptor is held securely by assembly in any orientation	Y	Y	Y
9	The compression plate is in good condition	Y	Y	Y
10	The compression breast thickness scale (analog or digital) is accurate and reproducible	Y	Y	Y
11	The automatic compression release following exposure functions correctly	Y	Y	Y
12	The manual release of compression is possible when power fails	Y	Y	Y
13	The compression release override works properly	Y	Y	Y
14	The radiation shield for the operator is adequate	Y	Y	Y
15	There are no sharp edges on the breast support or compression paddle	Y	Y	Y
16	The face guard is in place	Y	Y	Y
17	Confirm that appropriate, current operator technique control charts are posted.	N	N	N
18	Panel switches, Indicator lights and meters working properly	Y	Y	Y
19	Images contain institution ID, patient ID, image acquisition time and date and technique factors	Y	Y	Y
20	DICOM header is populated correctly with institution ID, patient ID, image acquisition time and date, and technique factors etc.	N	Y	Y

NB: Results are given in terms of compliance (Y) and failure to comply (N)

Table 11: Results of mammography equipment assembly evaluation for systems J – M

	MAMMOGRAPHY SYSTEMS	J	K	L	M
1	Free standing unit is mechanically stable.	Y	Y	Y	Y
2	Indicator lights working properly	Y	Y	Y	Y
3	All moving parts move smoothly, without obstructions to motion.	Y	Y	Y	Y
4	All locks and detents work properly.	Y	Y	Y	Y
5	Angulation indicators function properly	Y	Y	Y	Y
6	Image receptor and holder is free from vibrations during exposure	N/A	N/A	N/A	N/A
7	Image receptor slides smoothly into holder assembly	N/A	N/A	N/A	N/A
8	Image receptor is held securely by assembly in any orientation	N/A	N/A	N/A	N/A
9	The compression plate is in good condition	Y	Y	Y	Y
10	The compression breast thickness scale (analog or digital) is accurate and reproducible	Y	Y	Y	Y
11	The automatic compression release following exposure functions correctly	Y	Y	Y	Y
12	The manual release of compression is possible when power fails	Y	Y	Y	Y
13	The compression release override works properly	Y	Y	Y	Y
14	The radiation shield for the operator is adequate	Y	Y	Y	Y
15	There are no sharp edges on the breast support or compression paddle	Y	Y	Y	Y
16	The face guard is in place	Y	Y	Y	Y
17	Confirm that appropriate, current operator technique control charts are posted.	N	N	N	N
18	Panel switches, Indicator lights and meters working properly	Y	Y	Y	Y
19	Images contain institution ID, patient ID, image acquisition time and date and technique factors	Y	Y	Y	Y
20	DICOM header is populated correctly with institution ID, patient ID, image acquisition time and date, and technique factors etc.	Y	N	N	Y

NB: Results are given in terms of compliance (Y), failure to comply (N), and test not applicable to system (N/A)

X-ray Tube Performance Test

Results of X-ray tube performance test are presented in Table 12 to Table 27. For the purpose of this study, six (6) tests were performed under the X-ray tube performance test. Results of tube voltage accuracy and repeatability test, output repeatability & linearity test, short term automatic exposure control test are presented in Table 12 to Table 14 whiles results for half value layer (HVL) test are presented in Table 15 to Table 27.

Tube voltage accuracy and repeatability

The test was performed to verify the accuracy and repeatability of the tube voltage at a fixed kVp. With tolerance level of tube voltage accuracy of ±5 % recommended by the IAEA Human Health Series 2 (IAEA, 2009), it was realized from the results that all thirteen (13) mammography systems produced a good level of tube voltage accuracy. With a tolerance level of tube voltage repeatability of ≤5 % for the difference and ≤5 % for COV, it can be deduced that all thirteen (13) mammography systems passed the test. The results give the assurance that for patient examination, the tube voltage will be accurate and reliable. Details of raw values from which Table 12 was produced is presented in Appendix B.

Table 12: Results of Tube voltage accuracy and repeatability for all thirteen systems

Mammography systems	kVp accuracy (%)	kVp repeatability at 28 kVp	
		Difference (%)	COV (%)
A	2.20	0.20	0.20
B	2.14	0.04	0.50
C	1.55	0.04	0.88
D	2.50	0.10	0.10
E	0.68	0.47	0.23
F	0.64	0.14	0.07
G	1.06	0.69	0.43
H	2.76	2.70	1.18
I	2.70	0.63	1.32
J	0.50	0.39	0.21
K	0.08	0.10	0.21
L	1.95	0.11	0.24
M	1.69	2.10	0.88

Output repeatability & linearity test

The test was undertaken to evaluate the output repeatability of the air kerma for a given mAs and the linearity with the mAs. With a tolerance level of output repeatability of ≤5 % for the difference and ≤5 % for COV according to the International Atomic Energy Agency Human Health Series 2 (IAEA, 2009), it can be deduced that all thirteen (13) mammography systems passed the output test.

The results from the Linearity test, with tolerance level <10 %, indicate that all thirteen (13) mammography systems passed the test. Details of raw values from which Table 13 was produced is presented in Appendix C.

Table 13: Results of tube output repeatability and linearity test for all thirteen systems

Mammography systems	Output repeatability (%)		Output linearity (%)	
	Difference (%)	COV (%)	Max L_1	Max L_2
A	0.36	0.20	-0.48	0.01
B	3.50	2.00	3.03	2.71
C	0.92	1.11	-0.43	-0.32
D	0.10	0.05	-0.20	-0.08
E	2.10	0.99	0.22	-1.83
F	0.21	0.09	-0.82	0.06
G	1.04	0.84	-0.16	0.29
H	0.18	0.17	-0.06	0.09
I	0.19	0.10	-0.45	0.14
J	0.07	0.07	-0.06	-0.23
K	0.07	2.84	-3.83	-0.15
L	0.01	0.12	0.06	-0.01
M	0.28	0.13	-0.23	-.0.30

L_1 and L_2 are two Linearity values at consecutive mAs settings

Short Term Automatic Exposure Control test

The purpose of the test was to ensure that the AEC delivered consistent and reproducible exposures. The results from the assessment of the AEC for systems A – E, G and J – M, show that their AEC systems are functioning properly because the values calculated are within the tolerance limit. For systems 'F' and 'I' their AEC systems were not functioning and therefore were not in use. A value of 6.21 % was obtained for assessment of AEC of system 'H' which was more than the tolerance level of ≤ 5 %. This shows that the AEC system is not functioning well. This could lead to over or under exposure which may result in patient receiving an unusual amount of dose to the glandular tissue of the breast. Details of raw values from which Table 14 was produced is presented in Appendix D.

Table 14: Results of short term automatic exposure control test for all thirteen Systems

Mammography systems	Short term automatic exposure control (%)
A	1.22
B	2.45
C	3.19
D	1.70
E	3.30
F	-
G	0.00
H	6.21
I	-
J	2.76
K	1.97
L	3.79
M	4.41

Half Value Layer test

The HVL was measured to confirm that the total filtration of the X-ray beam over a wide range of kVp's is in agreement with international standards**.** Results of half value layer (HVL) test are presented in Table 15 to Table 27. The measurements were taken over the kVp range of the system (from the lowest to the highest with an increment of 1, 2 or 3 kVp) in both craniocaudal (CC) and mediolateral oblique (MLO) views. Results of the calculated HVL presented in Table 4.5 were compared with the results of the measured HVL in accordance with IAEA protocol (IAEA 2011). It was realized that the results were within acceptable limits. Therefore the beam quality over a range of kVp's is consistent. Details of raw values from which Table 15 to Table 27 were produced is presented in Appendix E.

Table 15: Results of half value layer test on mammography system A

Set kVp	Measured HVL value (mmAl)		Minimum HVL value (mmAl)	Maximum HVL value (mmAl)
	CC ± SD	MLO ± SD	CC & MLO	CC & MLO
23	0.30 ± 0.84E -3	0.30 ± 0.10E -2	0.26	0.42
25	0.32 ± 0.55E -3	0.32 ± 0.71E -3	0.28	0.44
27	0.34 ± 0.84E -3	0.35 ± 0.27E -1	0.30	0.46
29	0.36 ± 0.84E -3	0.36 ± 0.55E -3	0.32	0.48
31	0.37 ± 0.16E -2	0.37 ± 0.55E -3	0.34	0.50
33	0.39 ± 0.90E -3	0.39 ± 0.55E -3	0.36	0.52
35	0.40 ± 0.89E -3	0.40 ± 0.55E -3	0.38	0.54

Minimum HVL is calculated using equation 11 whiles maximum HVL is calculated using equation 12.

Table 16: Results of half value layer test on mammography system B

Set kVp	Measured HVL value (mmAl)		Minimum HVL value (mmAl)	Maximum HVL value (mmAl)
	CC ± SD	MLO ± SD	CC & MLO	CC & MLO
23	0.30 ± 0.84E -3	0.30 ± 0.10E -2	0.26	0.42
25	0.32 ± 0.55E -3	0.32 ± 0.71E -3	0.28	0.44
27	0.34 ± 0.84E -3	0.35 ± 0.27E -1	0.30	0.46
29	0.36 ± 0.84E -3	0.36 ± 0.55E -3	0.32	0.48
31	0.37 ± 0.16E -2	0.37 ± 0.55E -3	0.34	0.50
33	0.39 ± 0.90E -3	0.39 ± 0.55E -3	0.36	0.52
35	0.40 ± 0.89E -3	0.40 ± 0.55E -3	0.38	0.54

Minimum HVL is calculated using equation 11 whiles maximum HVL is calculated using equation 12.

Table 17: Results of half value layer test on mammography system C

Set kVp	Measured HVL value (mmAl)		Minimum HVL value (mmAl)	Maximum HVL value (mmAl)
	CC ± SD	MLO ± SD	CC & MLO	CC & MLO
23	0.30 ± 0.45E -3	0.30 ± 0.55E -3	0.26	0.42
25	0.32 ± 0.55E -3	0.32 ± 0.45E -3	0.28	0.44
27	0.34 ± 0.45E -3	0.34 ± 0.45E -3	0.30	0.46
29	0.36 ± 0.55E -3	0.36 ± 0.89E -3	0.32	0.48
31	0.38 ± 0.55E -3	0.38 ± 0.45E -3	0.34	0.50
33	0.39 ± 0.11E -2	0.39 ± 0.55E -3	0.36	0.52
35	0.41 ± 0.45E -3	0.41 ± 0.45E -3	0.38	0.54

Minimum HVL is calculated using equation 11 whiles maximum HVL is calculated using equation 12.

Table 18: Results of half value layer test on mammography system D

Set kVp	Measured HVL value (mmAl)		Minimum HVL value (mmAl)	Maximum HVL value (mmAl)
	CC ± SD	MLO ± SD	CC & MLO	CC & MLO
24	0.31 ± 0.15E -2	0.31 ± 0.11E -2	0.27	0.36
26	0.33 ± 0.55E -3	0.33 ± 0.55E -2	0.29	0.38
28	0.35 ± 0.84E -3	0.35 ± 0.89E -3	0.31	0.40
30	0.37 ± 0.11E -2	0.37 ± 0.55E -3	0.33	0.42
32	0.38 ± 0.55E -3	0.38 ± 0.55E -3	0.35	0.44
34	0.40 ± 0.50E -3	0.40 ± 0.55E -3	0.37	0.46
35	0.40 ± 0.89E -3	0.40 ± 0.55E -3	0.38	0.47

Minimum HVL is calculated using equation 11 whiles maximum HVL is calculated using equation 12.

Table 19: Results of half value layer test on mammography system E

Set kVp	Measured HVL value (mmAl)		Minimum HVL value (mmAl)	Maximum HVL value (mmAl)
	CC ± SD	MLO ± SD	CC & MLO	CC & MLO
23	0.30 ± 0.45E -3	0.30 ± 0.55E -3	0.26	0.42
25	0.32 ± 0.55E -3	0.32 ± 0.45E -3	0.28	0.44
27	0.34 ± 0.45E -3	0.34 ± 0.45E -3	0.30	0.46
29	0.36 ± 0.55E -3	0.36 ± 0.89E -3	0.32	0.48
31	0.38 ± 0.55E -3	0.38 ± 0.45E -3	0.34	0.50
33	0.39 ± 0.11E -2	0.39 ± 0.55E -3	0.36	0.52
35	0.41 ± 0.45E -3	0.41 ± 0.45E -3	0.38	0.54

Minimum HVL is calculated using equation 11 whiles maximum HVL is calculated using equation 12.

Table 20: Results of half value layer test on mammography system F

Set kVp	Measured HVL value (mmAl)		Minimum HVL value (mmAl)	Maximum HVL value (mmAl)
	CC ± SD	MLO ± SD	CC & MLO	CC & MLO
20	0.25 ± 0.55E -3	0.25 ± 0.55E -3	0.23	0.32
23	0.29 ± 0.89E -3	0.30 ± 0.26E -2	0.26	0.35
26	0.32 ± 0.45E -3	0.32 ± 0.55E -3	0.29	0.37
29	0.35 ± 0.45E -3	0.35 ± 0.55E -3	0.32	0.41
32	0.38 ± 0.45E -3	0.38 ± 0.45E -3	0.35	0.44
35	0.41 ± 0.40E -3	0.41 ± 0.55E -3	0.38	0.47

Minimum HVL is calculated using equation 11 whiles maximum HVL is calculated using equation 12.

Table 21: Results of half value layer test on mammography system G

Set kVp	Measured HVL value (mmAl)		Minimum HVL value (mmAl)	Maximum HVL value (mmAl)
	CC ± SD	MLO ± SD	CC & MLO	CC & MLO
20	0.26 ± 0.58E -3	0.26 ± 0.58E -3	0.23	0.32
23	0.30 ± 0.58E -3	0.30 ± 0.50E -3	0.26	0.35
25	0.32 ± 0.58E -3	0.32 ± 0.50E -3	0.28	0.37
27	0.33 ± 0.50E -3	0.33 ± 0.50E -3	0.30	0.39
29	0.35 ± 0.50E -3	0.35 ± 0.58E -3	0.32	0.41
31	0.36 ± 0.50E -3	0.36 ± 0.50E -3	0.34	0.43
33	0.38 ± 0.50E -3	0.38 ± 0.50E -3	0.36	0.45
35	0.39 ± 0.50E -3	0.39 ± 0.50E -3	0.38	0.47

Minimum HVL is calculated using equation 11 whiles maximum HVL is calculated using equation 12.

Table 22: Results of half value layer test on mammography system H

Set kVp	Measured HVL value (mmAl)		Minimum HVL value (mmAl)	Maximum HVL value (mmAl)
	CC ± SD	MLO ± SD	CC & MLO	CC & MLO
20	0.26 ± 0.50E -3	0.26 ± 0.58E -3	0.23	0.32
23	0.30 ± 0.58E -3	0.30 ± 0.58E -3	0.26	0.35
25	0.32 ± 0.58E -3	0.32 ± 0.50E -3	0.28	0.37
27	0.34 ± 0.58E -3	0.34 ± 0.50E -3	0.30	0.39
29	0.36 ± 0.58E -3	0.36 ± 0.50E -3	0.32	0.41
31	0.37 ± 0.58E -3	0.37 ± 0.50E -3	0.34	0.43
33	0.39 ± 0.60E -3	0.39 ± 0.50E -3	0.36	0.45
35	0.40 ± 0.50E -3	0.40 ± 0.50E -3	0.38	0.47

Minimum HVL is calculated using equation 11 whiles maximum HVL is calculated using equation 12.

Table 23: Results of half value layer test on mammography system I

Set kVp	Measured HVL value (mmAl)		Minimum HVL value (mmAl)	Maximum HVL value (mmAl)
	CC ± SD	MLO ± SD	CC & MLO	CC & MLO
23	0.35 ± 0.58E -3	0.35 ± 0.58E -3	0.26	0.42
25	0.39 ± 0.58E -3	0.39 ± 0.58E -3	0.28	0.44
27	0.42 ± 0.00	0.42 ± 0.58E -3	0.30	0.46
29	0.43 ± 0.58E -3	0.43 ± 0.00	0.32	0.48
31	0.45 ± 0.58E -2	0.45 ± 0.45E -3	0.34	0.50
33	0.46 ± 0.00	0.46 ± 0.00	0.36	0.52
35	0.48 ± 0.58E -3	0.48 ± 0.58E -3	0.38	0.54

Minimum HVL is calculated using equation 11 whiles maximum HVL is calculated using equation 12.

Table 24: Results of half value layer test on mammography system J

Set kVp	Measured HVL value (mmAl)		Minimum HVL value (mmAl)	Maximum HVL value (mmAl)
	CC ± SD	MLO ± SD	CC & MLO	CC & MLO
23	0.47 ± 0.55E -3	0.47 ± 0.55E -3	0.26	0.53
25	0.51 ± 0.84E -3	0.51 ± 0.55E -3	0.28	0.55
27	0.53 ± 0.11E -2	0.53 ± 0.55E -3	0.30	0.57
29	0.54 ± 0.10E -2	0.54 ± 0.55E -3	0.32	0.59
31	0.56 ± 0.55E -3	0.56 ± 0.55E -3	0.34	0.61
33	0.58 ± 0.50E -3	0.58 ± 0.55E -3	0.36	0.63
35	0.60 ± 0.55E -3	0.60 ± 0.55E -3	0.38	0.65

Minimum HVL is calculated using equation 11 whiles maximum HVL is calculated using equation 12.

Table 25: Results of half value layer test on mammography system K

Set kVp	Measured HVL value (mmAl)		Minimum HVL value (mmAl)	Maximum HVL value (mmAl)
	CC ± SD	MLO ± SD	CC & MLO	CC & MLO
23	0.47 ± 0.55E -3	0.47 ± 0.55E -3	0.26	0.53
25	0.51 ± 0.55E -3	0.51 ± 0.55E -3	0.28	0.55
27	0.53 ± 0.84E -3	0.53 ± 0.55E -3	0.30	0.57
29	0.54 ± 0.10E -2	0.54 ± 0.55E -3	0.32	0.59
31	0.56 ± 0.55E -3	0.57 ± 0.16E -3	0.34	0.61
33	0.58 ± 0.50E -3	0.58 ± 0.55E -3	0.36	0.63
35	0.60 ± 0.55E -3	0.60 ± 0.55E -3	0.38	0.65

Minimum HVL is calculated using equation 11 whiles maximum HVL is calculated using equation 12.

Table 26: Results of half value layer test on mammography system L

Set kVp	Measured HVL value (mmAl)		Minimum HVL value (mmAl)	Maximum HVL value (mmAl)
	CC ± SD	MLO ± SD	CC & MLO	CC & MLO
23	0.47 ± 0.45E -3	0.47 ± 0.45E -3	0.26	0.53
25	0.51 ± 0.55E -3	0.51 ± 0.89E -3	0.28	0.55
27	0.53 ± 0.55E -3	0.53 ± 0.55E -3	0.30	0.57
29	0.55 ± 0.45E -3	0.55 ± 0.22E -2	0.32	0.59
31	0.56 ± 0.55E -3	0.56 ± 0.55E -3	0.34	0.61
33	0.58 ± 0.50E -3	0.58 ± 0.55E -3	0.36	0.63
35	0.59 ± 0.51E -2	0.60 ± 0.48E -3	0.38	0.65

Minimum HVL is calculated using equation 11 whiles maximum HVL is calculated using equation 12.

Table 27: Results of half value layer test on mammography system M

Set kVp	Measured HVL value (mmAl)		Minimum HVL value (mmAl)	Maximum HVL value (mmAl)
	CC ± SD	MLO ± SD	CC & MLO	CC & MLO
23	0.47 ± 0.55E -3	0.47 ± 0.58E -3	0.26	0.53
25	0.51 ± 0.10E -2	0.51 ± 0.11E -2	0.28	0.55
27	0.53 ± 0.54E -3	0.53 ± 0.55E -3	0.30	0.57
29	0.55 ± 0.55E -3	0.55 ± 0.55E -3	0.32	0.59
31	0.56 ± 0.45E -3	0.56 ± 0.48E -3	0.34	0.61
33	0.58 ± 0.50E -3	0.58 ± 0.50E -3	0.36	0.63
35	0.59 ± 0.11E -2	0.59 ± 0.10E -2	0.38	0.65

Minimum HVL is calculated using equation 11 whiles maximum HVL is calculated using equation 12.

Compression Test

Breast compression is necessary because it reduces overlapping anatomy and decreases tissue thickness of the breast hence less scatter, more contrast, less geometric blurring of the anatomic structures, less motion and lower radiation dose to the tissues. Results from the compression force, thickness and alignment are presented in Table 28, Table 29 and Table 30 respectively.

Compression Force

Results from the compression force test is presented in Table 28. Systems A - C, E, and H – M passed both Power and Manual compression test performed on them according to the tolerance level (displayed value accuracy ± 20 N) set by IAEA Human Health Series 2 and 17 protocols (IAEA 2009, IAEA 2011). Details of raw values from which Table 28 was produced is presented in Appendix F.

Table 28: Results of compression force test for all thirteen systems

Mammography systems	Compression force accuracy (N)	
	Automatic Compression	Manual Compression
A	+10.00	+10.00
B	+7.04	+3.04
C	+15.00	+15.00
D	-	-
E	+15.00	+15.00
F	-	+630.00
G	+30.00	+10.00
H	+6.00	+10.00
I	+10.00	+10.00
J	+2.00	+3.00
K	+5.00	+6.00
L	+5.00	+4.00
M	+9.00	+17.00

Even though system "I" passed the test it was observed that the compression plate lacked the needed force to compress the breast. The compression was not firm enough hence during breast examinations, breast will not receive the maximum compression they require. System D has no display screen hence the compression force test could not be carried out. However under maximum compression, a force of 170 N and 200 N was calculated during Automatic Compression and Manual Compression respectively. These results can be used as baseline data for further studies. Power compression test was not performed on system F due to malfunctioning of the compression paddles. The system also failed the manual compression test recording a difference in value between the measured and displayed force of +630 N. Apart from results of Manual compression of system M, the FFDM systems recorded a relatively lower compression force difference than the CR systems.

Compression Thickness

Results from the compression thickness test is presented in Table 29. For the test to be passed, the displayed thickness must be within ± 5 mm of phantom thickness. System G failed the compression thickness test completely whiles system H failed the compression thickness accuracy test for the 45 mm PMMA phantom. This indicates that the breasts are not being compressed efficiently to the right thickness and hence can't achieve best image quality. Details of raw values from which Table 29 was produced is presented in Appendix G.

Table 29: Results of compression thickness test for all thirteen systems

Mammography systems	Compression thickness accuracy (mm) PMMA thickness		
	20 mm	45 mm	70 mm
A	4	3	3
B	2	4	1
C	5	5	1
D	0.5	1	2
E	3	3	2
F	4	1	0
G	11	10	11
H	2	6	5
I	3	3	1
J	4	4	3
K	4	2	3
L	3	4	3
M	2	2	3

Compression Alignment

Results from the compression alignment test is presented in Table 30. Results from system C shows that it failed the compression alignment test "Right Diff. (r-f)" which is the difference on the right side of the compression plate between the rear and front. Values obtained from system E's compression

alignment tests - Left Diff. (r-f) and Right Diff. (r-f) were 9 mm and 9 mm respectively. The values were more than the tolerance limit of ≤ 5 mm according to the European Quality Control of Physical and Technical Aspects of Mammography Screening protocol. The values measured indicate that the compression plate is misaligned for systems C and E which means patient breast is not optimally compressed during imaging. Details of raw values from which Table 30 was produced is presented in Appendix H.

Table 30: Results of compression alignment test for all thirteen systems

Mammography systems	Compression alignment accuracy (mm)			
	Rear Diff. (l-r)	Front Diff. (l-r)	Left Diff.(r-f)	Right Diff. (r-f)
A	1	0	2	3
B	1	0	2	1
C	0	1	5	6
D	1	1	1	3
E	0	0	9	9
F	1	2	1	2
G	4	3	5	4
H	3	0	4	3
I	1	1	1	1
J	0	0	0	2
K	4	0	3	1
L	1	1	1	1
M	1	1	2	0

Image Quality Test

The differences in attenuation of the various soft tissue structures in the female breast are small hence image quality is of high importance. Using the ImageJ software, circular Region-of-interest (ROI) was drawn on DICOM images (Figure 25 - Figure 27) obtained from the system for 20 mm, 45 mm and 70 mm PMMA slabs fitted with a spacer for an equivalent breast thickness of 21 mm, 53 mm and

90 mm respectively and data extracted from them which was used to calculate the signal – to – noise ratio (SNR). The results of the test are presented in Table 31. Details of raw values from which Table 31 was produced is presented in Appendix I.

Table 31: Results from Image Quality assessment for all thirteen systems

Mammography systems	*Signal to noise ratio (SNR)* PMMA Phantom thickness / equivalent breast thickness (mm)		
	20/21 mm	45/53 mm	70/90 mm
A	8.92	7.39	6.38
B	9.10	6.08	3.35
C	-	-	-
D	6.71	2.65	0.06
E	-	-	-
F	12.20	6.02	2.68
G	-	-	-
H	12.79	5.21	4.12
I	11.22	3.19	0.77
J	16.42	10.64	8.56
K	-	-	-
L	-	-	-
M	9.94	5.61	5.35

Quantitative image quality assessment was undertaken using the "Rose Model" for image quality assessment (Cunningham et al., 1999). DICOM images were not obtained from systems C, E, G, K and L because the DICOM package was not installed on the computer system as part of the purchasing agreement. This happened in three (3) private facilities and two (2) government facilities. Albert Rose Model for image quality states that "the ability to detect an object is related to the ratio of the signal to noise (SNR) and an object is distinguishable from the background if the SNR is equal to or greater than 5". The quality of images from

system A, J and M for all three thicknesses were of good quality. From Table 31 images from the test on the 20 mm phantom were of good quality for all the thirteen (13) systems. System B, F and H recorded good images for the 45 mm phantom. Systems D and I recorded poor image quality for the 45 mm phantom. Images of the 70 mm phantom from systems B, D, F, H and I were of poor quality. The images from the FFDM systems were generally of a better quality than the CR systems. Results also show that images of lower thickness was of better quality than those of high thickness which indicates that when the breast is well compressed during examination, the potential of achieving a high image quality is better.

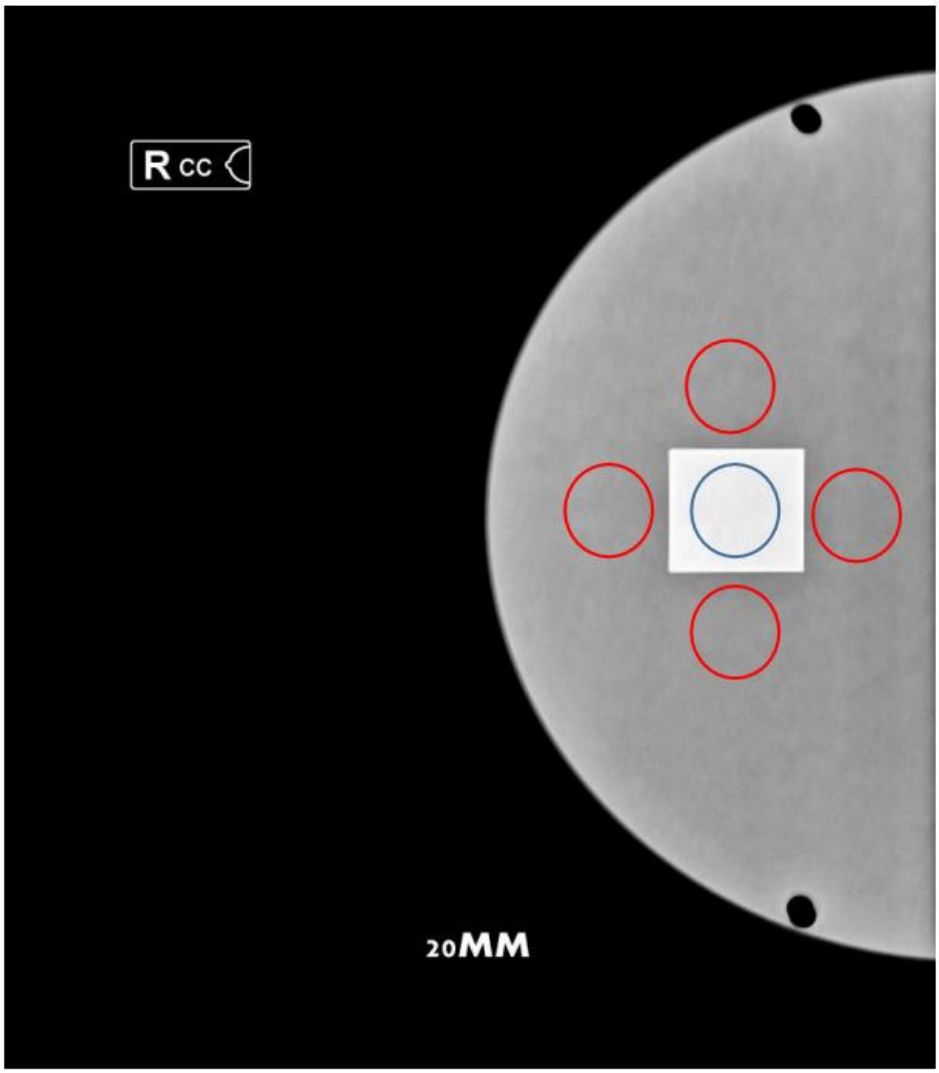

Figure 25: Circular ROI drawn on 20 mm phantom image

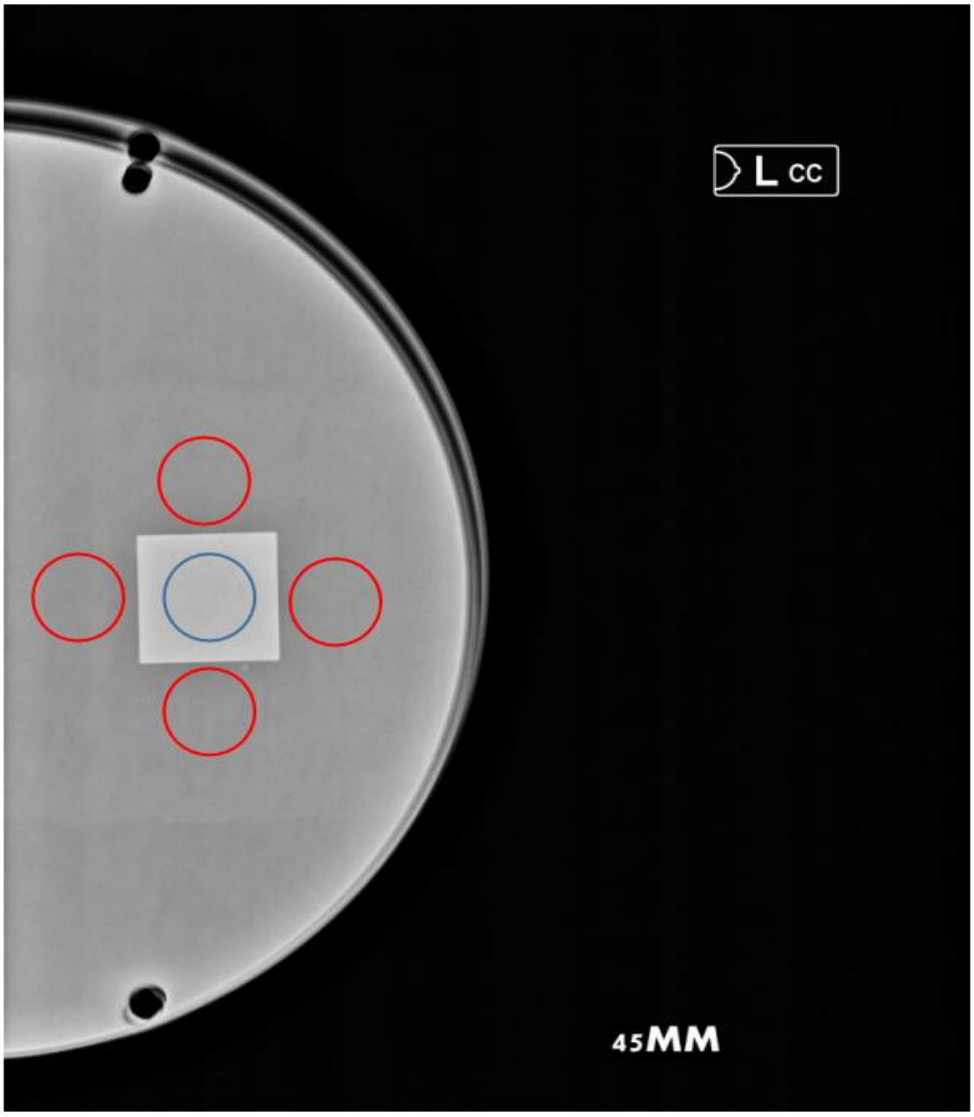

Figure 26: Circular ROI drawn on 45 mm phantom image

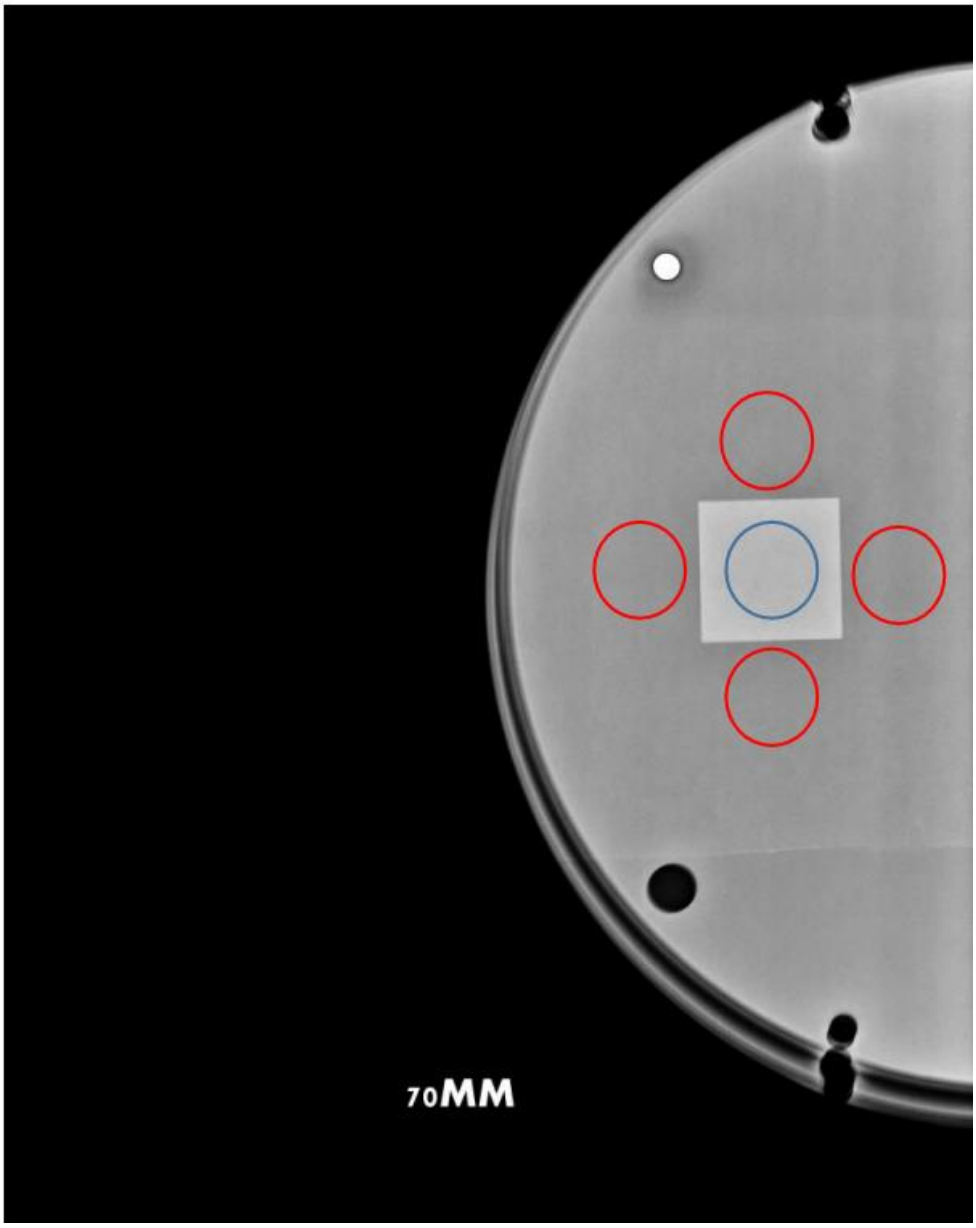

Figure 27: Circular ROI drawn on 70 mm phantom image

Estimation of Mean Glandular Dose (MGD)

MGD delivered by the systems at different equivalent breast thicknesses was estimated using the model as described by Dance and colleagues (Dance, 1990; Dance et al., 2000, 2009, 2011) and the results presented in Table 32. Details of raw values from which Table 32 was produced is presented in Appendix J.

The results were compared with the IAEA dosimetry protocol (IAEA, 2007) and the European Quality Control of Physical and Technical Aspects of Mammography Screening. Estimated value for system A's 60 mm and 75 mm equivalent breast thickness exceeded the acceptable limit by 17.07 % and 3.92 % respectively. System J's estimated mean glandular dose value for 75 mm equivalent breast phantom exceeded the acceptable limit by 9.52 %. All other estimated mean glandular doses were within the acceptable limits. A Graph of mean glandular dose against equivalent thickness of breast is presented in Figure 28. The graph shows a general increase in MGD values with increasing thickness with exceptions from system J.

Since systems J, K, L and M are FFDM systems the percentage difference between the displayed and estimated doses were determined. The result is presented in Table 33. It was found that the percentage difference between the patient (displayed) and estimated MGD for all four (4) systems were lower than 50%. The results show that the difference in all cases were below the set protocol level. Other authors report similar or even higher differences (Smans, Bosmans, Xiao, Carton & Marchal, 2006; Young et al., 2004). The possible reasons for the observed differences between phantom and patient (displayed) values are differences in

standard breast (represented by the phantom) composition and the composition of the real breasts, uncertainty in the breast thickness measurements, inaccuracies in the determination of HVL, some uncertainties related to the dosimeter and tube loading meter readings. The average of the MGD and standard deviation was also calculated for all the systems and the results presented in Table 34. From the results, system F recorded the lowest values of 1.07 ± 0.54 mGy and system A recorded the highest value of 2.74 ± 2.25 mGy. Both were CR systems. Among the FFDM systems, the highest value was recorded by system J whiles the lowest value was recorded by system K.

Table 35 presents a comparison amongst the mean glandular dose values from the study and the doses found in other studies using the same method i.e calculated incident air Kerma for 5 cm thick PMMA phantom (equivalent to a 6 cm thick breast). The results of this study compared favourably well.

For the FFDM systems, MGD was also measured using the ACR phantom and the values presented in Table 36. All four (4) systems complied with the maximum limit of 3 mGy for average patient breast (simulated by use of the mammographic phantom, approximately 4.2 cm compressed breast thickness of 50 % adipose – 50 % glandular composition at 28 kVp). It was realised that system M recorded the lowest MGD value during the ACR MAP test. All results obtained from the study can be used as baseline data for quality control at the Centres whose Mammography equipment was part of the study.

Table 32: Results of mean glandular dose assessment for all thirteen systems

PHANTOM THICKNESS / EQUIVALENT BREAST THICKNESS (mm)	ACCEPTABLE LEVEL (mGy)	RESULTS (mGy)												
		A	B	C	D	E	F	G	H	I	J	K	L	M
20/21	1.00	0.26	0.56	0.22	0.35	0.67	0.40	0.78	0.87	0.65	0.72	0.32	0.88	0.92
30/32	1.50	0.94	0.60	1.14	0.89	1.08	0.70	1.16	1.39	1.00	1.48	1.02	1.49	1.33
40/45	2.00	1.45	0.74	1.82	1.34	1.37	0.84	1.35	1.29	1.08	2.06	1.34	1.50	1.67
45/53	2.50	1.79	1.07	2.29	1.72	1.55	0.87	1.61	1.50	1.38	1.57	1.41	1.45	1.43
50/60	3.00	3.56	1.43	2.86	2.62	1.73	1.26	1.98	1.88	1.76	1.52	1.48	1.42	1.48
60/75	4.50	4.68	1.92	4.15	3.58	2.12	1.42	2.29	3.04	1.98	3.14	1.63	2.09	1.88
70/90	6.50	6.49	2.64	5.14	4.76	2.86	2.01	3.70	4.96	2.93	4.39	2.24	2.35	4.91

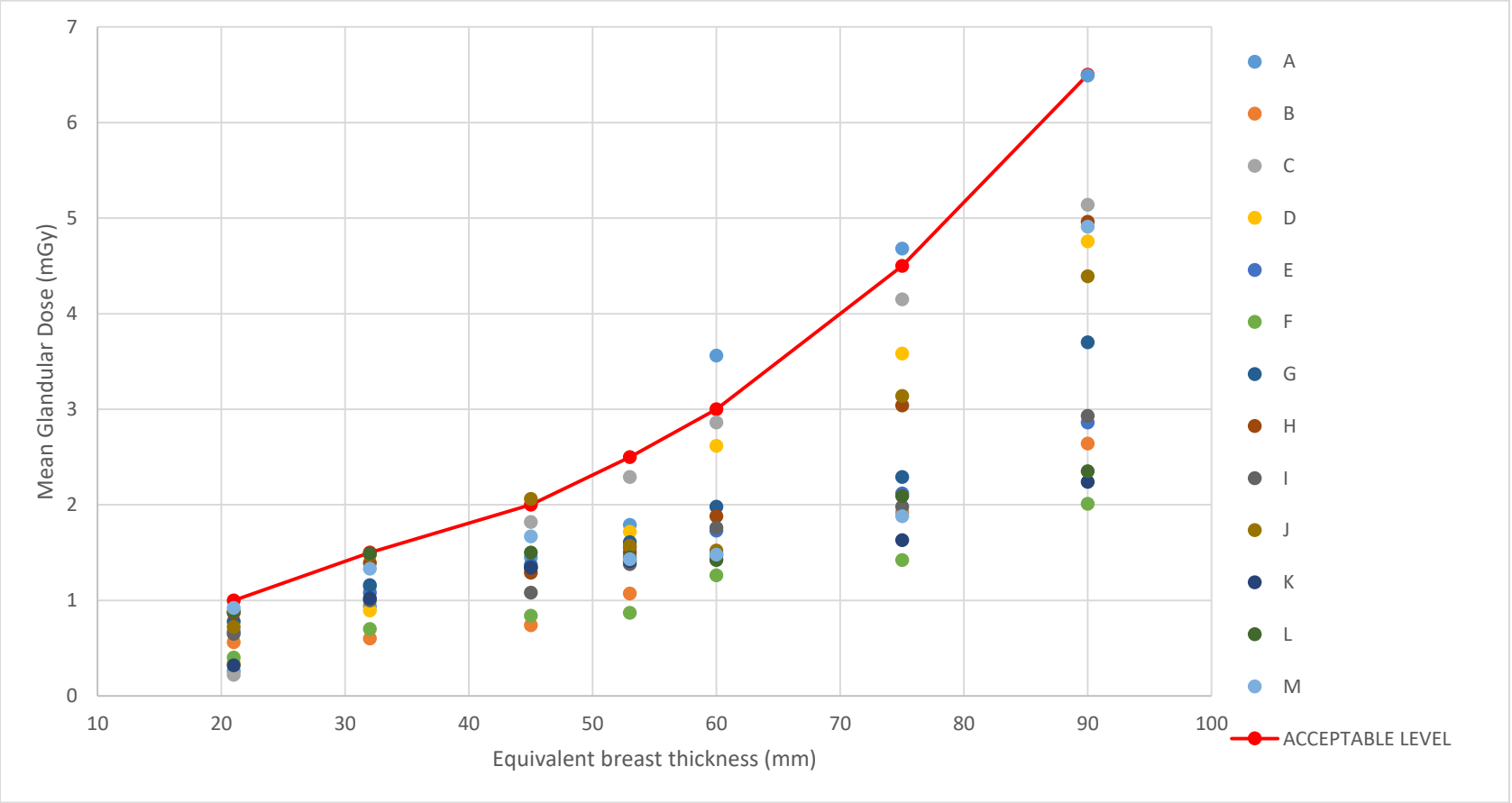

Figure 28: Graph of mean glandular dose against equivalent thickness of breast

Table 33: Results of percentage difference between displayed and estimated doses for FFDM systems

Thickness of equivalent breast (mm)	Percentage difference between calculated and displayed (%)			
	J	K	L	M
2.10	3.64	23.39	3.99	6.64
3.20	7.57	13.22	15.24	22.48
4.50	5.21	8.91	2.92	13.03
5.30	8.02	11.25	-0.38	5.71
6.00	18.60	1.81	19.16	15.17
7.50	33.64	22.19	34.49	29.56
9.00	42.17	14.23	36.72	37.44

Table 34: Results of average MGD with standard deviation

Mammography systems	Average MGD ± SD
A	2.74 ± 2.25
B	1.28 ± 0.77
C	2.52 ± 1.70
D	2.18 ± 1.57
E	1.63 ± 0.71
F	1.07 ± 0.54
G	1.84 ± 0.96
H	2.13 ± 1.42
I	1.54 ± 0.76
J	2.13 ± 1.24
K	1.35 ± 0.58
L	1.59 ± 0.48
M	1.95 ± 1.34

Table 35: Results compared with other studies

Study	MGD / mGy
This study	1.92 ± 0.68
Oliveira et al. (2011)	2.73 ± 0.10
Dantas el al. (2010)	2.20 ± 0.14
NHSBSP (2008)	2.29
NHSBSP (2009)	2.7
Wilson et al. (2010)	1.89 ± 0.98

Table 36: Results of MGD assessment using ACR MAP

FFDM System	Displayed MGD (mGy)
J	0.98
K	1.35
L	1.84
M	0.81

Establishment of Diagnostic Reference Levels (DRL)

The diagnostic reference levels (DRL) were determined for a range of PMMA thicknesses from 20 mm – 70 mm. The measured MGD was ordered from the lowest to the highest for a particular PMMA thickness. The 95th percentile of the mean glandular dose based on PMMA phantom measurements was calculated for the different equivalent breast thicknesses. The 95th percentile of the calculated mean glandular dose values refers to the point at which 5% of a calculated value exceeded the referenced value. The reason this statistic is so useful in measuring

data is that it gives a very accurate picture of the distribution of the values. The percentage difference between the DRL and the values that exceeded them was also calculated and the results presented in Table 37. MGD values for system A (50 mm and 70 mm) exceeded the DRL by 12.54% and 13.31% respectively), system J (30 mm, 40 mm and 60 mm) exceeded the DRL by 0.40%, 7.27% and 3.33% respectively), system M (20 mm) exceeded the DRL by 3.31% and system C (45 mm) exceeded the DRL by 14.02%.

Table 37: Results of 95th percentile calculations

PMMA thickness (mm)	95^{th} Percentile of MGD (mGy)	Percentage difference (%)
20	0.90	2.64
30	1.48	0.40
40	1.92	7.24
45	1.99	14.02
50	3.14	12.54
60	4.79	3.33
70	5.68	13.31

Results from Table 37 indicate that the percentage difference between the DRL and the values that exceeded them where less than 15%. This Figure can be used as a baseline data for further studies. A graphical presentation of the DRLs is shown in Figure 29 – 35.

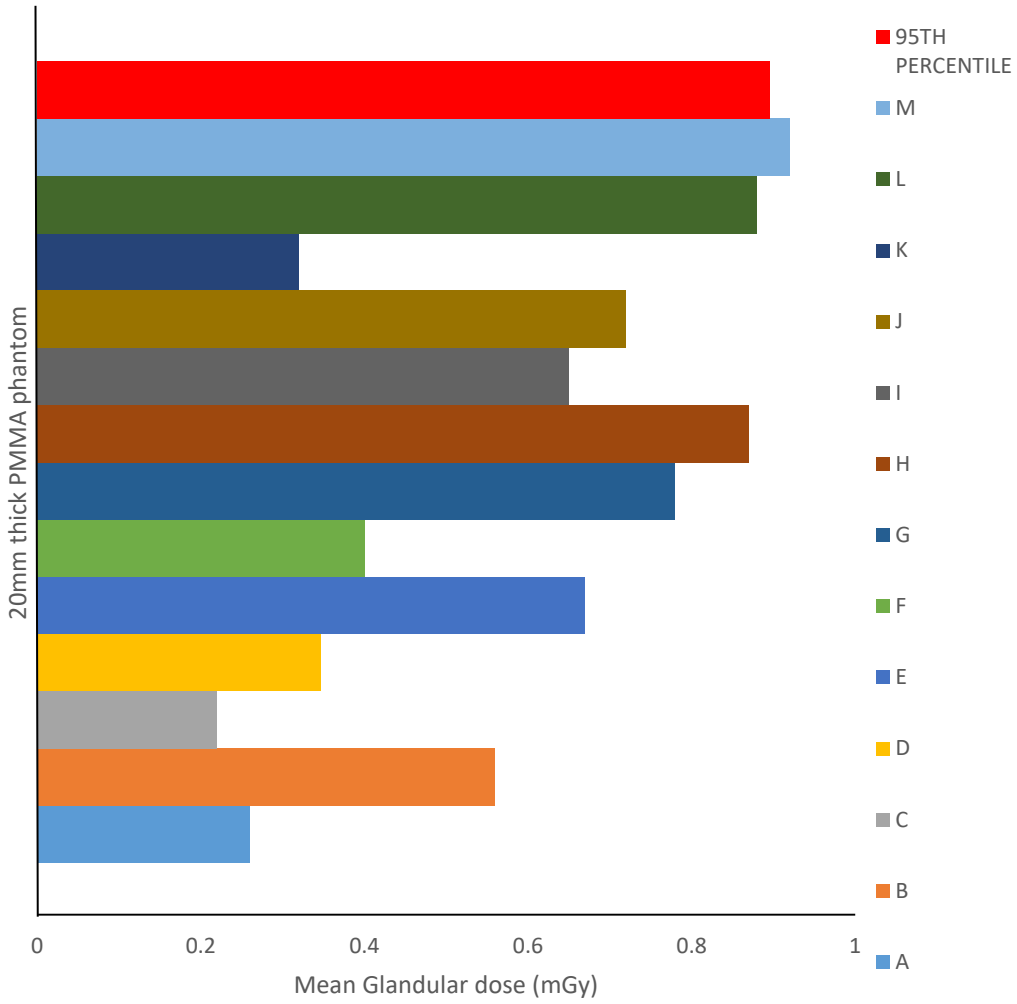

Figure 29: Graph of MGD for 20 mm thick PMMA Phantom compared with 95th percentile (DRL)

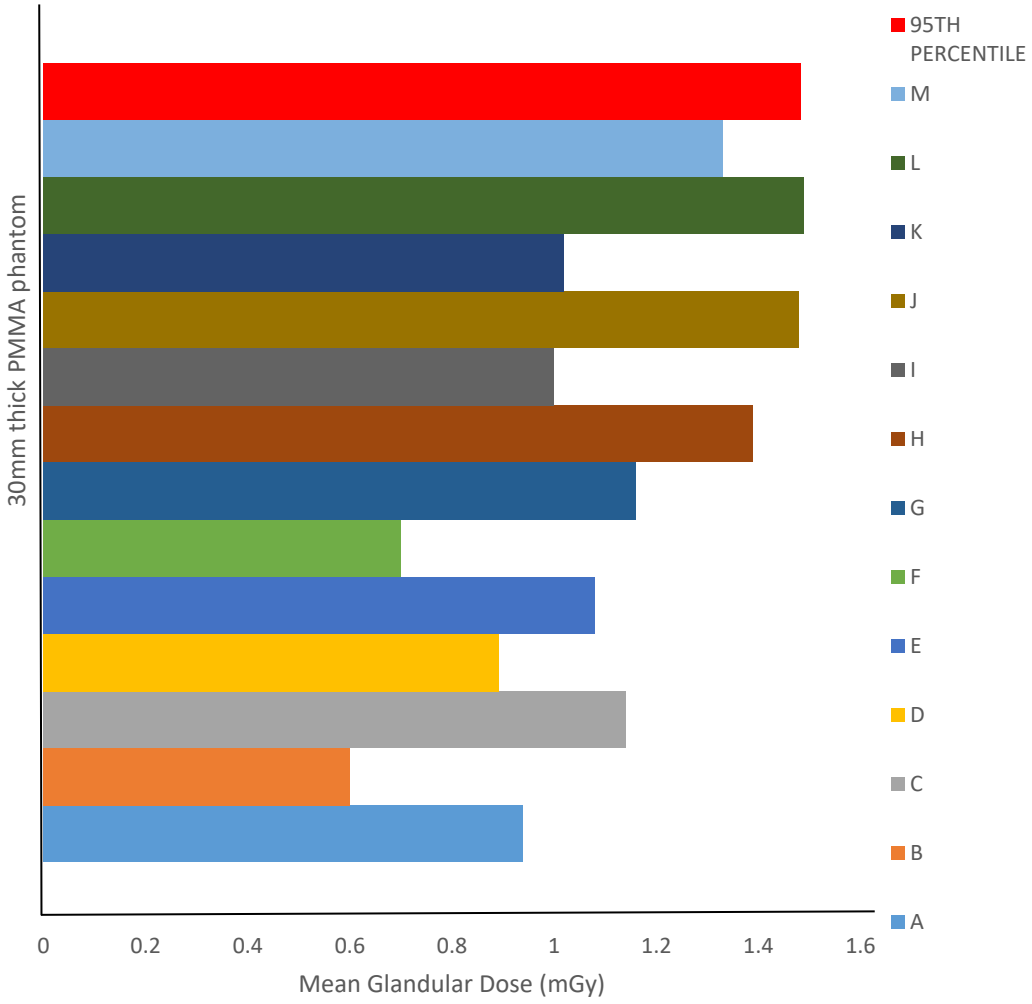

Figure 30: Graph of MGD for 30 mm thick PMMA Phantom compared with 95th percentile (DRL)

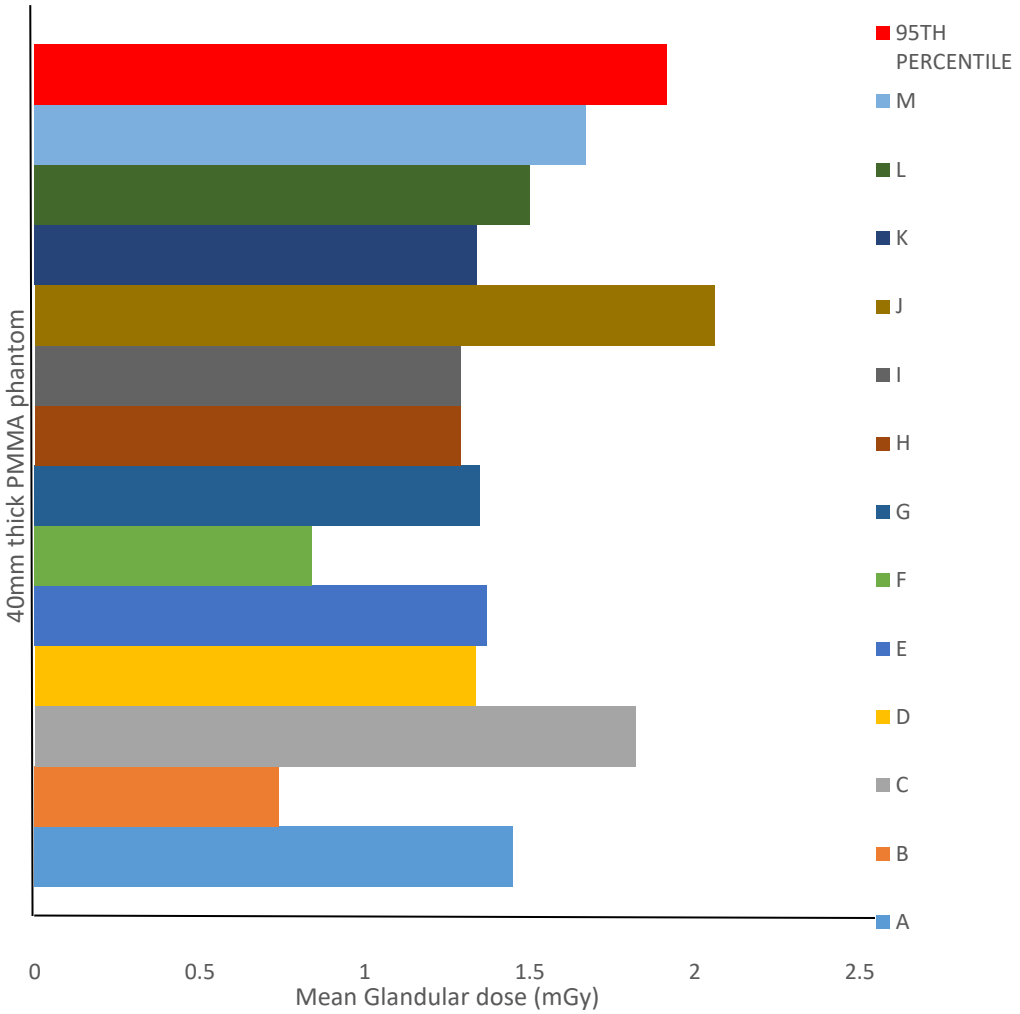

Figure 31: Graph of MGD for 40 mm thick PMMA Phantom compared with 95th percentile (DRL)

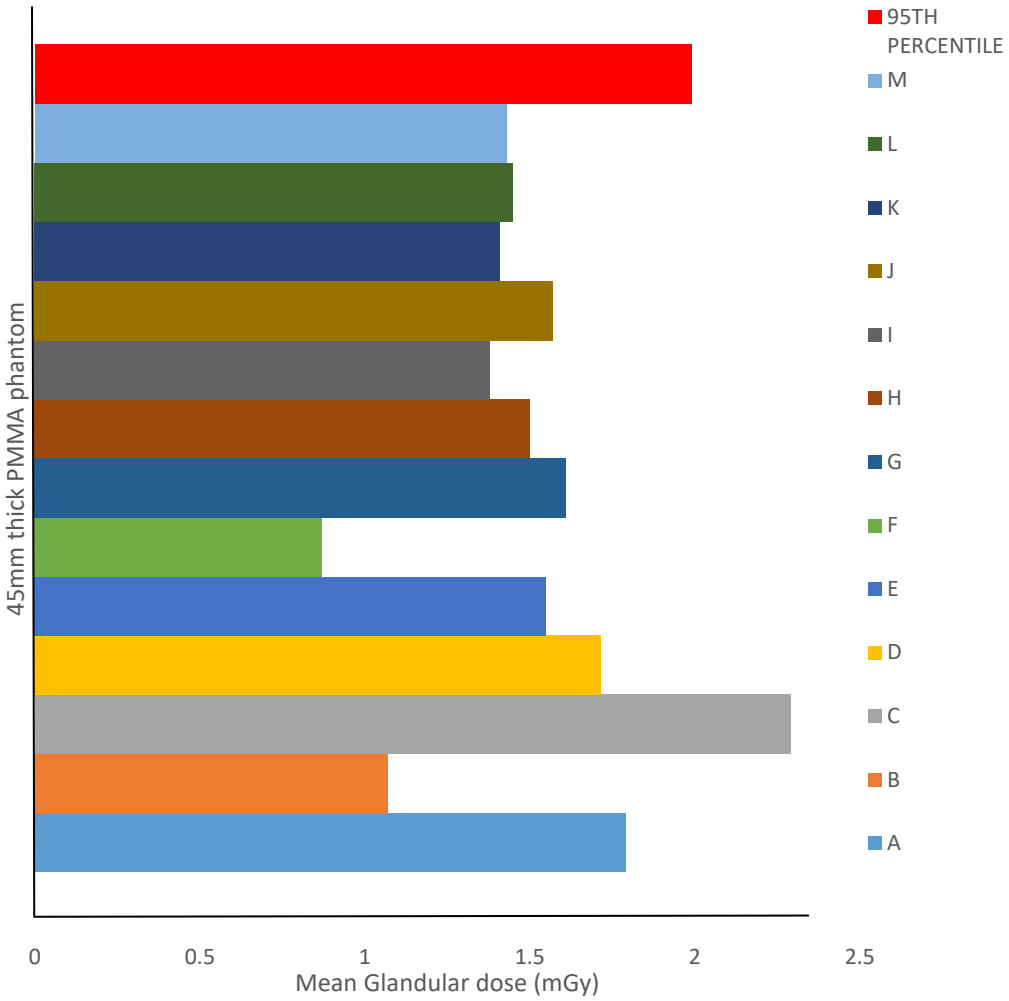

Figure 32: Graph of MGD for 45 mm thick PMMA Phantom compared with 95th percentile (DRL)

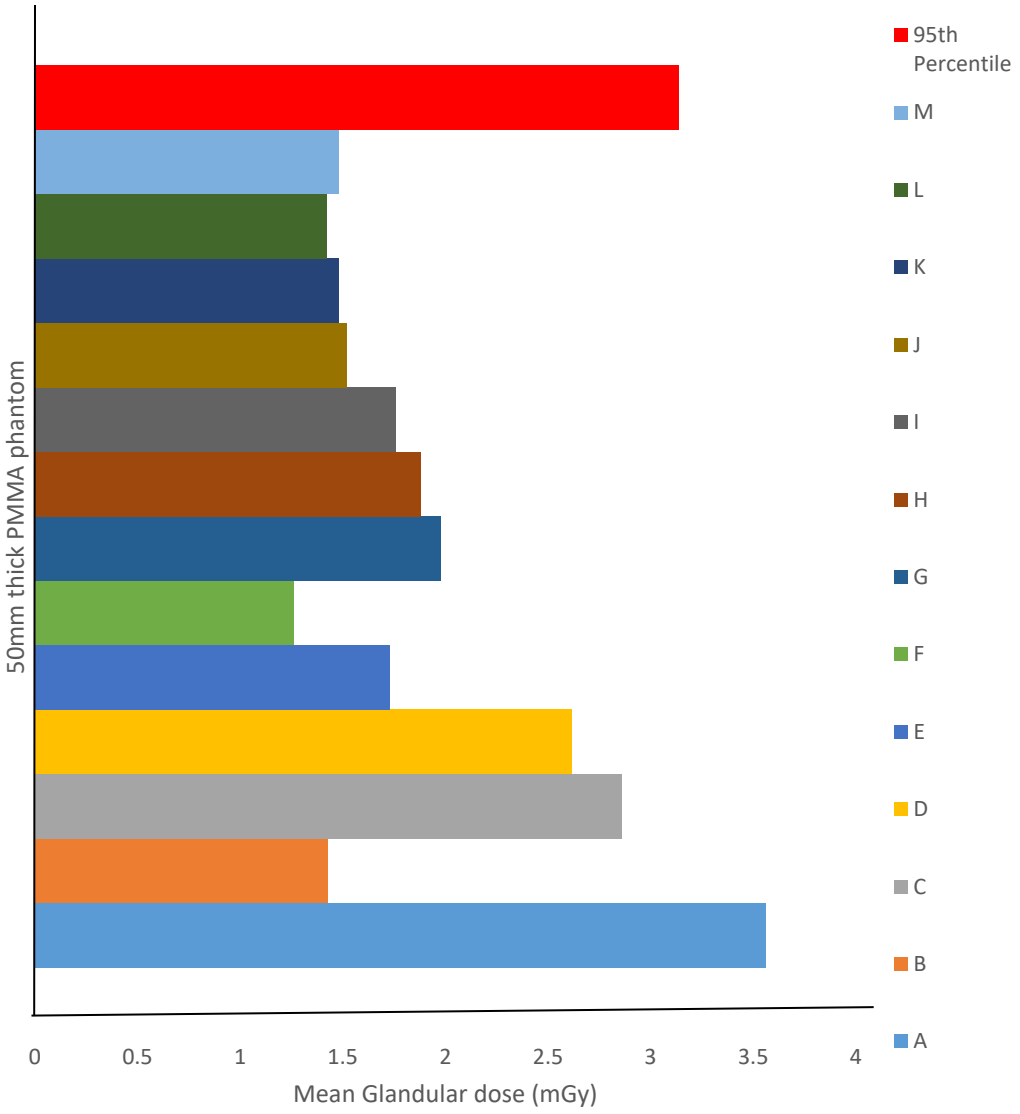

Figure 33: Graph of MGD for 50 mm thick PMMA Phantom compared with 95th percentile (DRL)

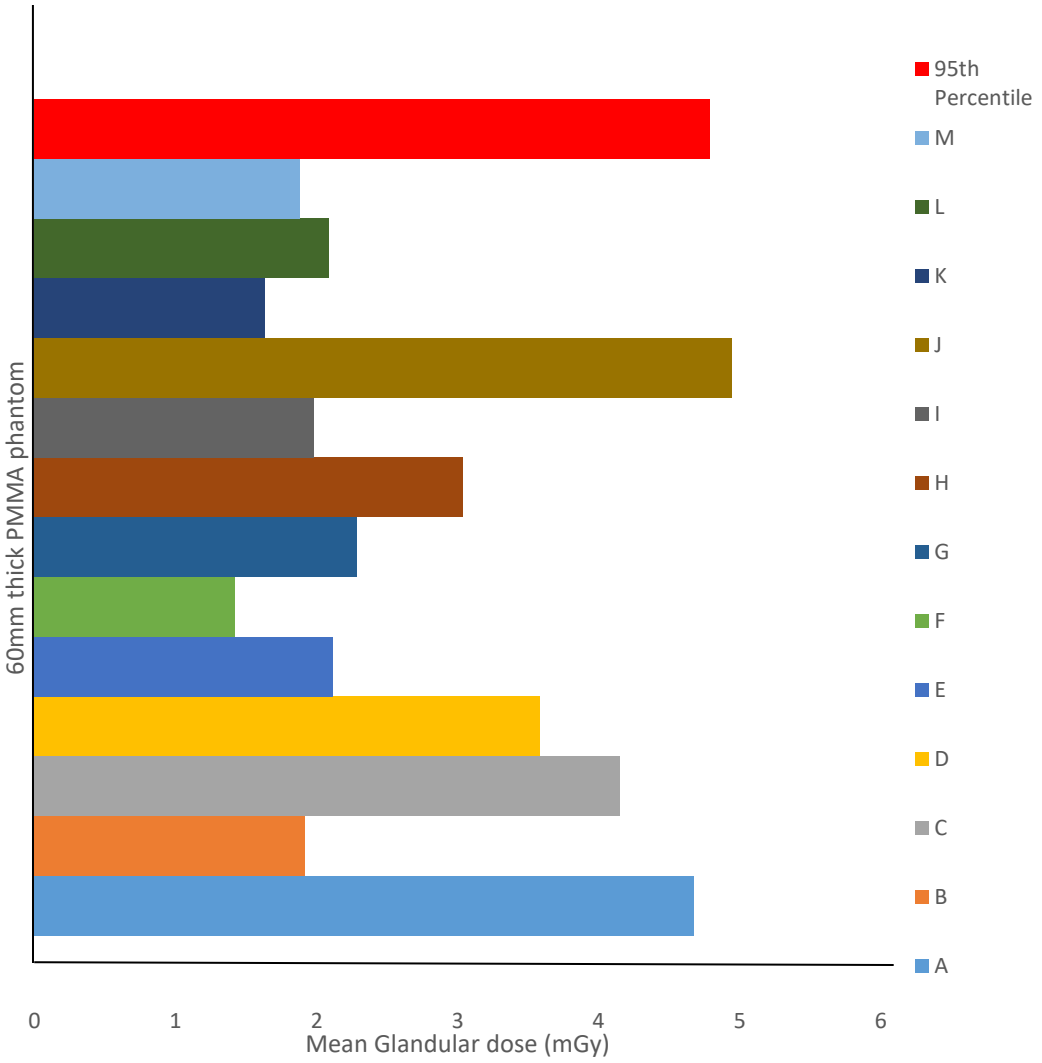

Figure 34: Graph of MGD for 60 mm thick PMMA Phantom compared with 95th percentile (DRL)

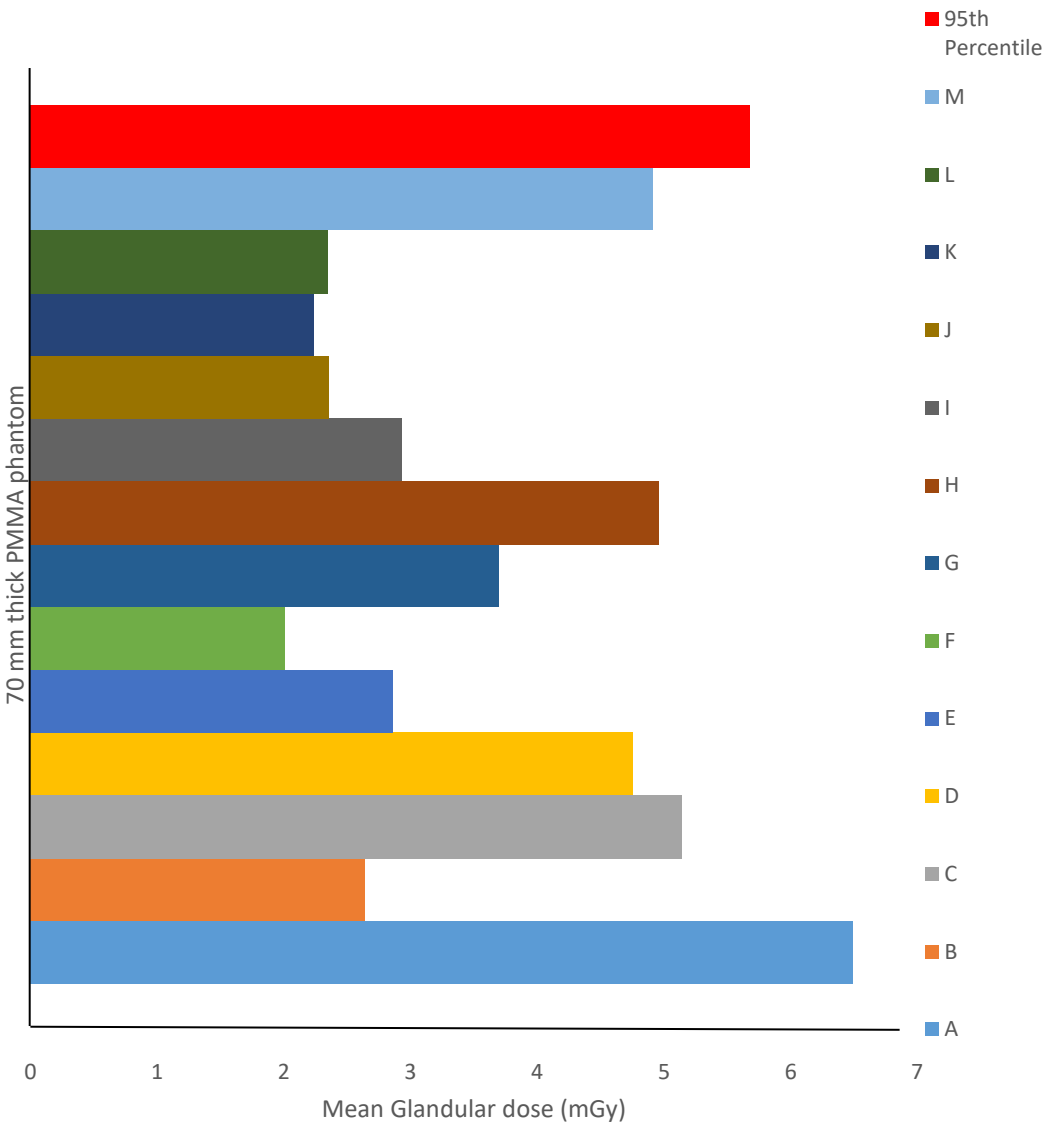

Figure 35: Graph of MGD for 70 mm thick PMMA Phantom compared with 95th percentile (DRL)

Modelled equations

Relationship between compressed breast thickness and tube voltage

With the aid of the MINITAB application software, the relationship between the compressed breast thickness and the tube voltage was modelled from phantom data and regression equation produced (equation 17). The equation has standard deviation of 0.60 and R^2 value of 89.95 %.

$$\boldsymbol{X = 23.9986 + 0.0862315\ (Y)} \quad (17)$$

where X denotes tube voltage and Y denotes compressed breast thickness.

Relationship between compressed breast thickness and tube output

With the aid of the MINITAB application software, the relationship between the compressed breast thickness and the tube output was modelled from phantom data and two regression equations were produced (equation 18 and equation 19). Equation 18 which was modelled for breast thicknesses between 5 mm and 20 mm had standard deviation of 0.233 and R^2 value of 81.04 %.

$$\boldsymbol{X_1 = 2.50493\ (Y_1) - 11.59459} \quad (18)$$

where X_1 denotes tube output and Y_1 denotes compressed breast thickness.

Equation 19 which was modelled for breast thicknesses between 20 mm and 85 mm had standard deviation of 0.123 and R^2 value of 89.66 %.

$$\boldsymbol{X_2 = 2.50493\ (Y_2) - 31.59459} \quad (19)$$

where X_2 denotes tube output and Y_2 denotes compressed breast thickness.

Relationship between tube voltage, tube output and mean glandular dose

MINITAB application software was used to model the relationship between the tube voltage, tube output and mean glandular dose. The model was developed from phantom measurement data and one regression equation was produced (equation 20). Equation 20 had standard deviation of 0.073 and R^2 value of 92.00 %.

$$\boldsymbol{X_3 = 3.5 - 0.109\ (Y_3) + \ 0.0103(Z_3)} \quad (20)$$

where X_3 denotes mean glandular dose, Y_3 denotes tube voltage and Z_3 denotes tube output.

Relationship between mean glandular dose and image quality

The relationship between the mean glandular dose and image quality was modelled from phantom measurement data and one regression equation was produced (equation 21) which had standard deviation of 0.408 and R^2 value of 79.50 %.

$$\boldsymbol{X_4 = 10.8 - 3.20\ (Y_4)} \quad (21)$$

where X_4 denotes the image quality and Y_4 denotes the mean glandular dose.
With these modelled equations, it was possible to predict closely the tube voltage, tube output, mean glandular dose and the quality of the image before patient was exposed.

The model equations were employed over a range of phantom thicknesses. In Manual mode, the exposure parameters were entered and exposure taken. Values recorded by the model and values recorded post exposure are presented in Table 38. From the results, it was found that the percentage deviation between the MGD

values for the model and the input data ranged from 2.27% – 29%. It was observed that the deviation was much less at lower thicknesses than at higher thicknesses. The image quality for all images were however of good quality. The model is therefore a good alternative to determining the exposure parameters before patient is exposed.

Table 38: Results from application of Model

Phantom Thickness / Equivalent breast thickness (mm)	kVp		mAs		MGD /mGy		Percentage difference (%)	SNR	
	Model generated Input	Console actual inputted	Model generated Input	Console actual inputted	Model expected results	Model Console output		Model expected results	Model calculated value
20/21	25.70	26.00	38.50	40.00	0.89	0.87	2.27	7.96	7.89
30/32	26.60	27.00	43.50	42.00	1.05	0.98	6.90	7.44	7.21
40/45	27.40	27.00	68.60	71.00	1.21	1.30	7.17	6.91	7.07
45/53	27.90	28.00	81.10	80.00	1.30	1.60	20.69	6.65	6.88
50/60	28.31	28.00	93.65	90.00	1.38	1.52	9.69	6.39	6.61
60/75	29.17	29.00	118.70	110.00	1.54	1.80	15.57	5.86	5.96
70/90	30.03	30.00	143.70	140.00	1.71	2.29	29.00	5.34	5.67

The model was also used to predict the quality of images from systems K and L and the result is presented in Table 39.

Table 39: Results of Image Quality as predicted by Model

Mammography systems	Signal-to-noise ratio (SNR) PMMA Phantom thickness / equivalent breast thickness (mm)		
	20/21 mm	45/53 mm	70/90 mm
K	9.78	6.29	3.63
L	7.98	6.16	3.28

Based on the modelled equation results, it indicates that systems K and L recorded good images for 21 mm and 53 mm equivalent breast thicknesses whereas images of the 90 mm equivalent breast thicknesses were not of standard quality.

Chapter Summary

In summary, this chapter presented the various results of the measured parameters in both tables and graphs. The results provides answers to the questions that were set out to be solved. It also describes the relationship between the various measurable quantities that were used to calculate the derived quantities in order to draw reasonable conclusions. Furthermore it gives explains the modelled equations and their implications on the mammography process.

.

CHAPTER FIVE

SUMMARY, CONCLUSIONS AND RECOMMENDATIONS

Overview

Quality control of the mammography equipment is very important in the imaging process to ensure that diagnostic outcomes are appropriate and treatment is reliable. Without it, both patients and reporting radiologist may be led in a false direction. This chapter presents summary of the findings from this study and its associated recommendations.

Conclusions

The study was conducted to review the overall condition of mammography practice in Ghana in order to suggest improvements in the practice. It involved undertaking a comprehensive quality control test on mammography machines used in Ghana. The results from the unit assembly evaluation show that the compression paddle of two (2) out of the thirteen (13) systems was not functioning. None of the 13 facilities accessed had exposure chats to aid radiographers in their work. DICOM header package was not installed on five (5) systems G, C, E, K. and L. Results for tube voltage accuracy and repeatability, output linearity and repeatability and half value layer measurement indicated satisfactory radiological performance of the systems. System H failed the short term automatic exposure control test whiles the test could not be performed on systems F and I due to malfunction of the AEC system.

The compression force, compression thickness and compression alignment were also assessed. Systems A – C, E, H – M, all passed the compression force

(both manual and power) test. System G failed the power compression test. The test was not performed on systems D because the system had no display force screen and could not be performed on system F because the compression paddle was not functioning. System F failed manual compression test. It was realised that even though system I passed the test, the compression plate lacked the needed force to compress the breast. One (1) system failed the compression test completely whiles one (1) system failed the test for the 45 mm thick PMMA phantom. Values from the compression alignment test Left Difference (rear – front) and Right Difference (rear – front) were outside the tolerance limit of ≤ 5 mm. Their values represent misalignment of the compression plate.

Quantitative image quality assessment was also conducted using ImageJ software applying Albert Rose's Model. DICOM images were not obtained from systems C, E, G, K and L because the DICOM package was not installed on the computer system as part of the purchasing agreement. Calculated values of signal – to – noise ratio (SNR) show that the quality of images from system A, J and M for all three thicknesses were of good quality. All images from the test on the 20 mm phantom were all of good quality. System B, F and H recorded good images for the 45 mm phantom. Systems D and I recorded poor image quality for the 45 mm phantom. Images of the 70 mm phantom from systems B, D, F, H and I were of poor quality.

Mean glandular dose delivered to the breast was also estimated using the PMMA phantoms at different thicknesses. Results show that doses being received are within the acceptable levels with the exception of systems A which recorded

MGD values of 3.56 mGy and 4.68 mGy for the 60 mm and 75 mm equivalent breast thicknesses and system L which recorded a MGD value of 4.95 mGy for the 75 mm equivalent breast thickness. Values obtained for the determination of accuracy of dose delivered for FFDM systems show that the results were all within acceptable limits. The MGD was also measured for the FFDM systems using the ACR MAP and the results were consistent with ACR protocols. The diagnostic reference levels based on PMMA was also established for a range of PMMA thicknesses from 20 mm – 70 mm whose equivalent breast thickness is 21 mm – 90 mm. The values for the 45 mm PMMA phantom compare well with the 95th percentile value for the DIMOND (Belgium) project.

Challenges

Some challenges were encountered during the study. These include:

(i) Refusal to be part of the study – some facilities mostly private ones refused to be part of the study stating reasons such as lack of interest in the outcome. This can be attributed to ignorance on the part of facility owners and/or management on the need for quality control assessment on their imaging systems.

(ii) Broken down / non-functional equipment – some equipment were not functioning due to reasons such as damaged X-ray tube and blown out power systems.

(iii) Delays in approval process – with some facilities, the delays in the approval process meant a delay in the start of the project.

(iv) Insufficient funding – six out of the eight regions with Mammography equipment were covered. The insufficient funds for the project made it impossible to travel the Brong Ahafo Region and the Northern Region.

Recommendations

The assessment of the performance of the mammography equipment in the country as at December 2016 will help to improve on mammography practice in Ghana. With the outcome of the study adequately presented, the following recommendations are made:

(i) The Ministry of Health / Ghana Health Service

Firstly, among all the Centres used in this study and others that were not used, there is currently no facility with an imaging centre that has a resident Medical Physicist. As a start Medical Physicists should be employed at all Teaching Hospitals and Regional Hospitals to ensure that quality control and quality assurance checks on all imaging equipment (ionizing and non-ionizing) should be performed. These Medical Physicists will be responsible to plan and execute a schedule QC/QA activities in accordance with International timelines such as weekly, monthly, quarterly, half – yearly and yearly. This will ultimately reduce equipment run down time, ensure that correct radiation doses are delivered to patients and adequate radiation protection of staff are ensured.

Secondly, purchase of medical imaging equipment should not be done without the express involvement of a Medical Physicist as part of the purchasing team.

Finally, as part of purchase agreement of diagnostic medical imaging equipment, phantoms for image quality and dosimetry assessment should be included.

(ii) Nuclear Regulatory Authority (NRA)

The Authority should ensure that acceptance testing is conducted on diagnostic radiology equipment post installation before the equipment is used for clinical activities. The Authority should also liaise with the Ministry of Health to ensure that the equipment is used for clinical activities who will be responsible for their quality control and quality assurance programme.

(iii) To research community

Currently there is no diagnostic reference level in mammography in Ghana based on patient data. Further to this work, this can be undertaken.

REFERENCES

ACS (2014). *Breast Cancer: Facts and Figures.* Atlanta, Georgia. USA: American Cancer Society.

ACS (2016). American Cancer Society recommendations for the early detection of breast cancer.https://www.cancer.org/cancer/breast-cancer/screening-tests-and-early-detection/american-cancer-society-recommendations-for-the-early-detection-of-breast-cancer.html, 2016

AJCC (2010). American Joint Committee on Cancer - Cancer Staging Handbook. (7th, Ed.). Springer-Verlag, New York. 749-756

ACS (2015). *www.cancer.org/cancer/breast-cancer*. Retrieved November 30th, 2015, from www.cancer.org: https://www.cancer.org/cancer/breast-cancer/screening-tests-and-early-detection.html

ArcGIS (2017). https://en.wikipedia.org/wiki/ArcGIS Retrieved March 13th 2017

Barnes, B.A., & Xuan, H. (2016). Lecture Notes. Screen Film Mammography Equipment Unit. 3. Slide21–26. Retrieved from www.santarosa.edu/~xho/ /Unit%203%20-%20Mammography%20. equipment. pdf on 6th November

Baxter, N. (2001). Canadian Task Force on Preventive Health Care. "Preventive health care, 2001 update: should women be routinely taught breast self-examination to screen for breast cancer?" 11 - 12

Beaman, S., Lillicrap, S. C. & Price, J. L. (1983). Tungsten anode tubes with K-edge filters for mammography British Journal of Radiology. Number 56. 721-727.

Berg, W. A., Gutierrez, L., NessAiver, M. S., Carter, Bhargavan, W. B., Lewis, M. Robert, S., & Loffe, O. B. (2004). Diagnostic accuracy of mammography, clinical examination, US, and MR imaging in preoperative assessment of breast cancer. *Radiology*, 233(3), 830 - 849.

Berrington de Gonzalez, A., & Reeves, G. (2005). Mammographic screening before age 50 years in the UK: comparison of the radiation risks with the mortality benefits. *British Journal of Cancer, 93*(5), 590-596.

Bick, U., & Diekmann, F. (2010). Digital mammography. Medical radiology-Diagnostic imaging. 332-345.

Blamey, R. W., Wilson, A. R., & Patnick, J. (2000). ABC of breast diseases: screening for breast cancer. British Medical Journal, **320**, 689-693.

Boadu, M., Sosu, E. K., Hasford, F., Nani, K., Sackey, T. A., Schandorf, C., & Addison, E. K. (2012). Mammography Examination in Ghana: Preliminary Survey of Patients' Profiles. Journal of Applied Science and Technology, **17**, Nos. 1 & 2, 87-92.

Boulet, P., Gérardin, J., Acem, Z., Parent, G., Collin, A., Pizzo, Y., & Porterie, B. (2014). Optical and radiative properties of clear PMMA samples exposed to a radiant heat flux. International Journal of Thermal Sciences **82**, 1-8

Broeders, J. M., Voorde, M., Veldkamp, W. J. H., Engen, R. E., Landsveld – Verhoeven, C., Jong – Gunneman, M. N. L., Win, J. , Greve, K. D., Paap, E. & Heeten, G. J. (2015). Comparison of a flexible versus a rigid breast compression paddle: pain experience, projected breast area, radiation dose

and technical image quality. European Radiology. **25**(3): 821–829. (Published online 2014 Dec 11. doi:10.1007/s00330-014-3422-4)

Bryan, T. & Snyder, E. (2013). The Clinical Breast Exam: A Skill that Should Not Be Abandoned. *J Gen Intern Med. May; 28(5)*: 719–722. Published online 2013 Feb 23.

Burgess, A. E., Jacobson, F. L. & Judy, P. F. (2001). Human observer detection experiments with mammograms and power-law noise *Med Phys*, *28*, 419-437

CMAJ (2011). Recommendations on screening for breast cancer in average-risk women aged 40–74 years. *Canadian Medical Association Journal, 183(17),* 1957. doi:doi:10.1503/cmaj.110334

Chevalier, M., Leyton, F., Tavares, M. N., Oliveira, M., Teogenes, A. & Peixoto, J. E. (2012). Image Quality Requirements for Digital Mammography in Breast Cancer Screening, Imaging of the Breast - Technical Aspects and Clinical Implication, Laszlo Tabar (Ed.), ISBN:978-953-51-0284-7. Retrieved from (http://www.intechopen.com/books/imaging-of-the-breast technical-aspects-and-clinical-implication/quality-requirements-of-image-in-digital-mammography-for-breastcancer-screening.)

Cunningham, I. A. & Shaw, R. (1999). Signal-to-noise optimization of medical imaging systems *Journal of Optical Society of America Volume 16, No. 3*, March. 621-632.

DATA TABLE FOR: Polymers: Commodity Polymers: PMMA (2017). Matbase.com. https://www.matbase.com/material-categories/natural-and-synt-hetic-polymers/thermoplastics/commodity-polymers/material-properties-of-pol-ymethyl-methacrylate-extruded-acrylic-pmma.html#properties) Retrieved 27th March, at 11:50pm

de Paredes, E. S., Fatouros, P. P., Thunberg, S., Cousins, J. F., Wilson, J. & Sedgwick, T. (1998). Evaluation of a digital spot mammographic unit using a contrast detail phantom. In Digital Mammography. The 4th International Workshop on Digital Mammography, IWDM, Nijmegen, the Netherlands. Edited by Karssemeijer N, Thijssen M, Hendriks J and van Erning L Kluwer Academic Publishers, Dordrecht, The Netherlands. 47-50.

Dance, D. R., Monte Carlo calculation of conversion factors for the estimation of mean glandular breast dose (1990). *Physics in Medicine and Biology. Number 35,* 1211 – 1219

Dance, D. R., Skinner, C. L., Young, K. C., Beckett, J. R. & Kotre, C. J. (2000). Additional factors for the estimation of mean glandular breast dose using the UK mammography dosimetry protocol. *Physics in Medicine and Biology 45 (2000)* 3225–3240.

Dantas, M. A. V. (2010). Glandular dose in mammography services with computed radiography systems in Belo Horizonte, Brazil. 5th Latin American Congress of Medical Physics. Cusco, Peru

Dance, D. R., Young, K. C., & van Engen, R. E. (2011). Estimation of mean glandular dose for breast tomosynthesis: factors for use with the UK, European and IAEA breast dosimetry protocols. *Phys. Med. Biol. 56* 453–471

Dance, D. R., Christofides, S., Maidment, A.D.A., Mclean, I. D., & Ng, K. H. (2014). Diagnostic Radiology Physics – A handbook for teachers and students. 274-300

EC (2006). European guidelines for quality assurance in breast cancer screening and diagnosis (4th Ed.). European Commission, Luxembourg, Office for Official Publications of the European Communities

Elmore, J. G., Miglioretti, D. L., & Carney, P. A. (2003). Does practice make perfect when interpreting mammography? Part II. *Journal of the National Cancer Institute, 95*, 250 - 252.

EMRO (2006). Technical Publication Series 30 - Guidelines for the early detection and screening of breast cancer. World Health Organization.

EUCAN (2015). http://eu-cancer.iarc.fr/. Retrieved February 10th, 2016, from http://eu-cancer.iarc.fr/cancer-13-breast-screening.html

GLOBOCAN (2012). Estimated cancer incidence, mortality and prevalence worldwide. (http://globocan.iarc.fr/Pages/fact_sheets_cancer.aspx). Retrieved from globocan.iarc.fr.

GNA (2015). Retrieved December 20th, 2015, from https://www.ghanabusiness-news.com/2015/10/26/breast-cancer-deaths-among-ghanaian-women high-who/

Gordis, L., Donald, B. A, Chu, S. Y., Fajardo, L. L., Hoel, G. D., Laufman, R. L., Rufenbarger, A., Constance, S. R., Sullivan, J. C., Wasson, D. H., Westhoff, L., Carolyn, Y. & Zern, T. R (1997). Breast Cancer Screening for women Ages 40 – 49. *Journal of the National Cancer Institute, Volume 89, Number 14*. 1015 – 1026.

Haffty, B. G., Buchholz, T. A., & Perez, C. A. (2008). Early stage breast cancer. In *Principles and practice of radiation oncology* (5th ed). 175–291) Philadelphia: Lippincott company.

Hall , E. J., & Giaccia, A. J. (2012). *Radiobiology for the Radiologist*. Philadelphia: Wolters Kluwer Health/Lippincott Williams & Wilkins.

Hammerstein, G. R., Miller, D. W., White, D. R., Masterson, M. E., Woodard, H. Q. & Laughlin, J. S. (1979). Absorbed radiation dose in mammography. *Radiology Number 130*, 485 – 491

Haus, A. G. (2001). Historical Technical Developments in Mammography. *International Conference on Technology in Cancer Research and Treatment in the New Millennium*, 3. New York. Retrieved March 28th, 2017 , from www.adeninepress.com/tech/abstracts2.cfm

Hendrick, R. E. (2010). Radiation doses and Cancer risk from Breast Imaging Studies. *Radiology, 257(1),* 246 – 253.

Hogg, P., Kelly J., & Mercer C. (2015). Digital Mammography: A Holistic Approach. Radiation Dose in Mammography. 153 – 161.

Huda, W., Sajewicz., A. M., Ogden, K. M. & Dance, D. R. (2003). Experimental investigation of the dose and image quality characteristics of a digital mammography imaging system. *Med. Phys.30, 442–448.*

IAEA. (2001). *Human Health Series No. 17 - Quality Assurance programme in Digital Mammography.* Vienna, Austria: IAEA.

IAEA. (2002). *Radiological protection for medical exposure to ionizing radiation. Safety Standard Series (No RS-G-1.5).* Vienna, Austria: IAEA.

IAEA. (2004). *Optimization of the radiological protection of patients undergoing radiography, fluoroscopy and computed tomography. (TECDOC – 1423).* Vienna, Austria: IAEA.

IAEA. (2005). *Optimization of the radiological protection of patients :image quality and dose in mammography (coordinated research in Europe).* IAEA-TECDOC-1447. Vienna: Internationa Atomic Energy Agency.

IAEA. (2006). Safety Reports Series No. 39. Applying Radiation Safety Standards in Diagnostic Radiology and Interventional procedures using X-rays. Vienna, Austria.

IAEA. (2009). *Human Health Series No. 2. Quality Assurance Program for Screen Film Mammography*. IAEA. 125-130/203-205

IAEA. (2011). *Human Health Series No. 17. Quality Assurance Program for Digital Mammography*. IAEA. 109-114

IAEA. (2014). Diagnostic Radiology Physics: A Handbook for teachers and students. 209 – 240.

ICRP (1991). Recommendations of the International Commission on Radiological Protection. ICRP Publication 60, Annals of the ICRP. Volume 21, 1 – 3.

ICRP (2001). Diagnostic Reference Levels in Medical Imaging: Review and additional advice. International Commission on Radiological Protection. Supporting Guidance 2. Annals of the ICRP. Volume 31. Number 4. Pages 33 - 52.

IMAGINIS. (2008). www.imaginis.com/breast-cancer-resource-center/general-information-on-breast-cancer. Retrieved from www.imaginis.com: http://www.imaginis.com/general-information-on-breast-cancer/what-is-breast-cancer-1 on June 11

IMAGINIS. (2015). Retrieved November 30th, 2015 ,from http://www.imaginis.com/ breast-cancer-screening-prevention/mammographic-screening-is-key-to-the-early-detection-of-breast-cancer

IPEM. (2005). The commissioning and routine testing of mammographic X - ray systems. IPEM Report 89. York, UK: Institute for Physics and Engineering in Medicine.

IPEM (2004). Institute of Physics and Engineering in Medicine Guidance on the Establishment and Use of Diagnostic Reference Levels for Medical X-ray Examinations. IPEM report 88.

IPSM (1989). The Commissioning and Routine Testing of Mammographic X-ray Systems. Topic group report 59 (York: IPSM - Institute of Physical Sciences in Medicine)

IPSM (1994). The commissioning and routine testing of mammographic X-ray systems. Institute of Physical Sciences in Medicine (IPSM) Report 59, 2nd Edn. IPSM, York. 11 – 12

John Hopkins Medicine. (2015). www.hopkinsmedicine.org. Retrieved December 15th, 2015, from www.hopkinsmedicine.org:Http://www.hopkinsmedicine.org/healthlibrary/test_procedures/gynecology/breast_magnetic_resonance_imaging_mri_92,P09110/

Khuwaja, G. A. (2006). Breast Cancer Detection Using Mammography. 5th WSEAS International Conference on Signal Processing. 27 – 29 May. 20 - 23. Istanbul, Turkey.

Kolb, T. M., Lichy, J. & Newhouse, J. H. (2002). Comparison of the performance of screening mammography, physical examination, and breast US and evaluation of factors that influence them: an analysis of 27,825 patient evaluations. *Radiology , 225(1),*165 - 175.

Kösters, J. P. & Gøtzsche, P. C. (2003). "Regular self-examination or clinical examination for early detection of breast cancer". Cochrane Database Syst Rev (2). 8 - 9

Krans, B. (2012). Breast self – examination. Healthline News letter. Retrieved from https://www.healthline.com/health/breast-lump-self-exam on 20 August 2016

Lanca, L. & Silva, A. (2013). Digital Radiography Detectors: A Technical Overview. In *Digital Imaging Systems for Plain Radiography* 9 – 19 . New York: Springer. doi:DOI 10.1007/978-1-4614-5067-2_2

Land, C. E. (1979). Low-Dose Radiation – A Cause of Breast Cancer. *National Conference on Breast Cancer – 1979. September 6 – 8, 1979. New York N.Y USA.* 12 – 18. New York N.Y USA: American Cancer Society.

Månsson, L. G., Båth, M. & Mattsson, S. (2005). Priorities in optimisation of medical X-ray imaging - A contribution to the debate. *Radiation Protection Dosimetry 114* (1-3) 298-302

MAP (1997). Mammography Accreditation Phantom User Guide. GAMMEX Publications. 1 – 12

Masselink, W. S. (2005). National Breast Screening Programmes. *The Trinity Student Medical Journal, 6,* 17 - 21.

MCHG. (2012). *www.moderncancerhospital.com/stay-healthy/86.html*. Retrieved December 5th, 2015, from www.moderncancerhospital.com. What Are High Risk Factors of Breast Cancer: http://www.modern cancer hospital .com/stay-healthy/86.html

MED. (1997). Medical Exposure Directives. COUNCIL DIRECTIVE 97/43/EURATOM of 30 June on health protection of individuals against the dangers of ionizing radiation in relation to medical exposure, and repealing Directive 84/466/Euratom. Retrieved from (http://eur-lex.europa.eu/legal-content/en/TXT/?uri=CELEX:31997L0043) March 2017 at 11:00am

Meyers, R. A. (1995), "Molecular biology and biotechnology: a comprehensive desk reference", Wiley-VCH, 722ISBN 1-56081-925-1

Michigan Medicine. (2015). *www.mcancer.org*. Retrieved November 20th, 2015, from www.mcancer.org/breast-cancer/detection-and-prevention/breast-cancer-risk-factors:http://www.mcancer.org/breast-cancer/detection-and-prevention/breast-cancer-risk-factors

MINITAB (2017). https://technology.ku.edu/software/minitab#top.Retrieved from http://www.ku.edu/ on May 15th, 2017 at 11pm

Mole , R. H. (1978). The Sensitivity of the Human Breast to cancer induction by ionization radiation. . *The British Journal of Radiology, 51(606),* 401 – 405.

NCRP. (1986). National Council on Radiation Protection and Measurements Mammography: a User's Guide. Report 85 (Bethesda, MD: NCRP)

NHS. (2016). National Health Services *http://www.nhs.uk*. Retrieved December 10th, 2016, from http://www.nhs.uk:. http://www.nhs.uk/Conditions/Cancer-of-the-breast-female/Pages/Introduction.aspx

NHSBSP (2008). National Health Services Breast Screening Programme Equipment Report 0803. Technical evaluation of GE Essential Full Field Digital Mammography systems. 12 - 18

NHSBSP (2009). National Health Services Breast Screening Programme Equipment Report 0604. Commissioning and Routine testing of Full Field Digital Mammography systems. 56 - 62

Nelson, H. D., Tyne, K., Naik, A., Bougatsos, C., Chan, B., Nygren, P., & Humphrey, L. (2009). Screening for Breast Cancer. Systematic Evidence - Review Update for the US Preventive Services Task Force. Evidence Syntheses. Retrieved from https://www.ncbi.nlm.nih.gov/books/NBK-36392/

NIH. (1997).National Institute of Health. Breast Cancer Screening for women Ages 40 – 49. Consensus Development Conference. January 21 – 23. Retrieved September 5th, 2015, from http://consensus.nih.gov/1997/1997BreastCancerScreening103html.htm

Nisha, S. K. (2013). Image Quality Assessment Techniques. *International Journal of Advanced Research in Computer Science and Software Engineering. 3(7),* 636 - 640

Nsiah-Akoto, I., Andam, A. B., Adisson, E. K., & Forson, A. J. (2011). Preliminary Studies into the Determination of Mean Glandular Dose During Diagnostic Mammography Procedure in Ghana. *Research Journal of Applied Sciences, Engineering and Technology 3(8),* 720-724.

Ocean 2014 (2015). Quality Assurance Software for Piranha. Reference Manual. Version 3.4A. 25 – 31

Oliveira, M. A., Dantas, M., Vicente, A., Santana, C. P., Squair, L. P., Gomes, S. D. & Nogueira, S. M. (2011).. Assessment of glandular dose and image quality in mammography using computerised radiography employing a polymethylmetacrilate breast simulator. *Radiation measurements. Volume 46*.2081 – 2085

Ozsaran, Z. & Alanyali, S. D. (2013). Staging of Breast Cancer. In A. Haydaroglu , & G. Ozyigit , *Principles and Practice of Modern Radiotherapy Techniques in Breast Cancer*. 13 - 19. New York: Springer. doi:DOI 10.1007/978-1-4614-5116-7_2

Parikh, J. R. (2007). America College of Radiology Appropriateness Criteria on Palpable Breast Masses. *Journal of the American College of Radiology, 4(5)*, 285 – 288.

Rasband, W. S. (1997 - 2012). ImageJ, United States National Institutes of Health, Bethesda, Maryland, USA, imagej.nih.gov/ij/.1997–2012

Rose, A. (1948). The sensitivity performance of the human eye on an absolute scale *Journal of Optical Society of America Volume 38* 196–208

Rose, A. (1953). "Quantum and noise limitations of the visual process," *Journal of Optical Society of America Volume 43*, Pages 715-716

Rosenstein, M., Andersen, L. W. & Warner, G. G. (1985). Handbook of Glandular Tissue Doses in Mammography FDA 85-8239 (Rockville, MD: US Department of Health and Human Services)

RPoP (2013) Radiation Protection of patients. Diagnostic Reference Levels (DRLs) in Medical Imaging. https://rpop.iaea.org/RPOP/RPoP/Content/InformationFor/HealthProfessionals/1_Radiology/Optimization/diagnostic-reference-levels.htm

RTI. (2014). Piranha Reference Manual (English) Version 5.5C. 4 – 50.

Ruschin, M., Timberg, P., Svahn, T., Andersson, I., Hemdal, B., Mattsson, S., Båth, M. & Tingberg, A. (2007). Improved in-plane visibility of tumors using breast tomosynthesis In: Medical imaging 2007: Physics of medical imaging (Ed by J Hsieh, M J Flynn) Proc SPIE 6510 65104R

Säbel, M., Willgeroth, F., Aichinger, H. & Dierker, J. (1986) X-ray spectra and image quality in mammography. *Electromedica. Number 54* 158 - 165

Säbel, M. (1996). Recent developments in breast imaging. *Physics in Medicine and Biology, Volume 41*, 315- 318.

Sackey, T. A. & Yarney, J. (2009). Survey on reported Cancers at The National Centre for Radiotherapy and Nuclear Medicine from 2004 – 2008. Accra.

Sams, K., Bosmans, H., Xiao, M., Carton, A. K., Marshall, N., Young, K. & Marchal, G. (2004). *Towards proposition of a diagnostic (dose) reference*

level for mammographic acquisitions in breast screening measurements in Belgium. Proceedings of the DIMOND3 Workshop. 1 - 4

Sandborg, M., Tingberg, A., Ullman, G., Dance, R. & Carlsson, G. A. (2006). Comparison of clinical and physical measures of image quality in chest and pelvis computed radiography at different tube voltages. *Med. Phys. 33(11)* 4169-4175

Saslow, D., Boetes, C., Burke, W., Harms, S., Leach, M. O., Lehman, C. D. & Russell, C. A. (2007). American Cancer Society Guidelines for Breast Screening with Magnetic Resonance Imaging as an Adjunct to. CA*: A Cancer Journal for Clinicians*, *57*(2),75–89.

Saunders, R. S., & Samei, E. (2008). The effect of breast compression on mass conspicuity in digital mammography. *Med Phys 35*, pp 4464-4473

Smans, K., Bosmans, H., Xiao, M., Carton, A. K. & Marchal, G. (2006). Towards a proposition of a diagnostic (dose) reference level for mammographic acquisitions in breast screening measurements in Belgium. *Radiation. Protection. Dosimetry. 117(1–3)*, 321–326.

Siu, A. L. (2016) United States Preventive Services Task Force. Screening for breast cancer: U.S. Preventive Services Task Force recommendation statement. *Annals of Internal Medicine. 164(4)*:279-296,

Stanton, L., Villafana, T., Day, J. L. & Lightfoot, D. A. (1984). Dosage evaluation in mammography *Radiology. Number 150*. 577-584

Storm, E. & Israel, H. I. (1970). Photon cross sections from 1 keV to 100 MeV for elements Z = 1 to Z =100. *Nuclear Data Tables. Volume A7* 565 - 681

TABAR, L. (2003). Mammography service screening and mortality in breast cancer patients: 20 year follow up before and after introduction of screening. *The Lancet - United Kingdom Medical Journal, 361* , 1405–1410.

USPSTF (2009). Retrieved November 30th, 2015, from www.uspreventiveservices taskforce.org: http://www.uspreventiveservicestaskforce.org/Page/Docume -nt/ UpdateSummaryFinal/breast-cancer-screening

Web MD. (2015). www.webmd.com/women/picture-of-the-breasts. Retrieved Dec -ember21st,2015,fromwww.webmd.com: www.webmd.com/women/pictu-re-of-the-breasts#1

WIKIPEDIA. (2015). Retrieved 15th December 2015, from https://en.wikipedia. org/ wiki/Mammography

WIKIPEDIA. (2016). Retrieved January 2017, from http://en.wikipedia.org/wiki /Styrofoam

World Health Organization. (2002). Breast Cancer Screening. IARC Handbooks of Cancer Prevention, 7, 2.

Yaffe, M.J., Barnes, G. T., Conway, B.J., Haus, A.G., Karellas, A., Kimme-Smith, C., Lin, P. J. P., Mawdsley, G., Rauch, P. & Rothenberg, L. N., (1990). Equipment requirements and quality control for mammography. [Report of

Task Group No 7, Diagnostic X-ray Imaging of the American Association of Physicist in Medicine]. [New York: American Institute of Physics. Report No 29]

Yaffe, M. J. (2006). The Biomedical Engineering Handbook. CRC Press, USA. 3rd Edition. Medical Devices and systems (X-rays). Ed Joseph D. Bronzino. Chapter 10. 210 – 227.

Yaffe, M. J., Bunch, P. C., Desponds, L., Jong, R. A., Nishikawa, R. M., Tapiovaara, M. J. & Young, K. C. (2009). Mammography - Assessment of Image Quality. Technical Aspects of Image Quality in Mammography. *Journal of International Commission on Radiation Units , Volume 9*, (Issue 2), 33-51. doi:doi.org/10.1093/jicru/ndp021

Young, K. C., Alsager, A., Oduko, J. M., Bosmans, H., Verbrugge, B., Geertse, T. & van Engen, R. (2008a). Evaluation of software for reading images of the CDMAM test object to assess digital mammography systems. In: Medical Imaging 2008: Physics of medical imaging (Ed by J Hsieh, E Samei) Proc SPIE 6913

Young, K. C., Oduko, J. M., Gundogdu, O. & Alsager, A. (2008b). "Comparing the performance of digital mammography systems." In: Eds. Krupinski EA, Proceedings of the 9th international workshop on digital mammography, IWDM. Tucson, Arizona, USA: Springer verlag Berlin, 732-739

APPENDICES

APPENDIX A

DATA SHEET FOR UNIT ASSEMBLY EVALUATION

	Parameter	Results Yes / No	Remarks Pass / Fail
1	Free standing unit is mechanically stable.		
2	Indicator lights working properly		
3	All moving parts move smoothly, without obstructions to motion.		
4	All locks and detents work properly.		
5	Angulation indicators function properly		
6	The compression plate is in good condition		
7	The compression breast thickness scale (analog or digital) is accurate and reproducible		
8	The automatic compression release following exposure functions correctly		
9	The manual release of compression is possible when power fails		
10	The compression release override works properly		
11	The radiation shield for the operator is adequate		
12	There are no sharp edges on the breast support or compression paddle		
13	The face guard is in place		
14	Panel switches, Indicator lights and meters working properly		
15	Images contain institution ID, patient ID, image acquisition time and date, and technique factors etc.		
16	DICOM header is populated correctly with institution ID, patient ID, image acquisition time and date, and technique factors etc.		

Unit assembly acceptable (Y/N)?

APPENDIX B

RAW DATA FOR THE ESTIMATION OF KVP ACCURACY AND REPEATABILITY

MAMMOGRAPHY SYSTEM	A	B	C	D	E	F	G	H	I	J	K	L	M
kVp1	27.37	27.36	27.44	27.40	28.09	28.20	27.85	27.76	28.71	28.10	28.07	27.41	27.10
kVp2	27.42	27.35	27.45	27.30	28.21	28.16	27.66	27.04	28.89	28.21	28.04	27.38	27.66
Repeatability – Difference (%)	0.20	0.04	0.04	0.10	0.47	0.14	0.69	2.70	0.63	0.39	0.10	0.11	2.10
kVp3	27.43	27.65	27.49	27.30	28.20	28.17	27.65	27.28	28.72	28.11	28.04	27.44	27.55
kVp4	27.34	27.34	27.45	27.28	28.27	28.21	27.80	26.96	29.26	28.15	28.04	27.55	27.64
kVp5	27.34	27.39	28.00	27.30	28.19	28.17	27.56	27.10	28.75	28.08	27.92	27.49	27.68
Mean kVp <kVp>	27.38	27.40	27.57	27.30	28.19	28.18	27.70	27.20	28.76	28.13	28.02	27.45	27.53
Standard deviation (SD)	0.04	0.13	0.24	0.01	0.07	0.02	0.12	0.32	0.38	0.05	0.05	0.07	0.24
Repeatibility: COV (%)	0.20	0.50	0.88	0.10	0.23	0.08	0.43	1.18	1.32	0.21	0.21	0.25	0.88
Nominal kVp - Mean kVp	0.62	0.60	0.43	0.70	0.19	0.18	0.30	0.80	0.76	0.13	0.02	0.55	0.47

APPENDIX C

RAW AND PROCESSED DATA FOR THE ESTIMATION OF OUTPUT REPEATABILITY AND LINEARITY

MAMMOGRAPHY SYSTEM	mAs	ER1	ER2	ER3	ER4	ER5	Average value	SD
	40	3.858	3.872	3.858	3.852	3.854	3.869	0.007
A	80	8.279	8.278				8.279	
	120	11.700	11.680				11.690	
	40	2.520	2.434	2.406	2.405	2.406	2.400	0.00
B	80	4.584	4.580				4.582	
	130	7.859	7.863				7.861	
	40	5.319	5.368	5.368	5.230	5.362	5.33	0.059
C	80	10.70	10.80				10.75	
	125	16.68	16.70				16.69	
	40	3.602	3.600	3.599	3.597	3.600	3.600	0.002
D	80	7.228	7.228				7.228	
	120	11.28	11.27				11.275	
	40	4.625	4.530	4.536	4.524	4.515	4.546	0.045
E	80	9.056	9.049				9.053	
	120	14.12	14.05				14.09	
	40	4.219	4.228	4.220	4.219	4.221	4.221	0.004
F	80	8.582	8.582				8.582	
	125	13.48	13.37				13.43	
	40	3.410	3.375	3.331	3.368	3.379	3.373	0.028
G	80	6.801	6.732				6.767	
	125	10.63	10.64				10.635	
H	40	4.508	4.500	4.505	4.488	4.501	4.500	0.008

APPENDIX C continued

	80	9.003	9.020				9.012	
	120	14.09	14.12				14.105	
	40	3.233	3.239	3.238	3.241	3.240	3.238	0.003
I	80	6.541	6.530				6.536	
	120	10.24	10.21				10.24	
	40	1.1514	1.515	1.513	1.515	1.513	1.514	0.066
J	80	3.028	3.035				3.032	
	125	4.715	4.715				4.715	
	40	1.479	1.478	1.507	1.405	1.508	1.475	0.024
K	80	3.187	3.185				3.186	
	125	4.960	4.967				4.964	
	40	1.500	1.499	1.496	1.497	1.500	1.498	0.002
L	80	2.991	2.995				2.993	
	125	4.677	4.674				4.676	
	40	1.414	1.418	1.415	1.417	1.414	1.416	0.002
M	80	2.848	2.841				2.845	
	125	4.417	4.419				4.418	

APPENDIX C continued

Repeatibility: Difference (%)	Repeatibility: COV (%)	Output (Y_1)	Output (Y_2)	Output (Y_3)	Linearity	
					L_1	L_2
0.36	0.20	0.097	0.103	0.097	-0.48	0.01
3.50	2.00	0.060	0.057	0.060	3.03	2.71
0.92	1.11	0.133	0.134	0.133	-0.43	-0.32
0.10	0.050	0.100	0.100	0.100	-0.20	-0.08
2.10	0.99	0.114	0.113	0.117	0.22	1.83
0.21	0.09	0.106	0.107	0.107	-0.82	0.06
0.69	0.84	0.084	0.085	0.085	-0.16	0.29
0.18	0.17	0.113	0.082	0.082	-0.06	0.09

APPENDIX C continued

0.19	0.10	0.081	0.082	0.082	-0.45	0.14
0.10	0.10	0.038	0.038	0.038	-0.06	-0.23
0.10	2.84	0.037	0.040	0.040	-3.83	-0.15
0.10	0.12	0.038	0.037	0.037	0.06	-0.01
0.28	0.13	0.035	0.036	0.035	-0.23	-0.30

APPENDIX D

RAW AND PROCESSED DATA FOR THE ESTIMATION OF SHORT TERM AUTOMATIC EXPOSURE CONTROL (AEC)

	Tube Load (mAs)												
Exposures	A	B	C	D	E	F	G	H	I	J	K	L	M
1	8.3	12.2	12.6	12.0	3.1	-	7.0	50.7	-	144.0	5.1	105.3	44.0
2	8.2	12.3	12.6	12.2	3.1	-	7.0	51.7	-	147.0	5.0	105.2	46.0
3	8.2	12.3	12.7	12.0	3.0	-	7.0	52.3	-	144.0	5.1	103.3	46.0
4	8.2	12.3	12.5	12.0	3.1	-	7.0	53.5	-	144.0	5.1	103.3	46.0
5	8.3	12.2	12.3	12.2	3.0	-	7.0	53.4	-	147.0	5.1	105.3	46.0
6	8.2	12.2	12.7	12.0	3.0	-	7.0	53.4	-	144.0	5.1	107.3	44.0
7	8.3	12.3	12.7	12.0	3.0	-	7.0	54.0	-	143.0	5.1	107.3	46.0
8	8.2	12.0	12.5	12.0	3.0	-	7.0	54.0	-	143.0	5.0	107.2	46.0
9	8.2	12.2	12.3	12.2	3.1	-	7.0	54.0	-	144.0	5.0	105.3	46.0
10	8.2	12.3	12.5	12.0	3.0	-	7.0	54.0	-	147.0	5.1	105.3	44.0
Mean	8.23	12.23	12.54	12.06	3.01	-	7.0	53.1	-	144.7	5.07	105.48	45.4
Maximum	8.30	12.30	12.7	12.2	3.1	-	7.0	54.0	-	147.0	5.1	107.3	46.0
Minimum	8.20	12.00	12.3	12.0	3.0	-	7.0	50.7	-	143.0	5.0	103.3	44.0
Deviation (%)	1.22	2.45	3.19	1.7	3.30	-	0.0	6.21	-	2.76	1.97	3.79	4.41

APPENDIX E

RAW DATA FOR MEASURING AND ESTIMATING HALF VALUE LAYER (HVL) FOR MAMMOGRAPHY SYSTEMS

Appendix E -1: Raw data for measuring and estimating HVL for mammography system A

MEASURED HVL			CALCULATED HVL			
23 kVp						
	CC	ML0	Equation 11		Equation 12	
	0.299	0.299	kVp	23	kVp	23
	0.298	0.298	Constant	0.03	Constant	0.19
	0.298	0.297				
	0.297	0.297	HVL	0.26	HVL	0.42
	0.299	0.299				
SD	0.000837	0.001				
Mean	0.30	0.30				
25 kVp						
	CC	ML0	Equation 11		Equation 12	
	0.321	0.319	kVp	25	kVp	25
	0.32	0.318	Constant	0.03	Constant	0.19
	0.32	0.319				
	0.321	0.319	HVL	0.28	HVL	0.44
	0.32	0.32				
SD	0.000548	0.000707				
Mean	0.32	0.32				
27 kVp						
	CC	ML0	Equation 11		Equation 12	
	0.34	0.34	kVp	27	kVp	27
	0.34	0.339	Constant	0.03	Constant	0.19
	0.339	0.34				
	0.338	0.34	HVL	0.30	HVL	0.46
	0.339	0.399				
SD	0.000837	0.026501				
Mean	0.34	0.35				
29 kVp						
	CC	ML0	Equation 11		Equation 12	
	0.357	0.356	kVp	29	kVp	29
	0.357	0.356	Constant	0.03	Constant	0.19
	0.358	0.357				
	0.356	0.357	HVL	0.32	HVL	0.48
	0.358	0.357				
SD	0.000837	0.000548				
Mean	0.36	0.36				
31 kVp						
	CC	ML0	Equation 11		Equation 12	
	0.373	0.373	kVp	31	kVp	31
	0.373	0.373	Constant	0.03	Constant	0.19
	0.374	0.372				
	0.374	0.373	HVL	0.34	HVL	0.50
	0.377	0.372				
SD	0.001643	0.000548				
Mean	0.37	0.37				

Raw data for measuring and estimating HVL for mammography system A continued

33 kVp						
	CC	ML0	Equation 11		Equation 12	
	0.39	0.389	kVp	33	kVp	33
	0.388	0.389	Constant	0.03	Constant	0.19
	0.39	0.39				
	0.389	0.39	HVL	0.36	HVL	0.52
	0.39	0.389				
SD	0.0009	0.000548				
Mean	0.39	0.39				
35 kVp						
	CC	ML0	Equation 11		Equation 12	
	0.404	0.404	kVp	35	kVp	35
	0.404	0.404	Constant	0.03	Constant	0.19
	0.403	0.404				
	0.402	0.403	HVL	0.38	HVL	0.54
	0.404	0.403				
SD	0.000894	0.000548				
Mean	0.40	0.40				

Appendix E -2: Raw data for measuring and estimating HVL for mammography system B

MEASURED HVL			CALCULATED HVL			
23 kVp						
	CC	ML0	Equation 11		Equation 12	
	0.361	0.362	kVp	23	kVp	23
						0.1
	0.362	0.361	Constant	0.03	Constant	9
	0.361	0.361				
						0.4
	0.362	0.362	HVL	0.26	HVL	2
	0.362	0.362				
SD	0.00055	0.00055				
Mean	0.36	0.36				
25 kVp						
	CC	ML0	Equation 11		Equation 12	
	0.372	0.371	kVp	25	kVp	25
						0.1
	0.371	0.371	Constant	0.03	Constant	9
	0.372	0.372				
						0.4
	0.372	0.374	HVL	0.28	HVL	4
	0.371	0.374				
SD	0.000548	0.001517				
Mean	0.37	0.37				
27 kVp						
	CC	ML0	Equation 11		Equation 12	
	0.381	0.380	kVp	27	kVp	27
						0.1
	0.381	0.382	Constant	0.03	Constant	9
	0.381	0.382				

						0.4
	0.382	0.381	HVL	0.30	HVL	6
	0.382	0.381				
SD	0.000548	0.000837				
Mean	0.38	0.38				
29 kVp						
	CC	ML0	Equation 11		Equation 12	
	0.358	0.360	kVp	29	kVp	29
						0.1
	0.359	0.359	Constant	0.03	Constant	9
	0.358	0.359				
						0.4
	0.358	0.358	HVL	0.32	HVL	8
	0.359	0.360				
SD	0.000548	0.00084				
Mean	0.36	0.36				
31 kVp						
	CC	ML0	Equation 11		Equation 12	
	0.378	0.379	kVp	31	kVp	31
						0.1
	0.377	0.378	Constant	0.03	Constant	9
	0.378	0.378				
						0.5
	0.379	0.360	HVL	0.34	HVL	0
	0.377	0.378				
SD	0.000837	0.008173				
Mean	0.38	0.37				
33 kVp						
	CC	ML0	Equation 11		Equation 12	
	0.394	0.395	kVp	33	kVp	33
						0.1
	0.394	0.395	Constant	0.03	Constant	9
	0.395	0.395				
						0.5
	0.392	0.394	HVL	0.36	HVL	2
	0.393	0.394				
SD	0.0011	0.000548				
Mean	0.39	0.39				
35 kVp						
	CC	ML0	Equation 11		Equation 12	
	0.409	0.409	kVp	35	kVp	35
						0.1
	0.407	0.409	Constant	0.03	Constant	9
	0.408	0.409				
						0.5
	0.409	0.408	HVL	0.38	HVL	4
	0.408	0.407				
SD	0.000837	0.000894				
Mean	0.41	0.41				

Appendix E -3: Raw data for measuring and estimating HVL for mammography system C

MEASURED HVL			CALCULATED HVL			
23 kVp						
	CC	ML0	Equation 11		Equation 12	
	0.299	0.299	kVp	23	kVp	23
	0.298	0.3	Constant	0.03	Constant	0.19
	0.299	0.3				
	0.299	0.3	HVL	0.26	HVL	0.42
	0.299	0.299				
SD	0.00045	0.00055				
Mean	0.30	0.30				
25 kVp						
	CC	ML0	Equation 11		Equation 12	
	0.321	0.322	kVp	25	kVp	25
	0.321	0.322	Constant	0.03	Constant	0.19
	0.322	0.322				
	0.322	0.321	HVL	0.28	HVL	0.44
	0.321	0.322				
SD	0.0005477	0.0004472				
Mean	0.32	0.32				
27 kVp						
	CC	ML0	Equation 11		Equation 12	
	0.341	0.342	kVp	27	kVp	27
	0.341	0.342	Constant	0.03	Constant	0.19
	0.341	0.342				
	0.34	0.342	HVL	0.30	HVL	0.46
	0.341	0.341				
SD	0.000447	0.000447				
Mean	0.34	0.34				
29 kVp						
	CC	ML0	Equation 11		Equation 12	
	0.36	0.359	kVp	29	kVp	29
	0.359	0.36	Constant	0.03	Constant	0.19
	0.359	0.359				
	0.359	0.359	HVL	0.32	HVL	0.48
	0.36	0.361				
SD	0.000548	0.00089				
Mean	0.36	0.36				
31 kVp						
	CC	ML0	Equation 11		Equation 12	
	0.377	0.377	kVp	31	kVp	31
	0.376	0.377	Constant	0.03	Constant	0.19
	0.377	0.377				
	0.376	0.376	HVL	0.34	HVL	0.50
	0.377	0.377				
SD	0.000548	0.000447				
Mean	0.38	0.38				
33 kVp						
	CC	ML0	Equation 11		Equation 12	

	0.393	0.394	kVp	33	kVp	33
	0.393	0.394	Constant	0.03	Constant	0.19
	0.392	0.393				
	0.395	0.393	HVL	0.36	HVL	0.52
	0.393	0.393				
SD	0.0011	0.000548				
Mean	0.39	0.39				
35 kVp						
	CC	ML0	Equation 11		Equation 12	
	0.408	0.408	kVp	35	kVp	35
	0.408	0.408	Constant	0.03	Constant	0.19
	0.407	0.408				
	0.408	0.409	HVL	0.38	HVL	0.54
	0.408	0.408				
SD	0.000447	0.000447				
Mean	0.41	0.41				

Appendix E – 4: Raw data for measuring and estimating HVL for mammography system D

MEASURED HVL			CALCULATED HVL			
24 kVp						
	CC	ML0	Equation 11		Equation 12	
	0.312	0.312	kVp	24	kVp	24
	0.314	0.314	Constant	0.03	Constant	0.12
	0.311	0.314				
	0.314	0.314	HVL	0.27	HVL	0.36
	0.311	0.312				
SD	0.001517	0.001095				
Mean	0.31	0.31				
26 kVp						
	CC	ML0	Equation 11		Equation 12	
	0.334	0.335	kVp	26	kVp	26
	0.333	0.334	Constant	0.03	Constant	0.12
	0.333	0.334				
	0.334	0.334	HVL	0.29	HVL	0.38
	0.334	0.335				
SD	0.000548	0.000548				
Mean	0.33	0.33				
28 kVp						
	CC	ML0	Equation 11		Equation 12	
	0.352	0.352	kVp	28	kVp	28
	0.35	0.352	Constant	0.03	Constant	0.12
	0.35	0.352				
	0.351	0.351	HVL	0.31	HVL	0.40
	0.351	0.35				
SD	0.000837	0.000894				
Mean	0.35	0.35				
30 kVp						

	CC	ML0	Equation 11		Equation 12	
	0.368	0.368	kVp	30	kVp	30
	0.366	0.367	Constant	0.03	Constant	0.12
	0.366	0.367				
	0.368	0.368	HVL	0.33	HVL	0.42
	0.368	0.367				
SD	0.001095	0.000548				
Mean	0.37	0.36				
32 kVp						
	CC	ML0	Equation 11		Equation 12	
	0.384	0.384	kVp	32	kVp	32
	0.383	0.383	Constant	0.03	Constant	0.12
	0.384	0.383				
	0.383	0.383	HVL	0.35	HVL	0.44
	0.383	0.384				
SD	0.000548	0.000548				
Mean	0.38	0.38				
34 kVp						
	CC	ML0	Equation 11		Equation 12	
	0.399	0.399	kVp	34	kVp	34
	0.398	0.399	Constant	0.03	Constant	0.12
	0.398	0.398				
	0.398	0.398	HVL	0.37	HVL	0.46
	0.399	0.399				
SD	0.0005	0.000548				
Mean	0.40	0.40				
35 kVp						
	CC	ML0	Equation 11		Equation 12	
	0.405	0.405	kVp	35	kVp	35
	0.405	0.405	Constant	0.03	Constant	0.12
	0.404	0.404				
	0.403	0.404	HVL	0.38	HVL	0.47
	0.405	0.405				
SD	0.000894	0.000548				
Mean	0.40	0.40				

Appendix E – 5: Raw data for measuring and estimating HVL for mammography system E

MEASURED HVL			CALCULATED HVL			
23 kVp						
	CC	ML0	Equation 11		Equation 12	
	0.299	0.299	kVp	23	kVp	23
	0.298	0.3	Constant	0.03	Constant	0.19
	0.299	0.3				
	0.299	0.3	HVL	0.26	HVL	0.42
	0.299	0.299				
SD	0.00045	0.00055				
Mean	0.30	0.30				
25 kVp						

	CC	ML0	Equation 11		Equation 12	
	0.321	0.322	kVp	25	kVp	25
	0.321	0.322	Constant	0.03	Constant	0.19
	0.322	0.322				
	0.322	0.321	HVL	0.28	HVL	0.44
	0.321	0.322				
SD	0.000548	0.000447				
Mean	0.32	0.32				
27 kVp						
	CC	ML0	Equation 11		Equation 12	
	0.341	0.342	kVp	27	kVp	27
	0.341	0.342	Constant	0.03	Constant	0.19
	0.341	0.342				
	0.34	0.342	HVL	0.30	HVL	0.46
	0.341	0.341				
SD	0.000447	0.000447				
Mean	0.34	0.34				
29 kVp						
	CC	ML0	Equation 11		Equation 12	
	0.36	0.359	kVp	29	kVp	29
	0.359	0.36	Constant	0.03	Constant	0.19
	0.359	0.359				
	0.359	0.359	HVL	0.32	HVL	0.48
	0.36	0.361				
SD	0.000548	0.00089				
Mean	0.36	0.36				
31 kVp						
	CC	ML0	Equation 11		Equation 12	
	0.377	0.377	kVp	31	kVp	31
	0.376	0.377	Constant	0.03	Constant	0.19
	0.377	0.377				
	0.376	0.376	HVL	0.34	HVL	0.50
	0.377	0.377				
SD	0.000548	0.000447				
Mean	0.38	0.38				
33 kVp						
	CC	ML0	Equation 11		Equation 12	
	0.393	0.394	kVp	33	kVp	33
	0.393	0.394	Constant	0.03	Constant	0.19
	0.392	0.393				
	0.395	0.393	HVL	0.36	HVL	0.52
	0.395	0.393				
SD	0.0013	0.000548				
Mean	0.39	0.39				
35 kVp						
	CC	ML0	Equation 11		Equation 12	
	0.445	0.444	kVp	35	kVp	35
	0.445	0.446	Constant	0.03	Constant	0.19
	0.444	0.444				
	0.445	0.445	HVL	0.38	HVL	0.54
	0.444	0.445				

SD	0.000548	0.000837
Mean	0.44	0.44

Appendix E – 6: Raw data for measuring and estimating HVL for mammography system F

MEASURED HVL			CALCULATED HVL			
20 kVp						
	CC	ML0	Equation 11		Equation 12	
	0.252	0.254	kVp	20	kVp	20
	0.252	0.254	Constant	0.03	Constant	0.12
	0.253	0.253				
	0.252	0.253	HVL	0.23	HVL	0.32
	0.253	0.254				
SD	0.000548	0.000548				
Mean	0.25	0.25				
23 kVp						
	CC	ML0	Equation 11		Equation 12	
	0.292	0.295	kVp	23	kVp	23
	0.292	0.295	Constant	0.03	Constant	0.12
	0.294	0.3				
	0.292	0.296	HVL	0.26	HVL	0.35
	0.292	0.3				
SD	0.000894	0.002588				
Mean	0.29	0.30				
26 kVp						
	CC	ML0	Equation 11		Equation 12	
	0.324	0.324	kVp	26	kVp	26
	0.325	0.324	Constant	0.03	Constant	0.12
	0.324	0.324				
	0.324	0.325	HVL	0.29	HVL	0.37
	0.324	0.325				
SD	0.000447	0.000548				
Mean	0.32	0.32				
29 kVp						
	CC	ML0	Equation 11		Equation 12	
	0.352	0.352	kVp	29	kVp	29
	0.352	0.352	Constant	0.03	Constant	0.12
	0.353	0.353				
	0.352	0.353	HVL	0.32	HVL	0.41
	0.352	0.352				
SD	0.000447	0.000548				
Mean	0.35	0.35				
32 kVp						
	CC	ML0	Equation 11		Equation 12	
	0.377	0.377	kVp	32	kVp	32
	0.377	0.377	Constant	0.03	Constant	0.12
	0.378	0.377				
	0.377	0.378	HVL	0.35	HVL	0.44
	0.377	0.377				

SD	0.000447	0.000447				
Mean	0.38	0.38				
35 kVp						
	CC	ML0	Equation 11		Equation 12	
	0.412	0.412	kVp	35	kVp	35
	0.412	0.413	Constant	0.03	Constant	0.12
	0.411	0.413				
	0.412	0.413	HVL	0.38	HVL	0.47
	0.412	0.412				
SD	0.0004	0.000548				
Mean	0.41	0.41				

Appendix E – 7: Raw data for measuring and estimating HVL for mammography system G

MEASURED HVL			CALCULATED HVL			
20 kVp						
	CC	ML0	Equation 11		Equation 12	
	0.262	0.263	kVp	20	kVp	20
	0.262	0.263	Constant	0.03	Constant	0.12
	0.263	0.262				
	0.263	0.262	HVL	0.23	HVL	0.32
SD	0.000577	0.000577				
Mean	0.26	0.26				
23 kVp						
	CC	ML0	Equation 11		Equation 12	
	0.297	0.299	kVp	23	kVp	23
	0.297	0.299	Constant	0.03	Constant	0.12
	0.298	0.299				
	0.298	0.298	HVL	0.26	HVL	0.35
SD	0.000577	0.0005				
Mean	0.30	0.30				
25 kVp						
	CC	ML0	Equation 11		Equation 12	
	0.316	0.317	kVp	25	kVp	25
	0.316	0.317	Constant	0.03	Constant	0.12
	0.317	0.317				
	0.317	0.316	HVL	0.28	HVL	0.37
SD	0.000577	0.0005				
Mean	0.32	0.32				
27 kVp						
	CC	ML0	Equation 11		Equation 12	
	0.332	0.333	kVp	27	kVp	27
	0.332	0.333	Constant	0.03	Constant	0.12
	0.332	0.332				
	0.331	0.333	HVL	0.30	HVL	0.39
SD	0.0005	0.0005				
Mean	0.33	0.33				
29 kVp						
	CC	ML0	Equation 11		Equation 12	

	0.348	0.349	kVp	29	kVp	29
	0.348	0.349	Constant	0.03	Constant	0.12
	0.348	0.348				
	0.347	0.348	HVL	0.32	HVL	0.41
SD	0.0005	0.000577				
Mean	0.35	0.35				
31 kVp						
	CC	ML0	Equation 11		Equation 12	
	0.364	0.365	kVp	31	kVp	31
	0.364	0.365	Constant	0.03	Constant	0.12
	0.364	0.364				
	0.365	0.365	HVL	0.34	HVL	0.43
SD	0.0005	0.0005				
Mean	0.36	0.36				
33 kVp						
	CC	ML0	Equation 11		Equation 12	
	0.378	0.379	kVp	33	kVp	33
	0.378	0.379	Constant	0.03	Constant	0.12
	0.378	0.379				
	0.377	0.378	HVL	0.36	HVL	0.45
SD	0.0005	0.0005				
Mean	0.38	0.38				
35 kVp						
	CC	ML0	Equation 11		Equation 12	
	0.393	0.394	kVp	35	kVp	35
	0.393	0.394	Constant	0.03	Constant	0.12
	0.393	0.394				
	0.394	0.395	HVL	0.38	HVL	0.47
SD	0.0005	0.0005				
Mean	0.39	0.40				

Appendix E – 8: Raw data for measuring and estimating HVL for mammography system H

MEASURED HVL			CALCULATED HVL			
20 kVp						
	CC	ML0	Equation 11		Equation 12	
	0.256	0.256	kVp	20	kVp	20
	0.256	0.255	Constant	0.03	Constant	0.12
	0.255	0.256				
	0.256	0.255	HVL	0.23	HVL	0.32
SD	0.000500	0.000577				
Mean	0.26	0.26				
23 kVp						
	CC	ML0	Equation 11		Equation 12	
	0.297	0.297	kVp	23	kVp	23
	0.297	0.297	Constant	0.03	Constant	0.12
	0.296	0.296				

	0.296	0.296	HVL	0.26	HVL	0.35
SD	0.000577	0.000577				
Mean	0.29	0.30				
25 kVp						
	CC	ML0	Equation 11		Equation 12	
	0.319	0.318	kVp	25	kVp	25
	0.319	0.318	Constant	0.03	Constant	0.12
	0.318	0.318				
	0.318	0.319	HVL	0.28	HVL	0.37
SD	0.000577	0.0005				
Mean	0.32	0.32				
27 kVp						
	CC	ML0	Equation 11		Equation 12	
	0.338	0.337	kVp	27	kVp	27
	0.338	0.337	Constant	0.03	Constant	0.12
	0.339	0.337				
	0.339	0.338	HVL	0.30	HVL	0.39
SD	0.000577	0.0005				
Mean	0.34	0.34				
29 kVp						
	CC	ML0	Equation 11		Equation 12	
	0.356	0.355	kVp	29	kVp	29
	0.356	0.355	Constant	0.03	Constant	0.12
	0.355	0.355				
	0.355	0.356	HVL	0.32	HVL	0.41
SD	0.000577	0.0005				
Mean	0.36	0.36				
31 kVp						
	CC	ML0	Equation 11		Equation 12	
	0.372	0.372	kVp	31	kVp	31
	0.372	0.372	Constant	0.03	Constant	0.12
	0.371	0.371				
	0.371	0.372	HVL	0.34	HVL	0.43
SD	0.000577	0.0005				
Mean	0.37	0.37				
33 kVp						
	CC	ML0	Equation 11		Equation 12	
	0.387	0.387	kVp	33	kVp	33
	0.388	0.387	Constant	0.03	Constant	0.12
	0.387	0.387				
	0.388	0.388	HVL	0.36	HVL	0.45
SD	0.0006	0.0005				
Mean	0.41	0.41				
35 kVp						
	CC	ML0	Equation 11		Equation 12	
	0.402	0.402	kVp	35	kVp	35
	0.402	0.402	Constant	0.03	Constant	0.12
	0.401	0.401				
	0.402	0.402	HVL	0.38	HVL	0.47
SD	0.0005	0.0005				
Mean	0.40	0.40				

Appendix E – 9: Raw data for measuring and estimating HVL for mammography system I

MEASURED HVL			CALCULATED HVL			
23 kVp						
	CC	ML0	Equation 11		Equation 12	
	0.352	0.354	kVp	23	kVp	23
	0.352	0.354	Constant	0.03	Constant	0.19
	0.351	0.355	HVL	0.26	HVL	0.42
SD	0.000577	0.000577				
Mean	0.35	0.35				
25 kVp						
	CC	ML0	Equation 11		Equation 12	
	0.393	0.394	kVp	25	kVp	25
	0.393	0.394	Constant	0.03	Constant	0.19
	0.392	0.395	HVL	0.28	HVL	0.44
SD	0.000577	0.000577				
Mean	0.39	0.39				
27 kVp						
	CC	ML0	Equation 11		Equation 12	
	0.415	0.415	kVp	27	kVp	27
	0.415	0.415	Constant	0.03	Constant	0.19
	0.415	0.416	HVL	0.30	HVL	0.46
SD	0.0000	0.000577				
Mean	0.42	0.42				
29 kVp						
	CC	ML0	Equation 11		Equation 12	
	0.431	0.431	kVp	29	kVp	29
	0.432	0.431	Constant	0.03	Constant	0.19
	0.431	0.431	HVL	0.32	HVL	0.48
SD	0.000577	0.000				
Mean	0.43	0.43				
31 kVp						
	CC	ML0	Equation 11		Equation 12	
	0.446	0.446	kVp	31	kVp	31
	0.445	0.445	Constant	0.03	Constant	0.19
	0.446	0.446	HVL	0.34	HVL	0.50
SD	0.000577	0.000577				
Mean	0.45	0.45				
33 kVp						
	CC	ML0	Equation 11		Equation 12	
	0.461	0.461	kVp	33	kVp	33
	0.461	0.461	Constant	0.03	Constant	0.19
	0.461	0.461	HVL	0.36	HVL	0.52
SD	0.0000	0.0005				
Mean	0.46	0.46				
35 kVp						
	CC	ML0	Equation 11		Equation 12	
	0.475	0.475	kVp	35	kVp	35
	0.476	0.476	Constant	0.03	Constant	0.19
	0.475	0.475	HVL	0.38	HVL	0.54

SD	0.000577	0.000577
Mean	0.48	0.48

Appendix E – 10: Raw data for measuring and estimating HVL for mammography system J

MEASURED HVL			CALCULATED HVL			
23 kVp						
	CC	ML0	Equation 11		Equation 12	
	0.466	0.466	kVp	23	kVp	23
	0.467	0.466	Constant	0.03	Constant	0.3
	0.466	0.466				
	0.467	0.465	HVL	0.26	HVL	0.53
	0.466	0.465				
SD	0.000548	0.000548				
Mean	0.47	0.47				
25 kVp						
	CC	ML0	Equation 11		Equation 12	
	0.507	0.506	kVp	25	kVp	25
	0.506	0.507	Constant	0.03	Constant	0.3
	0.508	0.506				
	0.507	0.507	HVL	0.28	HVL	0.55
	0.506	0.506				
SD	0.000837	0.000548				
Mean	0.51	0.51				
27 kVp						
	CC	ML0	Equation 11		Equation 12	
	0.526	0.527	kVp	27	kVp	27
	0.527	0.526	Constant	0.03	Constant	0.3
	0.527	0.526				
	0.527	0.527	HVL	0.30	HVL	0.57
	0.529	0.526				
SD	0.001095	0.000548				
Mean	0.53	0.53				
29 kVp						
	CC	ML0	Equation 11		Equation 12	
	0.544	0.543	kVp	29	kVp	29
	0.543	0.542	Constant	0.03	Constant	0.3
	0.543	0.542				
	0.545	0.542	HVL	0.32	HVL	0.59
	0.545	0.543				
SD	0.001000	0.000548				
Mean	0.54	0.54				
31 kVp						
	CC	ML0	Equation 11		Equation 12	
	0.558	0.558	kVp	31	kVp	31
	0.558	0.558	Constant	0.03	Constant	0.3
	0.559	0.557				
	0.559	0.558	HVL	0.34	HVL	0.61

	0.558	0.557				
SD	0.000548	0.000548				
Mean	0.56	0.56				
33 kVp						
	CC	ML0	Equation 11		Equation 12	
	0.576	0.576	kVp	33	kVp	33
	0.576	0.576	Constant	0.03	Constant	0.3
	0.576	0.577				
	0.577	0.576	HVL	0.36	HVL	0.63
	0.577	0.577				
SD	0.0005	0.000548				
Mean	0.58	0.58				
35 kVp						
	CC	ML0	Equation 11		Equation 12	
	0.595	0.596	kVp	35	kVp	35
	0.595	0.596	Constant	0.03	Constant	0.3
	0.596	0.595				
	0.596	0.595	HVL	0.38	HVL	0.65
	0.596	0.595				
SD	0.000548	0.000548				
Mean	0.60	0.60				

Appendix E – 11: Raw data for measuring and estimating HVL for mammography system K

MEASURED HVL			CALCULATED HVL			
23 kVp						
	CC	ML0	Equation 11		Equation 12	
	0.466	0.466	kVp	23	kVp	23
	0.467	0.466	Constant	0.03	Constant	0.3
	0.466	0.466				
	0.467	0.465	HVL	0.26	HVL	0.53
	0.466	0.465				
SD	0.000548	0.000548				
Mean	0.47	0.47				
25 kVp						
	CC	ML0	Equation 11		Equation 12	
	0.507	0.506	kVp	25	kVp	25
	0.506	0.507	Constant	0.03	Constant	0.3
	0.506	0.506				
	0.507	0.507	HVL	0.28	HVL	0.55
	0.506	0.506				
SD	0.000548	0.000548				
Mean	0.51	0.51				
27 kVp						
	CC	ML0	Equation 11		Equation 12	
	0.526	0.527	kVp	27	kVp	27
	0.527	0.526	Constant	0.03	Constant	0.3
	0.527	0.526				

	0.528	0.527	HVL	0.30	HVL	0.57
	0.526	0.526				
SD	0.000837	0.000548				
Mean	0.53	0.53				
29 kVp						
	CC	ML0	Equation 11		Equation 12	
	0.544	0.543	kVp	29	kVp	29
	0.543	0.543	Constant	0.03	Constant	0.3
	0.543	0.544				
	0.545	0.544	HVL	0.32	HVL	0.59
	0.545	0.543				
SD	0.001000	0.000548				
Mean	0.55	0.36				
31 kVp						
	CC	ML0	Equation 11		Equation 12	
	0.559	0.559	kVp	31	kVp	31
	0.56	0.559	Constant	0.03	Constant	0.3
	0.559	0.559				
	0.559	0.588	HVL	0.34	HVL	0.61
	0.56	0.588				
SD	0.000548	0.015884				
Mean	0.56	0.57				
33 kVp						
	CC	ML0	Equation 11		Equation 12	
	0.576	0.577	kVp	33	kVp	33
	0.576	0.577	Constant	0.03	Constant	0.3
	0.576	0.577				
	0.577	0.576	HVL	0.36	HVL	0.63
	0.577	0.576				
SD	0.0005	0.000548				
Mean	0.58	0.58				
35 kVp						
	CC	ML0	Equation 11		Equation 12	
	0.596	0.596	kVp	35	kVp	35
	0.597	0.596	Constant	0.03	Constant	0.3
	0.596	0.595				
	0.597	0.595	HVL	0.38	HVL	0.65
	0.596	0.596				
SD	0.000548	0.000548				
Mean	0.60	0.60				

Appendix E – 12: Raw data for measuring and estimating HVL for mammography system L

MEASURED HVL			CALCULATED HVL			
23 kVp						
	CC	ML0	Equation 11		Equation 12	
	0.466	0.466	kVp	23	kVp	23
	0.466	0.466	Constant	0.03	Constant	0.3

	0.466	0.466				
	0.467	0.466	HVL	0.26	HVL	0.53
	0.466	0.467				
SD	0.000447	0.000447				
Mean	0.47	0.47				
25 kVp						
	CC	ML0	Equation 11		Equation 12	
	0.51	0.51	kVp	25	kVp	25
	0.51	0.51	Constant	0.03	Constant	0.3
	0.509	0.51				
	0.509	0.512	HVL	0.28	HVL	0.55
	0.509	0.511				
SD	0.000548	0.000894				
Mean	0.51	0.51				
27 kVp						
	CC	ML0	Equation 11		Equation 12	
	0.53	0.53	kVp	27	kVp	27
	0.53	0.53	Constant	0.03	Constant	0.3
	0.531	0.531				
	0.53	0.531	HVL	0.30	HVL	0.57
	0.531	0.53				
SD	0.000548	0.000548				
Mean	0.53	0.53				
29 kVp						
	CC	ML0	Equation 11		Equation 12	
	0.546	0.546	kVp	29	kVp	29
	0.546	0.546	Constant	0.03	Constant	0.3
	0.545	0.546				
	0.546	0.55	HVL	0.32	HVL	0.59
	0.546	0.55				
SD	0.000447	0.002191				
Mean	0.55	0.55				
31 kVp						
	CC	ML0	Equation 11		Equation 12	
	0.562	0.561	kVp	31	kVp	31
	0.562	0.561	Constant	0.03	Constant	0.3
	0.562	0.56				
	0.561	0.56	HVL	0.34	HVL	0.61
	0.561	0.56				
SD	0.000548	0.000548				
Mean	0.56	0.56				
33 kVp						
	CC	ML0	Equation 11		Equation 12	
	0.578	0.578	kVp	33	kVp	33
	0.578	0.578	Constant	0.03	Constant	0.3
	0.578	0.577				
	0.577	0.577	HVL	0.36	HVL	0.63
	0.577	0.577				
SD	0.0005	0.000548				
Mean	0.58	0.58				
35 kVp						
	CC	ML0	Equation 11		Equation 12	

	0.597	0.597	kVp	35	kVp	35
	0.597	0.597	Constant	0.03	Constant	0.3
	0.588	0.597				
	0.588	0.597	HVL	0.38	HVL	0.65
	0.587	0.598				
SD	0.005128	0.000447				
Mean	0.59	0.60				

Appendix E – 13: Raw data for measuring and estimating HVL for mammography system M

MEASURED HVL			CALCULATED HVL			
23 kVp						
	CC	ML0	Equation 11		Equation 12	
	0.466	0.466	kVp	23	kVp	23
	0.467	0.467	Constant	0.03	Constant	0.3
	0.466	0.466				
	0.467	0.466	HVL	0.26	HVL	0.53
	0.466	0.467				
SD	0.000548	0.000548				
Mean	0.30	0.30				
25 kVp						
	CC	ML0	Equation 11		Equation 12	
	0.51	0.51	kVp	25	kVp	25
	0.51	0.51	Constant	0.03	Constant	0.3
	0.512	0.512				
	0.512	0.512	HVL	0.28	HVL	0.55
	0.511	0.511				
SD	0.001	0.001				
Mean	0.51	0.51				
27 kVp						
	CC	ML0	Equation 11		Equation 12	
	0.531	0.34	kVp	27	kVp	27
	0.53	0.339	Constant	0.03	Constant	0.3
	0.531	0.34				
	0.53	0.34	HVL	0.30	HVL	0.57
	0.53	0.399				
SD	0.000548	0.026501				
Mean	0.53	0.35				
29 kVp						
	CC	ML0	Equation 11		Equation 12	
	0.546	0.356	kVp	29	kVp	29
	0.546	0.356	Constant	0.03	Constant	0.3
	0.545	0.357				
	0.546	0.357	HVL	0.32	HVL	0.59
	0.545	0.357				
SD	0.000548	0.000548				
Mean	0.55	0.36				
31 kVp						

	CC	ML0	Equation 11		Equation 12	
	0.562	0.373	kVp	31	kVp	31
	0.561	0.373	Constant	0.03	Constant	0.3
	0.562	0.372				
	0.562	0.373	HVL	0.34	HVL	0.61
	0.562	0.372				
SD	0.000447	0.000548				
Mean	0.56	0.37				
33 kVp						
	CC	ML0	Equation 11		Equation 12	
	0.576	0.389	kVp	33	kVp	33
	0.576	0.389	Constant	0.03	Constant	0.3
	0.576	0.39				
	0.577	0.39	HVL	0.36	HVL	0.63
	0.577	0.389				
SD	0.0005	0.000548				
Mean	0.58	0.39				
35 kVp						
	CC	ML0	Equation 11		Equation 12	
	0.59	0.404	kVp	35	kVp	35
	0.588	0.404	Constant	0.03	Constant	0.3
	0.588	0.404				
	0.59	0.403	HVL	0.38	HVL	0.65
	0.59	0.403				
SD	0.001095	0.000548				
Mean	0.59	0.40				

APPENDIX F

RAW DATA FOR THE ESTIMATION OF COMPRESSION FORCE

Compression mode	Automatic		Manual	
Mammography systems	Maximum force measured (N)	Displayed force value (N)	Maximum force measured (N)	Displayed force value (N)
A	186	176	196	186
B	166.96	174	156.96	160
C	175	190	215	200
D	170	-	200	-
E	110	110	200	200
F	N/A	N/A	170	800
G	140	110	220	210
H	220	214	140	130
I	20	30	110	120
J	150	152	200	197
K	190	185	220	226
L	170	165	200	196
M	161	170	177	160

APPENDIX G

RAW DATA FOR THE ESTIMATION OF COMPRESSION THICKNESS

Mammography systems	PMMA thickness (mm)					
	20		45		70	
	Measured thickness (mm)	Displayed thickness (mm)	Measured thickness (mm)	Displayed thickness (mm)	Measured thickness (mm)	Displayed thickness (mm)
A	20	16	43	40	68	65
B	21	23	44	48	72	73
C	20	15	40	45	70	69
D	19.5	-	44	-	68	-
E	23	20	48	45	68	70
F	21	25	44	45	70	70
G	10	21	45	35	70	59
H	20	18	44	38	68	63
I	24	21	48	45	71	70
J	18	14	44	40	69	66
K	18	14	41	37	67	63
L	20	17	45	41	68	65
M	20	18	45	43	69	66

APPENDIX H

RAW DATA FOR THE ESTIMATION OF COMPRESSION ALIGNMENT

Mammography systems	Compression alignment accuracy (mm)			
	Rear Left	Front Left	Rear Right	Front Right
A	32	34	31	34
B	44	46	45	46
C	35	40	35	41
D	19	18	20	17
E	40	49	40	49
F	78	77	77	75
G	43	48	47	51
H	40	44	41	44
I	48	49	47	48
J	45	45	45	47
K	39	42	41	42
L	40	41	41	42
M	51	53	52	52

APPENDIX I

RAW DATA FOR DETERMINING IMAGE QUALITY

Mammography system	A						B					
PMMA THICNESS (mm)	20		45		70		20		45		70	
	MPV	STDEV	MPV	STDEV	MPV	STDEV	MPV	STDEV	MPV	STDEV	MPV	STDEV
AL	44.06	1.18	49.31	1.25	104.53	1.94	80.449	9.053	104.405	9.245	92.198	6.589
PMMA BKG - 1	55.20	1.24	59.99	1.40	118.50	2.08	32.276	4.439	63.378	6.459	65.582	5.291
PMMA BKG - 2	55.39	1.23	58.92	1.38	116.52	2.06	36.864	5.402	70.036	7.907	74.828	7.362
PMMA BKG - 3	54.65	1.26	60.10	1.38	118.35	2.05	35.409	5.188	58.693	5.559	71.344	6.722
PMMA BKG - 4	55.61	1.26	59.33	1.40	117.82	2.11						

APPENDIX I continued

Mammography system	D						F					
PMMA THICNESS (mm)	20		45		70		20		45		70	
	MPV	STDEV	MPV	STDEV	MPV	STDEV	MPV	STDEV	MPV	STDEV	MPV	STDEV
AL	156.92	10.30	118.53	16.06	98.71	2.421	3196.68	48.528	2195.367	122.47	2679.49	223.02
PMMA BKG - 1	94.91	8.39	80.59	14.11	99.04	8.499	2740.93	64.747	1825.204	107.075	2124.90	218.94
PMMA BKG - 2	106.88	9.44	72.14	12.86	99.15	8.457	2357.48	64.034	1574.941	97.987	2474.69	219.37
PMMA BKG - 3	98.427	9.41	83.03	14.45	98.99	8.459	2194.84	59.612	1388.768	88.257	2177.27	227.31
PMMA BKG - 4	91.11	7.97	88.64	15.14	97.43	8.457	2434.52	62.105	1624.215	100.241	1318.90	312.17

APPENDIX I continued

Mammography system	H						I					
PMMA THICNESS (mm)	20		45		70		20		45		70	
	MPV	STDEV	MPV	STDEV	MPV	STDEV	MPV	STDEV	MPV	STDEV	MPV	STDEV
AL	2180.7	79.79	2955.30	175.56	2958.783	173.536	125.122	13.677	109.423	12.026	114.839	25.03
PMMA BKG - 1	2901.875	58.879	3260.21	129.835	3258.026	130.147	43.985	6.13	68.918	9.088	91.778	20.812
PMMA BKG - 2	2763.856	77.165	3205.46	139.552	3231.962	133.843	53.83	8.34	87.091	12.657	102.337	23.348
PMMA BKG - 3	3050.376	52.215	3378.68	111.304	3374.058	111.698	47.549	6.776	72.956	9.778	93.082	21.166
PMMA BKG - 4	3084.298	52.4	3426.44	110.651	3419.145	108.159	44.739	6.424	75.616	10.164	103.978	23.08

APPENDIX I continued

Mammography system	J						M					
PMMA THICNESS (mm)	20		45		70		20		45		70	
	MPV	STDEV	MPV	STDEV	MPV	STDEV	MPV	STDEV	MPV	STDEV	MPV	STDEV
AL	208.55	4.004	154.556	3.62	150.871	3.403	324.533	102.402	1160.521	96.153	1180.982	98.996
PMMA BKG - 1	136.79	4.916	115.195	4.041	118.286	3.607	1625.6	126.375	1774.542	102.829	1731.064	107.41
PMMA BKG - 2	128.28	5.085	112.527	3.673	115.104	3.802	1714.74	144.331	1759.173	106.664	1717.251	104.72
PMMA BKG - 3	124.88	4.624	113.421	3.748	117.693	4.256	1708.738	134.628	1795.035	110.635	1782.618	103.208
PMMA BKG - 4	128.48	4.611	117.152	3.563	121.599	3.618	1618.39	134.873	1703.206	105.512	1741.416	105.124

APPENDIX J

RAW DATA FOR ESTIMATION OF MEAN GLANDULAR DOSE

Appendix J-1: Raw data for estimation of mean glandular dose for mammography system A

Equivalent Brest thickness / cm	Output	ESAK	I_1	D_2	$(D_2)^2$	I_2
2.1	0.045	0.55035	0.55035	62.9	3956.41	0.587712
3.2	0.08296	2.65472	2.65472	61.8	3819.24	2.93676
4.5	0.08302	5.23026	5.23026	60.5	3660.25	6.037251
5.3	0.08302	7.314062	7.314062	59.7	3564.09	8.670351
6.0	0.08296	16.01128	16.01128	59	3481	19.4334
7.5	0.08286	24.94086	24.94086	57.5	3306.25	31.8715
9.0	0.08286	39.44136	39.44136	56	3136	53.13767

NB: $D_1 = 65$ cm and $(D_1)^2 = 4225$ cm^2

Appendix J-2: Raw data for estimation of mean glandular dose for mammography system B

Equivalent Brest thickness / cm	Output	ESAK	I_1	D_2	$(D_2)^2$	I_2
2.1	0.042	1.134	1.134	57.9	3352.41	1.217751
3.2	0.04232	1.60816	1.60816	56.8	3226.24	1.794465
4.5	0.04226	2.49334	2.49334	55.5	3080.25	2.914057
5.3	0.04218	4.09146	4.09146	54.7	2992.09	4.922732
6.0	0.04232	6.00944	6.00944	54	2916	7.419062
7.5	0.04092	9.53436	9.53436	52.5	2756.25	12.4530
9.0	0.04984	15.89896	15.89896	51	2601	22.00548

NB: $D_1 = 60$ cm and $(D_1)^2 = 3600$ cm^2

Appendix J-3: Raw data for estimation of mean glandular dose for mammography system C

Equivalent Brest thickness / cm	Output	ESAK	I_1	D_2	$(D_2)^2$	I_2
2.1	0.12	0.468	0.468	57.9	3352.41	0.502564
3.2	0.12184	3.16784	3.16784	56.8	3226.24	3.534834
4.5	0.122	6.466	6.466	55.5	3080.25	7.557049
5.3	0.10884	9.36024	9.36024	54.7	2992.09	11.26198
6.0	0.10898	12.85964	12.85964	54	2916	15.8761
7.5	0.12164	21.53028	21.53028	52.5	2756.25	28.12118
9.0	0.1084	30.894	30.894	51	2601	42.75986

NB: $D_1 = 60$ cm and $(D_1)^2 = 3600$ cm^2

Appendix J-4: Raw data for estimation of mean glandular dose for mammography system D

Equivalent Brest thickness / cm	Output	ESAK	I_1	D_2	$(D_2)^2$	I_2
2.1	0.069	0.71745	0.71745	63.9	4083.21	0.769342
3.2	0.082373	2.476907	2.476907	62.8	3943.84	2.755353
4.5	0.082427	4.729867	4.729867	61.5	3782.25	5.502786
5.3	0.078013	6.921921	6.921921	60.7	3684.49	8.285022
6.0	0.078087	11.62679	11.62679	60	3600	14.24285
7.5	0.081807	18.6685	18.6685	58.5	3422.25	24.14857
9.0	0.080367	28.74477	28.74477	57	3249	39.30101

NB: $D_1 = 66$ cm and $(D_1)^2 = 4356$ cm^2

Appendix J-5: Raw data for estimation of mean glandular dose for mammography system E

Equivalent Brest thickness / cm	Output	ESAK	I_1	D_2	$(D_2)^2$	I_2
2.1	0.0979	1.4685	1.4685	57.9	3352.41	0.672584
3.2	0.1034	3.102	3.102	56.8	3226.24	3.461367
4.5	0.10266	5.03034	5.03034	55.5	3080.25	5.879141
5.3	0.10378	6.2268	6.2268	54.7	2992.09	7.491914
6.0	0.10322	7.84472	7.84472	54	2916	9.68484
7.5	0.10306	11.3366	11.3366	52.5	2756.25	14.80699
9.0	0.10336	17.36448	17.36448	51	2601	24.03388

NB: $D_1 = 60$ cm and $(D_1)^2 = 3600$ cm^2

Appendix J-6: Raw data for estimation of mean glandular dose for mammography system F

Equivalent Brest thickness / cm	Output	ESAK	I_1	D_2	$(D_2)^2$	I_2
2.1	0.03626	0.951825	0.951825	63.9	4083.21	1.015414
3.2	0.05524	2.2096	2.2096	62.8	3943.84	2.440519
4.5	0.06748	3.374	3.374	61.5	3782.25	3.88582
5.3	0.07722	3.861	3.861	60.7	3684.49	4.56468
6.0	0.0982	6.1866	6.1866	60	3600	7.485786
7.5	0.1265	7.9695	7.9695	58.5	3422.25	10.14395
9.0	0.1604	12.832	12.832	57	3249	17.20412

NB: $D_1 = 66$ cm and $(D_1)^2 = 4356$ cm^2

Appendix J-7: Raw data for estimation of mean glandular dose for mammography system G

Equivalent Brest thickness / cm	Output	ESAK	I_1	D_2	$(D_2)^2$	I_2
2.1	0.086	1.72	1.72	63.9	4083.21	1.834909
3.2	0.08746	3.41094	3.41094	62.8	3943.84	3.767408
4.5	0.08714	5.05412	5.05412	61.5	3782.25	5.820807
5.3	0.08776	6.84528	6.84528	60.7	3684.49	8.092854
6.0	0.08692	9.30044	9.30044	60	3600	11.25353
7.5	0.0868	12.7596	12.7596	58.5	3422.25	16.24102
9.0	0.08714	23.17924	23.17924	57	3249	31.07688

NB: $D_1 = 66$ cm and $(D_1)^2 = 4356$ cm^2

Appendix J-8: Raw data for estimation of mean glandular dose for mammography system H

Equivalent Brest thickness / cm	Output	ESAK	I_1	D_2	$(D_2)^2$	I_2
2.1	0.11378	2.61694	2.61694	62.9	3956.41	2.794597
3.2	0.11482	4.0187	4.0187	61.8	3819.24	4.445651
4.5	0.1148	4.7642	4.7642	60.5	3660.25	5.499281
5.3	0.11446	6.2953	6.2953	59.7	3564.09	7.462674
6.0	0.11544	8.658	8.658	59	3481	10.50849
7.5	0.1155	16.632	16.632	57.5	3306.25	21.25375
9.0	0.11524	30.88432	30.88432	56	3136	41.60914

NB: $D_1 = 65$ cm and $(D_1)^2 = 4225$ cm^2

Appendix J-9: Raw data for estimation of mean glandular dose for mammography system I

Equivalent Brest thickness / cm	Output	ESAK	I_1	D_2	$(D_2)^2$	I_2
2.1	0.0562	1.2926	1.2926	62.9	3956.41	1.380351
3.2	0.05728	2.5776	2.5776	61.8	3819.24	2.851447
4.5	0.0572	3.5464	3.5464	60.5	3660.25	4.093584
5.3	0.0579	5.0952	5.0952	59.7	3564.09	6.040033
6.0	0.05792	7.18208	7.18208	59	3481	8.717118
7.5	0.05684	9.54912	9.54912	57.5	3306.25	12.20266
9.0	0.0563	16.0455	16.0455	56	3136	21.61742

NB: $D_1 = 65$ cm and $(D_1)^2 = 4225$ cm^2

Appendix J-10: Raw data for estimation of mean glandular dose for mammography system J

Equivalent Brest thickness / cm	Output	ESAK	I_1	D_2	$(D_2)^2$	I_2
2.1	0.03802	2.0911	2.0911	62.9	3956.41	2.233059
3.2	0.03818	3.0544	3.0544	61.8	3819.24	3.378903
4.5	0.03818	5.23066	5.23066	60.5	3660.25	6.037713
5.3	0.03816	4.31208	4.31208	59.7	3564.09	5.111694
6.0	0.037782	4.647208	4.647208	59	3481	5.640464
7.5	0.0382	17.6866	17.6866	57.5	3306.25	22.6014
9.0	0.03826	9.52674	9.52674	56	3136	12.83497

Appendix J-11: Raw data for estimation of mean glandular dose for mammography system K

Equivalent Brest thickness / cm	Output	ESAK	I_1	D_2	$(D_2)^2$	I_2
2.1	0.038373	2.11049	2.11049	61.8	3819.24	2.334711
3.2	0.04236	3.3888	3.3888	60.5	3660.25	3.911667
4.5	0.04236	3.3888	3.3888	60.5	3660.25	3.911667
5.3	0.044843	3.901353	3.901353	59.7	3564.09	4.624804
6.0	0.04574	4.43678	4.43678	59	3481	5.38506
7.5	0.044745	5.727373	5.727373	57.5	3306.25	7.318911
9.0	0.05206	8.5899	8.5899	56	3136	11.57281

NB: $D_1 = 65$ cm and $(D_1)^2 = 4225$ cm^2

Appendix J-12: Raw data for estimation of mean glandular dose for mammography system L

Equivalent Brest thickness / cm	Output	ESAK	I_1	D_2	$(D_2)^2$	I_2
2.1	0.03858	1.46604	1.46604	62.9	3956.41	1.565566
3.2	0.037922	3.071647	3.071647	61.8	3819.24	3.397982
4.5	0.037882	3.788235	3.788235	60.5	3660.25	4.372732
5.3	0.03858	4.0509	4.0509	59.7	3564.09	4.802082
6.0	0.037922	4.323059	4.323059	59	3481	5.247033
7.5	0.037882	7.424941	7.424941	57.5	3306.25	9.488205
9.0	0.037922	9.442471	9.442471	56	3136	12.72144

NB: $D_1 = 65$ cm and $(D_1)^2 = 4225$ cm^2

Appendix J-13: Raw data for estimation of mean glandular dose for mammography system M

Equivalent Brest thickness / cm	Output	ESAK	I_1	D_2	$(D_2)^2$	I_2
2.1	0.038	1.52	1.52	62.9	3956.41	1.623189
3.2	0.037902	2.728941	2.728941	61.8	3819.24	3.018867
4.5	0.03862	4.20958	4.20958	60.5	3660.25	4.859088
5.3	0.037922	3.981765	3.981765	59.7	3564.09	4.720127
6.0	0.03868	4.48688	4.48688	59	3481	5.445868
7.5	0.03798	6.646569	6.646569	57.5	3306.25	8.493536
9.0	0.03864	19.62912	19.62912	56	3136	26.44548

NB: $D_1 = 65$ cm and $(D_1)^2 = 4225$ cm^2

APPENDIX K

PUBLISHED ARTICLES FROM THESIS

1. Edem Sosu, Mary Boadu, Samuel Yeboah Mensah. Quantitative assessment of Image Quality in mammography: Results from phantom studies in Ghana. International Journal of Scientific Research in Science and Technology. Volume 3, Issue 7. September - October 2017. Pages 73 – 77
2. Edem Sosu, Mary Boadu, Samuel Yeboah Mensah. Optimization of Radiological protection of patients in mammography examination using compression analysis. International Journal of Scientific Research in Science, Engineering and Technology (IJSRSET), Volume 4 Issue 1, January – February 2018, Pages 459 – 463.
3. Edem Sosu, Mary Boadu, Samuel Yeboah Mensah. Determination of dose delivery accuracy and image quality in Full - Field digital mammography. Journal of Radiation Research and Applied Sciences (2018); 8(1):1 - 5

APPENDIX L

PUBLISHED ARTICLES RELATED TO THESIS

1. Ernest Agyemang - Oko, Edem Sosu, Baah Sefa - Ntiri, " Comparative study of mean Glandular dose between two Mammography Systems with Similar Target - Filter Combination", International Journal of Scientific Research in Science, Engineering and Technology(IJSRSET), Volume 3 Issue 6, September-October 2017, Pages 700-703.
2. Pwamang C, Sosu E, Schandorf C, Boadu M, Hewlett V. Assessment of Dose to Glandular Tissue of Patients Undergoing Mammography Examinations.. J Radiol Radiat Ther 4(2): 1062. 2016. Pages 2 – 5

APPENDIX M

CONFERENCE POSTER PRESENTATIONS

1. E. K. Sosu, F. Hasford, T. B. Dery, E. W. Fiagbedzi, Y. Serfor - Armah, A.W.K Kyere. Medical Physics in Ghana. The Abdus Salam International Centre for Theoretical Physics, (ICTP). College on Medical Physics, 1st – 19th September, 2014. Trieste, Italy.
2. Edem Sosu, Mary Boadu, Samuel Mensah. Mammography Dose Audit in Ghana: results of a phantom studies. International Conference on radiation protection in medicine: achieving change in practice. (IAEA CN-255). 11th – 15th December 2017. Vienna, Austria.
3. Edem Sosu, Mary Boadu, Samuel Mensah. Towards establishing Diagnostic reference levels in mammography practice: preliminary results basedon phantom studies in Ghana. International Conference on radiation protection in medicine: achieving change in practice. (IAEA CN-255). 11th – 15th December 2017. Vienna, Austria.

APPENDIX N

AWARD

Winner, TAQI BINESH Award for Best Poster Presentation during the College on Medical Physics held from 1st – 19th September, 2014 at The Abdus Salam International Centre for Theoretical Physics, (ICTP), Trieste, Italy.

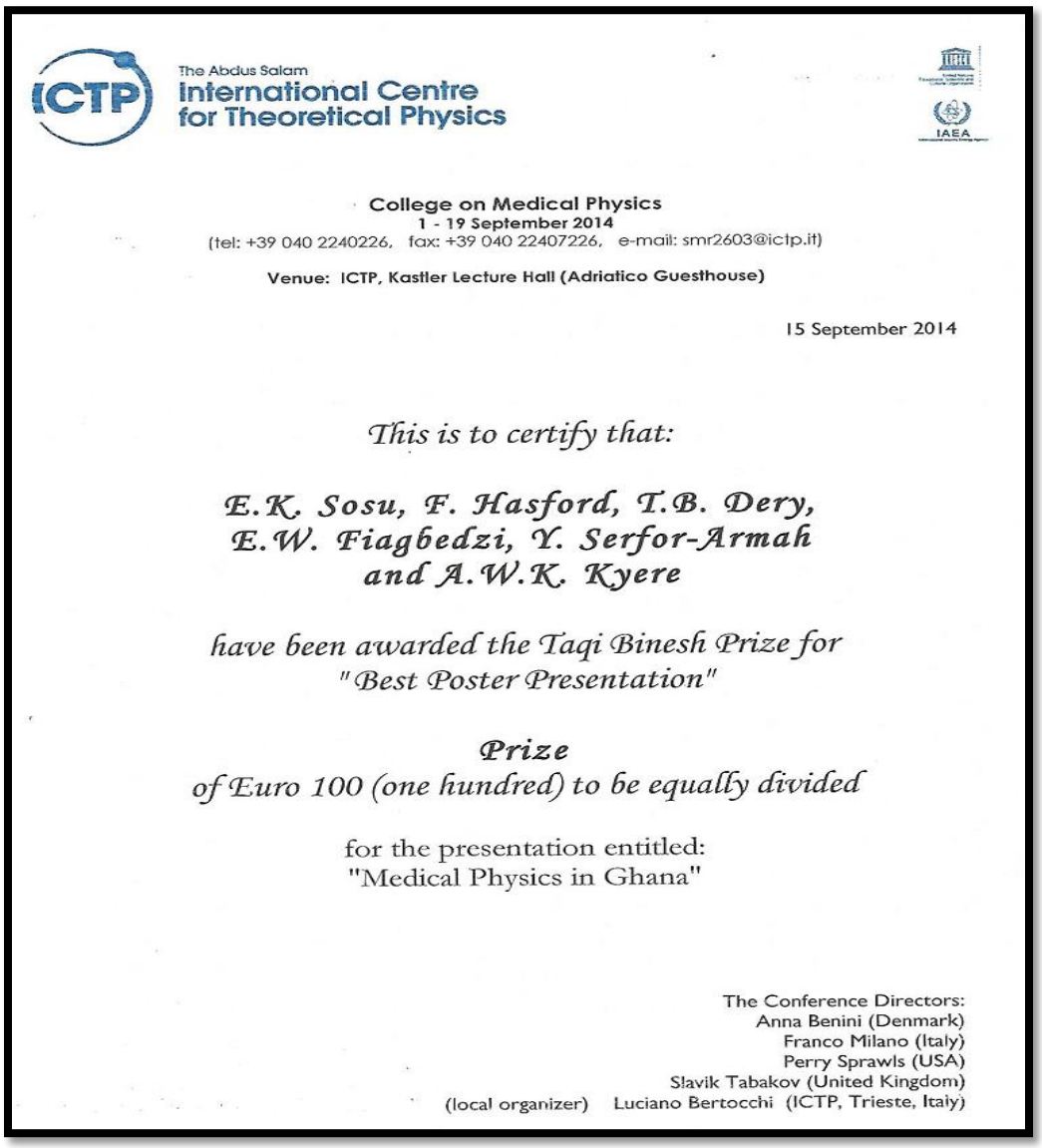

The Abdus Salam
International Centre
for Theoretical Physics

IAEA

College on Medical Physics
1 - 19 September 2014
(tel: +39 040 2240226, fax: +39 040 22407226, e-mail: smr2603@ictp.it)

Venue: ICTP, Kastler Lecture Hall (Adriatico Guesthouse)

15 September 2014

This is to certify that:

E.K. Sosu, F. Hasford, T.B. Dery, E.W. Fiagbedzi, Y. Serfor-Armah and A.W.K. Kyere

have been awarded the Taqi Binesh Prize for "Best Poster Presentation"

Prize
of Euro 100 (one hundred) to be equally divided

for the presentation entitled:
"Medical Physics in Ghana"

The Conference Directors:
Anna Benini (Denmark)
Franco Milano (Italy)
Perry Sprawls (USA)
Slavik Tabakov (United Kingdom)
(local organizer) Luciano Bertocchi (ICTP, Trieste, Italy)

APPENDIX O

COPIES OF PUBLISHED ARTICLES AND CONFERENCE PRESENTATIONS